DEPOLYMERIZATION OF LIGNIN FOR VALUE-ADDED PRODUCTS BY CATALYTIC OXIDATION

A Dissertation
Presented to
The Academic Faculty

by

Xu Du

In Partial Fulfillment
of the Requirements for the Degree
Doctor of Philosophy in the
School of Chemical and Biomolecular Engineering

Georgia Institute of Technology
December 2018

DEPOLYMERIZATION OF LIGNIN FOR VALUE-ADDED PRODUCTS BY CATALYTIC OXIDATION

Approved by:

Dr. Yulin Deng, Advisor
School of Chemical and Biomolecular Engineering
Georgia Institute of Technology

Dr. Preet Singh
School of Materials Science and Engineering
Georgia Institute of Technology

Dr. Sven Behrens
School of Chemical and Biomolecular Engineering
Georgia Institute of Technology

Dr. Zhiqun Lin
School of Materials Science and Engineering
Georgia Institute of Technology

Dr. Chris Luettgen
School of Chemical and Biomolecular Engineering
Georgia Institute of Technology

Date Approved: August 13, 2018

To my parents for their unconditional support and love

ACKNOWLEDGEMENTS

In this thesis, I would like to thank all the people who helped and supported me during my life, especially during these precious five years in Atlanta. Over the past five years, I studied a different major, experienced different cultures, made many friends from different backgrounds, and learned a lot of knowledge and skills that will support me for my future development and have a good life. Firstly, I would like to thank my supervisor, Dr. Yulin Deng, for accepting me to be member of your group. Thank you for supporting me in my hardest times. You always gave me a quick feedback for my questions at any time. It has been very enjoyable for me to work in your group. I would never have gained so much without your advice and support. I would like to acknowledge my PhD committee, Professor Zhiqun Lin, Professor Chris Luettgen, Professor Sven Behrens, and Professor Preet Singh for your useful suggestions and encouragements in my PhD study.

Many colleagues have assisted and helped me during my PhD research. Wei Liu, thanks for your help and discussions of the problems I met during my PhD studies. You are a talented researcher and nice person. I have no doubt you will be a shining star in academia in future. Wei Mu and Xiaodan Zhang, thanks for your help in the beginning of PhD and my job hunting period. Arie Mulyadi, Zhe Zhang, Vincent Li, Jie Tao, Weisheng Yang, Dr. Jian Gong, Dr. Yong Cui, Dr. Parikshit Gogoi, Junli Zhou, Xihong Zu thanks for your help when we worked together. My gratitude also goes to all other our group members for sharing the memorable time.

I also would like to thank my colleagues in my department. Andrew Tricker, my best American friend, thanks for helping me to do a lot of lignin characterizations and

manuscript revision. Without your help, it would be extremely hard for me to finish the analysis of my samples. Sireesha Aluri, thanks for your encouragement in my hard time and help for GC analysis. Alex Brittain, thanks for your help in GC-MS analysis. I also would like to thank the staff in RBI building for their work and support for solving day-to-day problems, especially, Jerry Nunn, Lloyd Williams, Bob Davis, Charles Brookshire, Lavon Harper, Dione Morton, Mary Williams, and Hank (Major) White.

For the officers in TAPPI student chapter at Georgia Tech, Thomas Kwok, Chinmay Satam, Yoon Joo Na, Nikolay Semenikhin and Zihao Qu, thanks for your support when I was the president. I could not have made this organization run without your support and hardworking. Thank our supervisors, Dr. Chris Luettgen and Dr. Norman Marsolan, for your support and supervision for our organization. For the colleagues in Lignin group, Thomas Kwok, Andrew Tricker, Michael Stellato, Nick Kruyer, and Zhongzhen Wang, thanks for your help in lignin study. Thank the faculty members Dr. Andreas Bommarius, Dr. Matthew Realff, Dr. Carsten Sievers, and Dr. Sankar Nair for your suggestions.

Last but not least, thanks my lifetime friends Ningyuan Cao, Feifei Sun, Zihao Qu, Weize Hu, Yi Zhang, Xiaotang Du, Pan Wu, Hongfu Pan, Yang Wang, and Qiaoli Xu for your strong support and sharing the precious moments with me. You are the reason for me to live without fear and hesitate. I also would like to thank other Chinese friends here for spending memorable time, especially Xinyuan Nan, Yanchao He, Shuai Tan, Lu Jiang, Sen Yang, Rui Chang, Siwei Guo, Ruian Duan, Yuze Zhang, Liang He,Yang Jiao, Xiaoming Mu, Qianhui Chen, Chao Tai, Ningquan Wang, Songcheng Wang, Xueju Wang, Lu Xu, and Yuehui Zhao.

TABLE OF CONTENTS

LIST OF TABLES

LIST OF FIGURES

LIST OF SYMBOLS AND ABBREVIATIONS

GPC	Gel Permeation chromatography
NMR	Nuclear Magnetic Resonance
HSQC	Heteronuclear Single-Quantum Correlation
GC	Gas Chromatography
MS	Mass Spectroscopy
FID	Flame Ionization Detector
FTIR	Fourier Transform infrared
XPS	X-ray photoelectron spectroscopy
UV	Ultraviolet
TGA	Thermogravimetric Analysis
RT	Retention Time
T	Temperature
t	time
M_n	Number average molecular weight
M_w	Weight average molecular weight
POM	Polyoxometalates
PMo_{12}	Phosphomolybdic acid ($H_3PMo_{12}O_{40}$)
DCM	Dichloromethane
DMSO	Dimethyl sulfoxide
THF	Tetrahydrofuran
MeOH	Methanol
EtOH	Ethanol

MeCN	Acetonitrile
HCl	Hydrochloric acid
H_3PO_4	Phosphoric acid
HNO_3	Nitric acid
TEMPO	2,2,6,6-Tetramethyl -1-piperidinyloxy
Pt	Platinum
$FeCl_3$	Ferric (III) chloride
H_2	Hydrogen gas
N_2	Nitrogen gas
O_2	Oxygen gas
nm	Nanometer
μm	Micrometer
wt	Weight
vol	Volume
ppm	part per million
Ar	Aromatic

SUMMARY

Lignin is the second most abundant component of lignocellulosic biomass after cellulose. It is a natural cross-linked amorphous polymer that acts as the bridge in the plants structure.[1] However, compared with cellulose, lignin has always been considered a low-quality feedstock and used in low-value-added materials. Considering its rich aromatic structure and huge production, lignin has potential to be the major resource for renewable aromatic chemicals. However, there are three major concerns for effective lignin valorization. **First,** the condensation reaction of the lignin fragments through positive α carbocation (C_{α}^{+}) coupled with electron-rich lignin aromatic rings that occurs during the depolymerization process which increases the recalcitrance of the lignin and limits product yields. **Second,** the use of acid or alkali during lignin fractionation (e.g. delignification in pulping) results in the variation of the ether linkages and lignin condensation with the formation of interunit C-C linkages. This can reduce the amount of breakable ether bonds and increase the recalcitrance of lignin that suppress the depolymerization of isolated lignin in the subsequent process. **Third,** the current studies only focus on the production of chemicals from lignin but ignores the possibilities to combine the lignin depolymerization with other processes to make extra value. To respond these three concerns, my PhD study focuses on three parts, (1) suppress lignin condensation during depolymerization by selective oxidation of active benzyl alcohol to facilitate lignin depolymerization; (2) fractionate lignin from biomass for *in situ* depolymerization towards complete biomass valorization; and (3) combine lignin depolymerization to chemicals and electrolysis to hydrogen together to maximize lignin valorization.

1. Lignin depolymerization by a two-step oxidation strategy

The key to suppress condensation of β-O-4 linkages during depolymerization is to modify or block the active α-OH in β-O-4 moieties to avoid formation of the active C_α^+ that can lead to additional C-C linkages formation. My study employed two-step oxidation (preoxidation – depolymerization) strategies in two ways. In the preoxidation process, the secondary benzylic alcohol (C_α-OH) in the lignin structure is oxidized to a carbonyl (C_α=O) at low temperature. In the second depolymerization process, the lignin is depolymerized via oxidative cleavage to aromatic chemicals at an elevated temperature. In the first approach, the TEMPO was used to selectively oxidize the C_α-OH to a ketone.[2, 3] Polyoxometalate (POM), which can be completely regenerated by oxygen under relatively mild conditions (150 °C, 10 bar O_2), was used as oxidative catalyst for further degradation of the modified lignin. The lignin depolymerization efficiency could be remarkably improved by converting the active C_α-OH to the stable C_α=O. Under optimized conditions, 74.5% of the lignin was converted to low-molecular-weight (LMW) products, and 32.8 wt% of the lignin was converted to monomeric compounds. **(Chapter 3)**

However, all the current two-step processes need to be conducted in two different catalysis systems (*i.e.* solvents, catalysts),[2-5] which becomes a significant hurdle for employing this strategy in industrial practice. For the first time, we conducted a two-step oxidation protocol which was achieved in one pot by the same polyoxometalate catalysis system. First, the benzyl alcohols in industrial lignin was oxidized to ketones in methanol by POM under mild condition (<80 ^oC). Then the preoxidized lignin was further depolymerized to aromatics at an elevated temperature (e.g. 140 ^oC). 58.0 % of industrial lignin without purification can be converted to LMW products. **(Chapter 4)**

2. Lignin-first biomass fractionation towards complete biomass valorization

Although the condensation during lignin depolymerization can be suppressed by applying preoxidation process, the recalcitrant condensed structure of lignin that has been formed during biomass fractionation is a barrier for further lignin depolymerization. Current biorefineries are focus on cellulose valorization, and consider lignin a low-value byproduct.[6] New biorefinery schemes are needed for complete utilization of biomass, where both the valorizations of lignin and cellulose are regarded as a primary targets. In my study, the low concentration POM catalyst is employed to extract lignin from wood sawdust, under mild condition (100 ^{o}C) in methanol, while avoiding structural lignin condensation and degradation. Then extracted lignin is further oxidized to LMW products with 86.2 wt% yield, and the remaining cellulose can be further used to produce bio-ethanol towards biomass complete valorization. **(Chapter 5)**

3. Catalytic electrolysis for simultaneously H_2 evolution and lignin depolymerization

The last part of my study focused on designing a new electro-catalytic process to extract extra value from lignin, instead of only focusing on the production of aromatics. Hereby we present a novel proton exchange membrane (PEM) electrolysis process in which lignin was used as the hydrogen source at anode for hydrogen production. POM was used as the catalyst and charge transfer agent in anode. Over 90% Faraday efficiency was achieved. In a thermal insulation reactor, the input heat energy can be maintained at a very low stage for continuous operation. Compared to the alkaline water electrolysis reported in literature, the electrical energy consumption could be 40% lower with novel lignin electrolysis method. At the anode, the Kraft lignin (KL) was oxidized to aromatic

chemicals by POM, and reduced POM was regenerated during the electrolysis. Structure analysis of the residual KL indicated the reduction of hydroxyl group number and the cleavage of ether bonds. Our results suggest that POM-mediated electrolysis process can significantly reduce the electrolysis energy consumption in hydrogen production and, simultaneously, depolymerize lignin to low molecular weight value-added aromatic chemicals.[7] **(Chapter 6)**

POM is chemically stable and effective mediator and charge transfer catalyst, but the molecular weight of POM is very high (molecular weight of $H_3PMo_{12}O_{40}$ is 1,825.25 g mol^{-1}), which reduces the diffusibility and dischargeability on the anode. With such an extremely high molecular weight catalyst, it is also difficult to obtain a high molar concertation solution that is important for increasing both lignin oxidation and anode discharge rate. The Fe^{3+}/Fe^{2+} ion pair is an excellent candidate to realize the lignin oxidation and anode discharge circle due to its low cost and small ion pair. The standard potential of Fe^{3+}/Fe^{2+} is 0.77 V vs. NHE. The KL was oxidized to aromatic chemicals by $FeCl_3$, and Fe^{2+} was reoxidized by electrolysis. Similarly, over 40% of electrical energy consumption was saved compared to the alkline water electrolysis and 90% Faraday efficiency was achieved. **(Chapter 7)**

In summary, this dissertation attempts to understand the catalytic valorization of lignin better mainly using polyoxometalates as catalyst due to its special properties, including catalysis process design, catalyst preparation, depolymerization of lignin (or lignocellulose), and lignin (and its products) characterization. Most of the effort has been put into developing the novel catalytic oxidation process in order to design an effective process for lignin conversion with high yield and low energy input.

CHAPTER 1. INTRODUCTION AND LITERATURE REVIEW

Biomass is one of the most valuable renewable resources on earth. 170 billion tons of biomass are produced in nature by photosynthesis every year, among which only 3-4% is further utilized.[8] Apart from providing food, feed, and energy, only a small fraction of utilized biomass was employed to produce valuable chemicals such as medicinal drugs, cellulose esters, oxidized linseed oil, flavors and fragrances.[9] The main reason being that carbon-based chemical can be synthesized from cheaper petroleum by conventional routes. The rising cost and dwindling supply of oil in the foreseeable future has led to increasing concerns regarding energy security, environmental stewardship, and rural development. For these reasons, ever-increasing studies has been focused on possible ways to produce fuels and chemicals from biomass, especially lignocellulosic biomass.[10] Some excellent studies have been made for the development of novel processes for the fractionation of lignocellulose to cellulose, hemicellulose, and lignin with high purity.[11, 12] However, the traditional lignocellulosic biorefineries focus on producing valuable products from the carbohydrate fractions: cellulose and hemicellulose. Lignin has always been considered as an unwanted, low-quality and low-value-added product as it results in the recalcitrance of biomass and inhibit the efficient fractionation of the carbohydrates. In pulp and paper industry, only 2% lignin is used for producing value-added products, while over 95% is simply incinerated for heat.[13]

Lignin is second abundant component of lignocellulosic biomass after cellulose. Its valorization is a key point to create economically feasible and sustainable biorefineries. Due to its aromatic-rich structure, lignin is a promising renewable source for aromatic

chemicals production in the future. Until recently, there has been no efficient way to recover these aromatic chemicals.[10] Developing techniques to produce aromatics from lignin is not only urgent and challenging, but also a visible long-term opportunity. The increasing awareness in lignin as a renewable resource has launched enormous researches into its valorization, via dissolution, biological, thermal disruption, reduction and oxidation methods (Figure 1.1), for the production of chemicals.[1, 14-16] As a promising and economically feasible technique, oxidative methods can convert lignin to chemicals under a generally mild conditions. This study will focus on the oxidative thermal- and electro-catalytic approaches for lignin depolymerization (highlighted by red in Figure 1.1).

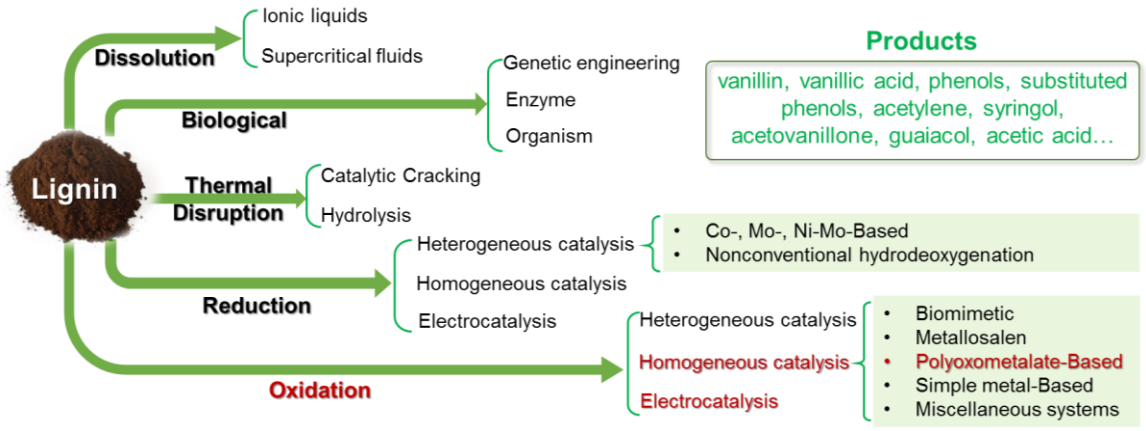

Figure 1.1 The studies in lignin valorization for the production of renewable chemicals.

1.1 Lignocellulose: structure and composition

Lignocellulose has been widely considered as a promising renewable resource to produce alternative transportation fuels and chemicals in recent decades. Cellulose, hemicellulose and lignin (Figure 1.2) are the three main components of lignocellulosic

biomass. Their proportions vary with material sources. The major part of plant cell walls is cellulose, in which glucose molecules are linked by glycosidic bonds. Hemicellulose, the third component of lignocellulose, is a polymer containing several different 5- and 6-carbon monosaccharide units. It provides structural strength to the plant cell wall by binding cellulose fibers together and by cross-linking with lignin. Lignin is the second major component with a three-dimensional structure that provides compressive strength to the plant tissue and the individual fibers and stiffness to the cell wall.

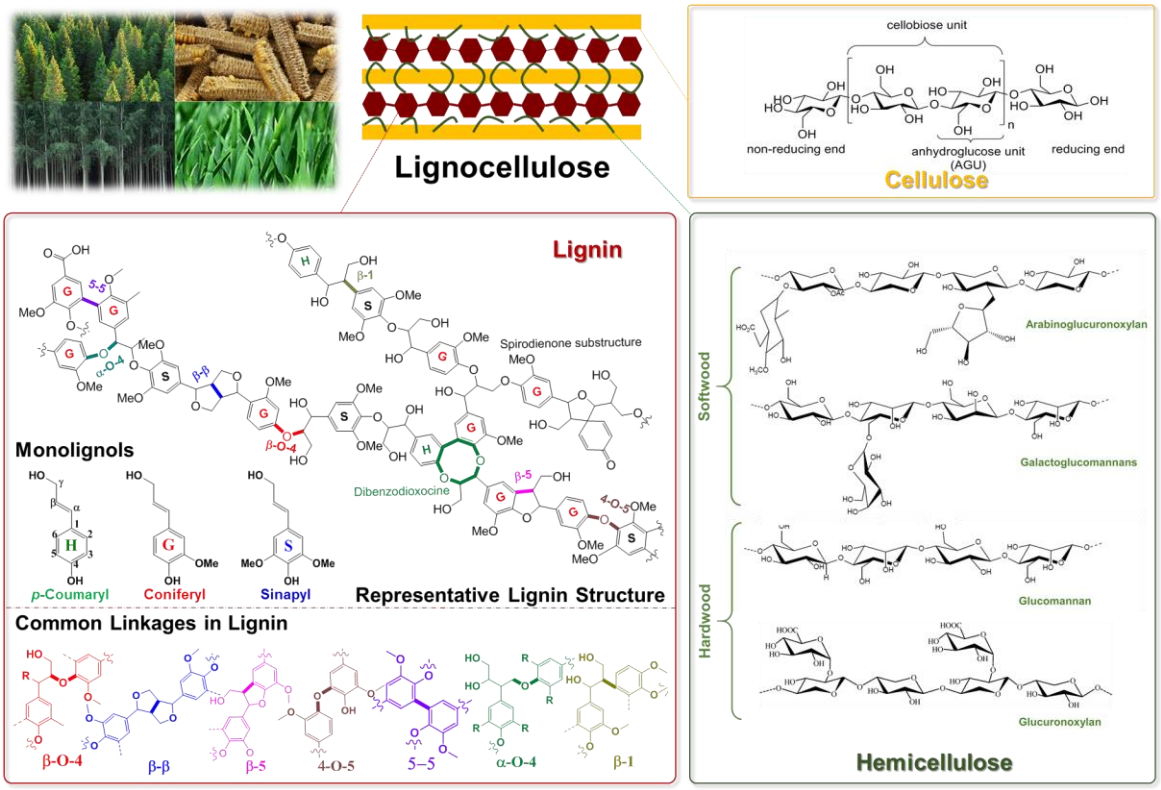

Figure 1.2 Structure of lignocellulose, highlighting the three main components (cellulose, hemicellulose and lignin).

1.1.1 Lignin

Considerable effort has gone into elucidating the native structure of lignin and its role in the cell wall. Lignin is a three-dimensional amorphous polymer containing methoxylated phenyl-propane structures, [17] but the exact structure is highly dependent on the plant species. In the plant cell wall, the lignin acts as a resin in between the cellulose and hemicellulose, holding the lignocellulosic matrix together. The abundance of lignin in softwoods, hardwoods, agriculture waste and grasses are shown in Table 1.1.

Table 1.1 Major biomass components indifferent hardwoods, softwoods, agriculture waster and grass.[16, 18-20]

Lignocellulose		Cellulose (%)	Hemicellulose (%)	Lignin (%)
Hardwood		43-47	36-39	17-23
		45-47	26-33	18-21
Softwood		46	23	28
Agriculture Waste		35-39	23-30	12-16
		34-41	32-46	6-16
Grass		35-40	25-30	15-20
		24-33	45-52	9-13

The exact structure of lignin is still unknown, but three monolignols (Figure 1.2), *p*-coumaryl (H unit), coniferyl (G unit), and sinapyl (S unit) alcohol, are widely accepted as the primary units to polymerize during lignin biosynthesis.[17] The common linkages in lignin are shown in Figure 1.2, include β-O-4, 5-5, β-5, α-O-4, β-1, 4-O-5 and β-β. For softwoods (spruce) and hardwoods (birch) the abundances of the common linkages are summarized in Table 1.2. β-O-4 is the most abundant linkage in both softwood and hardwood, consisting of about 50% in softwood (spruce) and 60% in hardwood (birch) of all linkages. The next most common are the 5-5 and β-5 linkage. [1, 17] Although the advanced NMR techniques were developed in recent years, it should be noted that to identify and quantify the different linkages and structures in lignin is a challenging task due to the complex moieties and chemical alteration from varying fractionation methods. [21-29]

Table 1.2 Common linkages and approximate abundance in softwood (Spruce) and hardwood (Birch)[1, 30]

Linkage	β-O-4	5-5	β-5	α-O-4	β-1	4-O-5	β-β	D*
Softwood	45-50	19-27	9-12	6-8	1-9	nd*-7	2-6	nd-7
Hardwood	60	9	6	6-8	1-7	6.5	3	nd

*nd = not determined, D = Dibenzodioxocin, Abundance per 100 C_9-units

1.1.2 Cellulose and hemicellulose

Cellulose, the main component of lignocellulose, is the most plentiful renewable bio-polymeric resource, having an annual estimated production of approximately 1×10^{11} metric tons. It is generally used in either fibre form, as an additive, or for bio-ethanol.

Irrespective of its source, cellulose can be regarded as a homopolymer molecule with 1,4-linked anhydro-D-glucose units. The dimer of glucose, cellobiose, is often counted as the repeated segment (Figure 1.2). The degree of polymerization (DP) for cellulose is up to 20000. The smaller cellulose are localized in the primary cell wall. [31] Hydrogen bonding between the different polysaccharide layers contribute to the resilience of the crystalline cellulose. [32]

Hemicellulose, another major component of lignocellulosic biomass, contains a set of 5- and 6-carbon sugars including galactose, arabinose, mannose, xylose, and glucose.[32] The major components of hemicellulose in softwoods (SW) are galactoglucomannans and arabinoglucuronoxylan, small amount of xyloglucan, arabinogalactan, and other glucans. For hardwoods, the glucuronoxylan and glucomannan is predominant in hemicellulose with limited amount of glucans and galactans.[33] The major types of hemicelluloses in softwoods and hardwoods are shown in Figure 1.2.

1.2 Lignin fractionations and structural considerations

Pretreatment of biomass and lignin fractionation are vital early stages in biorefinery. During pretreatment, the chemical transformations of lignin are conducted in the process of lignin fractionation, including the incorporation of sulfur and the condensation of lignin. These changes are dependent on the pretreatment approaches. Biomass pretreatment is a major challenge to the biorefinery because the recalcitrance offered by the semi-crystalline structure of cellulose and complex structure of the plant cell wall makes separation into constituent components difficult. The structure of the lignin depends on the isolation method employed.

Recently, Dale et al. comprehensively reviewed the pretreatment technologies, wherein were divided into four categories: chemical treatment (Kraft, alkaline, sulfide, and Klason), physical treatment (extensive grinding), solvent fractionation (organosolv process, including ethanol/water and ionic liquids treatment), and biological treatment (using cellulolytic enzyme).[34] Among these methods, the chemical pretreatment can lead to significant structural changes in the lignin while the others three can result in mild structure changes as shown in Figure 1.3. Gaspar et al. reviewed a green catalyst, polyoxometalates (POMs), to replace the chlorine-based chemical in current Kraft pulping process for delignification, [35] which will be discussed in detail in section 1.4.

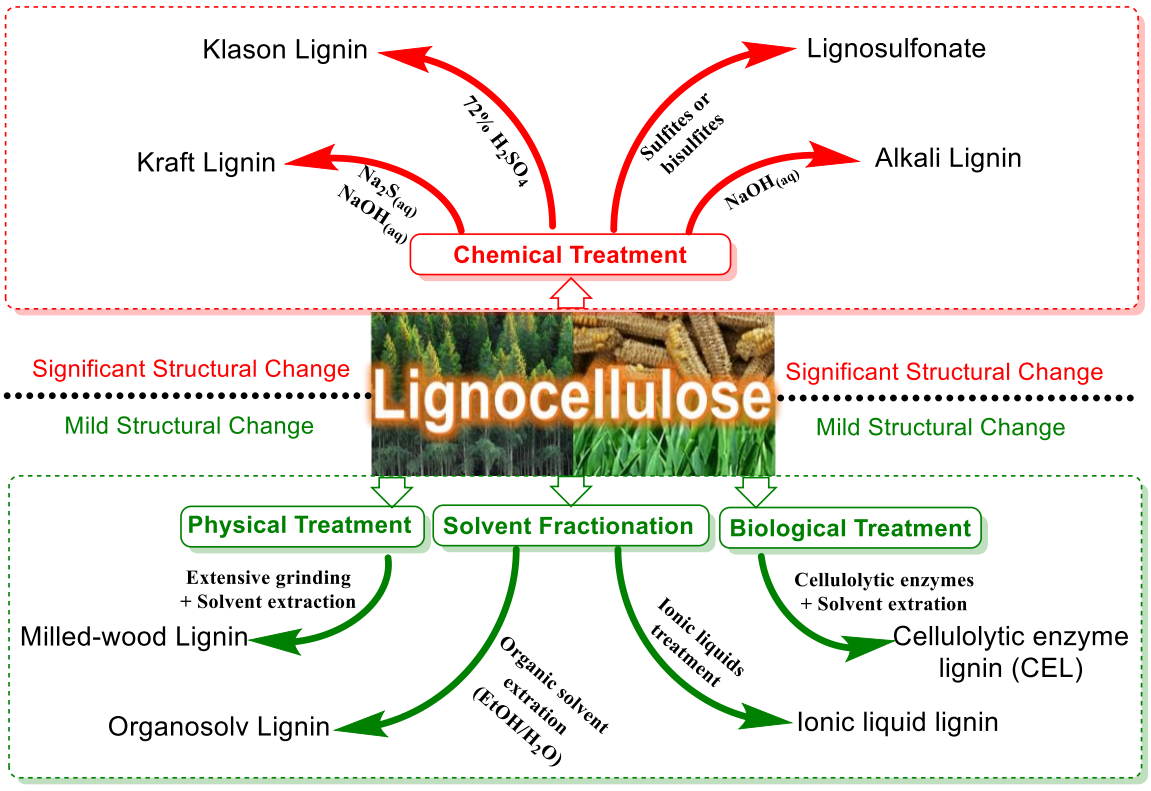

Figure 1.3 A summary of procedures for isolation of lignin from lignocellulose. Adapted with premission from reference[14]. Open access article 2018 American Chemistry Society.

1.2.1 Fractionation methods leading to significant lignin structural changes

The chemical pulping methods such as the Kraft,[17] sulfite,[36] Klason[37] and alkaline[38-40] process (Figure 1.3) usually focus on separating high quality cellulose. The harsh processing conditions due to the employment of inorganic salts, bases, or acids leads to significant structural changes in the lignin.[41] The Kraft pulping approach is the dominate process in current paper industry. The lignocellulose is treated by intensively using aqueous sodium hydroxide (NaOH) and sodium sulfide (NaS) at high temperature (423-453 K) and pH to fractionate the lignin. The pulping process is initiated by nucleophilic attacks on electron-deficient carbonyl structures. Bleaching, on the other hand, used electrophiles to attack electron-rich centers of aromatic nuclei, unsaturated and ring-conjugated side chains. [42, 43] Gierer et al. reported the structural changes of lignin during chemical bleaching in the Kraft pulping process.[42, 43] The 5-5 linkages of lignin are usually reserved due to the highly stable C-C bond. Since Kraft pulping is one of the most dominant processes, considerable developments have been made in infrastructure industrially. The sulfite pulping is another commonly applied method in pulping process to produce water soluble lignosulfonates. Lignosulfonates include about 4-8% sulfur due to the formation of sulfonate groups. The negative effect of the incorporated sulfur during catalytic depolymerisation of lignosulfonate to aromatics should be considered. The Klason process was originally developed to measure lignin content in wood by employing 72% sulfuric acid that significant modified the native lignin structure.[37] The alkaline pulping processes (soda, sulfate, and semi-chemical)[40] show a less structural modification as other chemical pulping processes.[15]

1.2.2 Fractionation methods leading to mild lignin structural changes

The physical, biological treatment, and solvent fractionation (organosolv and ionic liquid treatment) will result in mild structural changes due to their relatively mild processing conditions. The physical treatment to produce milled wood lignin (MWL) comprises of extensive grinding to different mesh sizes followed by organic solvent or water extraction. The widely used solvent system is mixture of dioxane and water. The lignin obtained preserved more native lignin structures since the mild conditions applied in lignin fractionation process. However, in case of hardwoods, the lignin suffer more structural transformations including the formation of new carbonyl and hydroxyl groups.[40] In the biological treatment, cellulolytic enzymes can isolate the lignin, which is called cellulolytic lignin (CEL), from finely ground wood, which result in partial hydrolysis of carbohydrates. The lignin residue is subsequently extracted by solvent (e.g. dioxane/water) and precipitated in water with protein and carbohydrates impurities. This process usually takes several days to process.

The solvent fractionation of lignin includes the commercialized organosolv pulping and recently extensively studied ionic liquids treatment. Organosolv lignin is obtained by treatment of lignocellulose with various organic solvents. The most commonly used solvent is ethanol/water. The main advantage of this process is that it completely separates the major constituents of lignocellulose individually and facilitate the valorization of all components in benign, environmentally friendly conditions. The high purity and less structural changes of organosolv lignin will help the following lignin valorization to chemicals. However, the high cost of recovery of solvent is major hurdle to prevent its application. It is worth mentioning that ionic liquids (IL), molten salts of organic cations

or anions are used as solvents in delignification due to some of their distinct solvent properties.[44-49] Some ILs can efficiently fractionate lignin without significant reduction in cellulose crystallinity.[49] However, limitations persist due to the cost of IL, the product separation from the reaction media, and solvent recyclability. Moreover, ILs can act as reaction media with its catalytic properties for dissolution of lignin and depolymerization to lower molecular weight compounds.[50-52]

1.3 Depolymerization of lignin into chemicals

The concept of lignin as a renewable feedstock to produce aromatic chemicals was raised by Freudenberg in 1929.[53] With increasing number of academic achievements to clarify the structure of lignin, increasing researchers realized the enormous potential of lignin as the resource for chemicals. In the last two decades, the literature on lignin valorization has been multifarious. Several recent reviews provide comprehensive research progresses on the transformation of lignin into value-added chemicals[16, 54], including thermal degradation[55-59], biological degradation[60, 61], oxidation[62], hydrodeoxygenation[63], and ionic liquids [64, 65]. Within so many routes, the novel catalytic methodologies are the most widely studied and can be grouped into seven main strategies (shown in Figure 1.4). This part is not meant to cover all published references on lignin valorization; rather, the major catalytic lignin valorization methods will be shown, including oxidative, reductive depolymerization, highly efficient stabilization-depolymerization, lignin-first biomass fractionation, and electrocatalytic depolymerization.

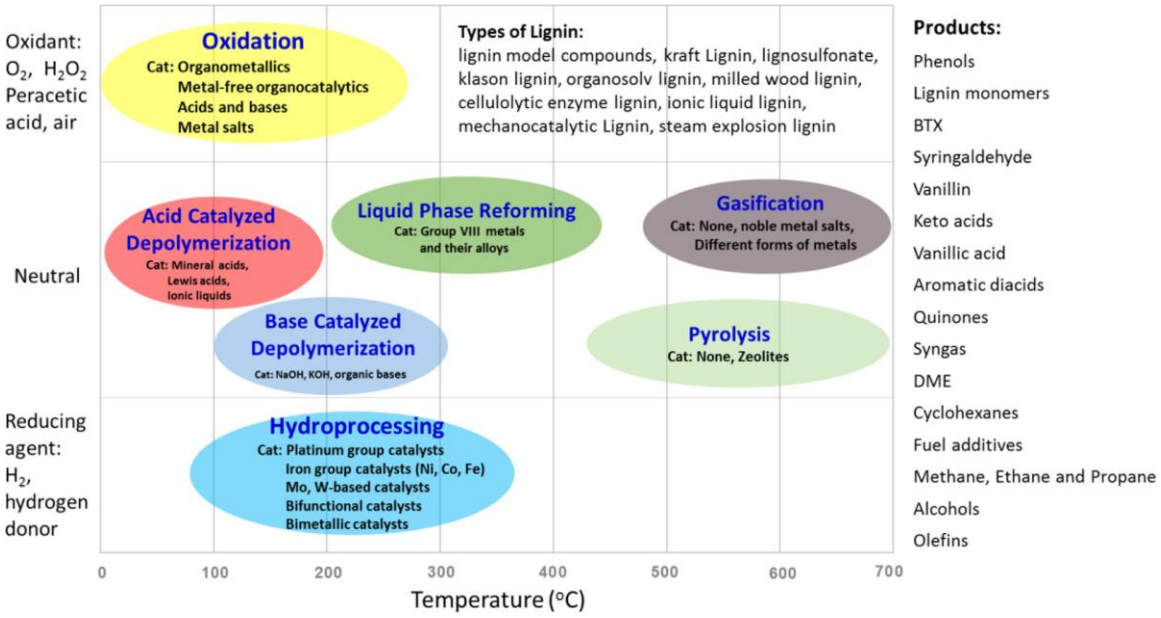

Figure 1.4 Summary of processes for conversion of lignin (Note: the abscissa represents the typical temperature range of the lignin conversion processes). Reprinted with permission from reference [15]. Copyright 2015 American Chemistry Society.

1.3.1 Oxidative depolymerisation

Oxidative depolymerization of lignin is one of the most important and economically feasible valorization strategies since it has been widely used in industry (e.g. papermaking). The oxidative cracking reaction usually aim to cleave the aryl ether bond. Under harsh conditions, the carbon-carbon (C-C) bonds, aromatic rings and other linkages also can be cleaved. Oxygen, hydrogen peroxide, peroxyacids, nitrobenzene, and metal oxides are the most popular oxidants. In a recent review, Li et al. divided the catalytic systems into four categories: metal salts catalysis, acid or base catalysis, metal-free organic catalysis, and organometallic catalysis.[15] Oxidative methods can employ mild reaction conditions, but still runs the risk of over-oxidizing the substrate and aromatic products to gaseous products.

Table 1.3 Strategies and yields of main products established for the oxidative depolymerization of lignins isolated from lignocellulose prior to catalytic treatment.

Oxidative Depolymerization Strategy	Ref.
Lin & Liu (cornstalk lignin) $LaCoO_3$, NaOH, H_2O, 120°C, O_2 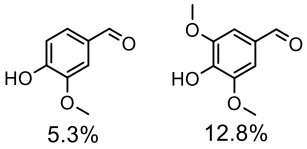 5.3% 12.8%	66
Gu (beech lignin) La/SBA-15, H_2O_2, microwave irradiation 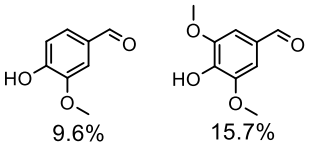 9.6% 15.7%	67
Bösmann & Wasserscheid (beech lignin) $[EMIM][CF_3SO_3]$,$Mn(NO_3)_2$, 100°C, O_2 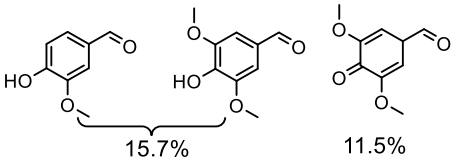 15.7% 11.5%	68
Liu (mixed hardwood lignin) $[mmim][Me_2PO_4]$,$CuSO_4$, 175°C, O_2 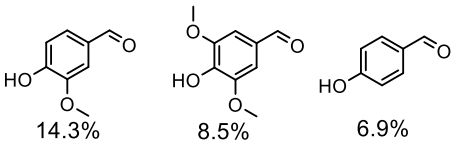 14.3% 8.5% 6.9%	69
Miyafuji (cedar lignin) $Bu_4NOH{\cdot}30H_2O$, 120°C, 2.5h, air  25.7% 1.9%	70

As compared to reductive depolymerization approaches, oxidation methods usually result in more diverse lignin derived aromatic compounds by adding functionalities, which gives more complex obtained products. Depending on the severity of the lignin oxidation,

a set of products from aromatic aldehydes to carboxylic acids are produced, in which vanillin, 4-hydroxybenzaldehyde, syringaldehyde, and muconic acid are major products.[71] In some cases, radicals are formed during oxidation which leads to repolymerization of lignin and decreased product yield. Preferably, oxidation methods under mild conditions result in efficient depolymerization of lignin to fine chemicals without severe condensation and overoxidation. [65, 72, 73] In homogeneous catalytic systems of lignin oxidation, they have several advantages, especially easily to tailor the solubility, activity and stability of catalyst by modifying their electronic and steric properties. Several recent works are summarized in Table 1.3.

1.3.2 Reductive depolymerisation

The reductive depolymerization of lignin has attracted lots of attentions since the reductive deoxygenation of lignin improves the selectivity of aromatics by decreasing the complexity of the reaction mixture.[74] In reductive approaches, the catalyst should selectively break C−O bonds leading to depolymerization to aromatic monomers.[75, 76] A negative effect is that the presence of competing ring hydrogenation reactions can increase the complexity of the products. Some studies developed catalysts that suppressed over-reduction of the obtained aromatic monomer.[77-79] Several outstanding reviews comprehensively summarized the homogeneous and heterogeneous catalyzed reductive depolymerization of lignin and model compounds to visualize the overall adaptability of lignin valorization.[1, 14, 15, 80, 81] Hydrogen gas or hydrogen-donor solvents are usually employed to produce or upgrade bio-oils to fuels in reductive approaches.[82-84] **Error! Not**

a valid bookmark self-reference. highlights some of the recent important studies about the reductive depolymerization of lignin.

Table 1.4 Strategies and yields of main products established for the reductive depolymerization of lignins isolated from lignocellulose prior to catalytic treatment.

Reductive Depolymerization Strategy	Ref.
Anastas (candlenut lignin) Cu-PMO, CH_3OH, 180°C, H_2 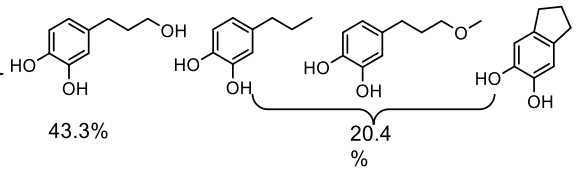 	85
Hartwig (miscanthus giganteus lignin) Pd/C, dioxane, 200°C, H_2 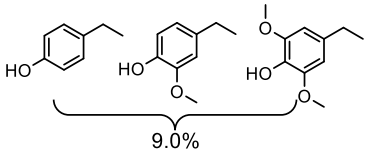 	86
Zeng & Lin (bamboo lignin) H-USY/Raney Ni, H_2O/CH_3OH, 270°C, N_2 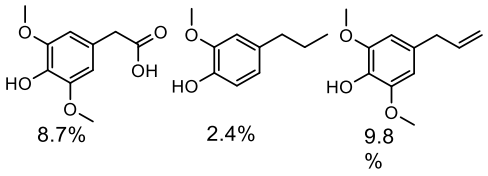 	87
Prechtl & Yan (birch lignin) Ni_7Au_3, NaOH, H_2O, 160°C, H_2 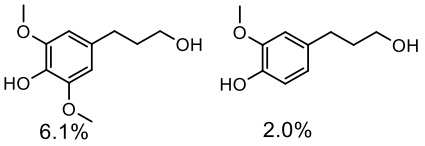 	88
Lu & Xu (beech THFA lignin) Ni/C, THFA/1,4-dioxane, 220°C, H_2 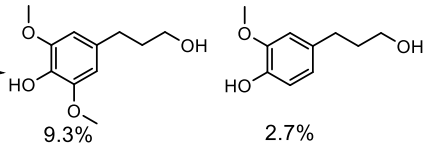 	89
Yang & Wang (birch lignin) Ru/Nb_2O_5, H_2O, 250°C, H_2 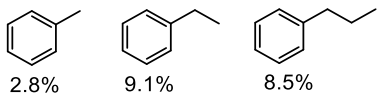 	90

1.3.3 Highly efficient two-step (stabilization-depolymerization) strategy

Recently, several innovative two-step methodologies have been developed to effectively depolymerize lignin by selectively oxidize the secondary alcohol in β-O-4 linkage followed by ether bond cleavage. [2-5] By the calculations of density functional theory (DFT), the bond dissociation enthalpy (BDE) of C_β-O bond in β-O-4 linkage decrease after oxidation of $C_\alpha H{-}OH$ (68.2-71.8 kcal mol^{-1}) to $C_\alpha{=}O$ (55.9-57.1 kcal mol^{-1}) [91] thus making bond more labile (Figure 1.5). The stable $C_\alpha{=}O$ also can prevent the generation the reactive carbonations and further condensation. A feasible strategy to overcome the recalcitrance of lignin is to weaken the $C_\beta{-}O$ in β-O-4 linkage by oxidizing the $C_\alpha H{-}OH$.

As shown in Figure 1.5, successful generation of oxidized β-O-4 ketone and further cleavage to aromatics has been studied by several routes including: (1) acetamido-TEMPO[2, 3] was applied to oxidize Aspen lignin and further depolymerized to 60wt% yield of low-molecular-weight (LMW) aromatics in aqueous formic acid by Stahl's lab[3]; (2) 2,3-dichloro-5,6-dicyano-1,4-benzoquinone (DDQ) was used to oxidize a Birch lignin and then reduced by Zn/NH_4Cl in aqueous solution to 6 wt% phenolic monomers by Westwood's lab;[5] (3) DDQ/ N-hydroxyphthalimide (NHPI)-mediated benzylic oxidation of the ($C_\alpha H{-}OH$) moieties followed by further hydrogenation in a NiMo sulfide catalysis process resulting in the cleavage of ether bonds to aromatic monomers by Wang's lab.[4]

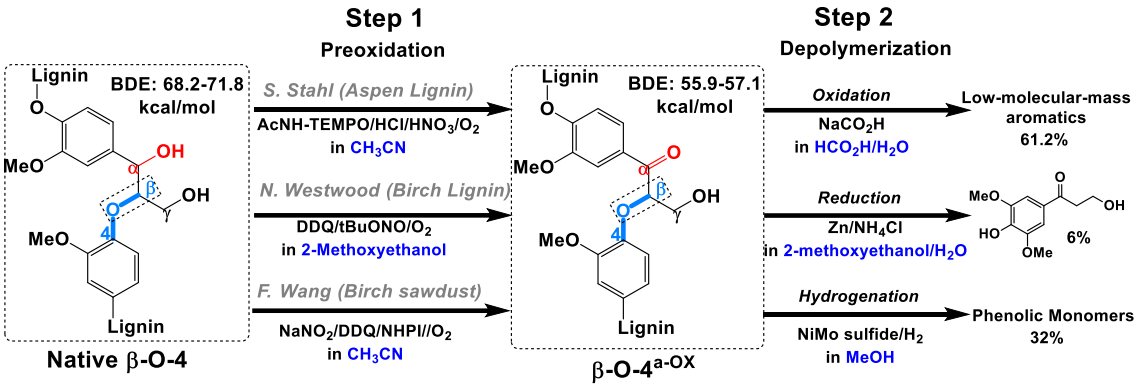

Figure 1.5 Previous studies to depolymerize lignin by benzylic oxidation methods to lower C–O-aryl ether bond dissociation enthalpies (BDEs) in the β–O–4 units (preoxidation step) and further facilitate subsequent cleavages (depolymerization step).[2-5]

1.3.4 Lignin-first biomass fractionation and deployerization

In traditional lignocellulosic biorefineries, the ultimate objective is to isolate valuable products from the carbohydrate fractions, especially from cellulose. The lignin is fractionated by harsh processing conditions (e.g., Kraft pulping) in industrial delignification process to avoid lignin residual in carbohydrate. However, the lignin endures irreversible condensation and degradation in such severe environment, resulting in ineffective depolymerization. The efficient utilization of all components of lignocellulose is a visible long-term opportunity. Exploiting this potential requires fundamentally innovative biorefinery processes and new catalytic methods that can deal with the structural complexity of lignocellulose and create value from all its major components.[6, 92] All of three major components in lignocellulose should be considered as primary targets to maximize both economic and ecologic incentives.

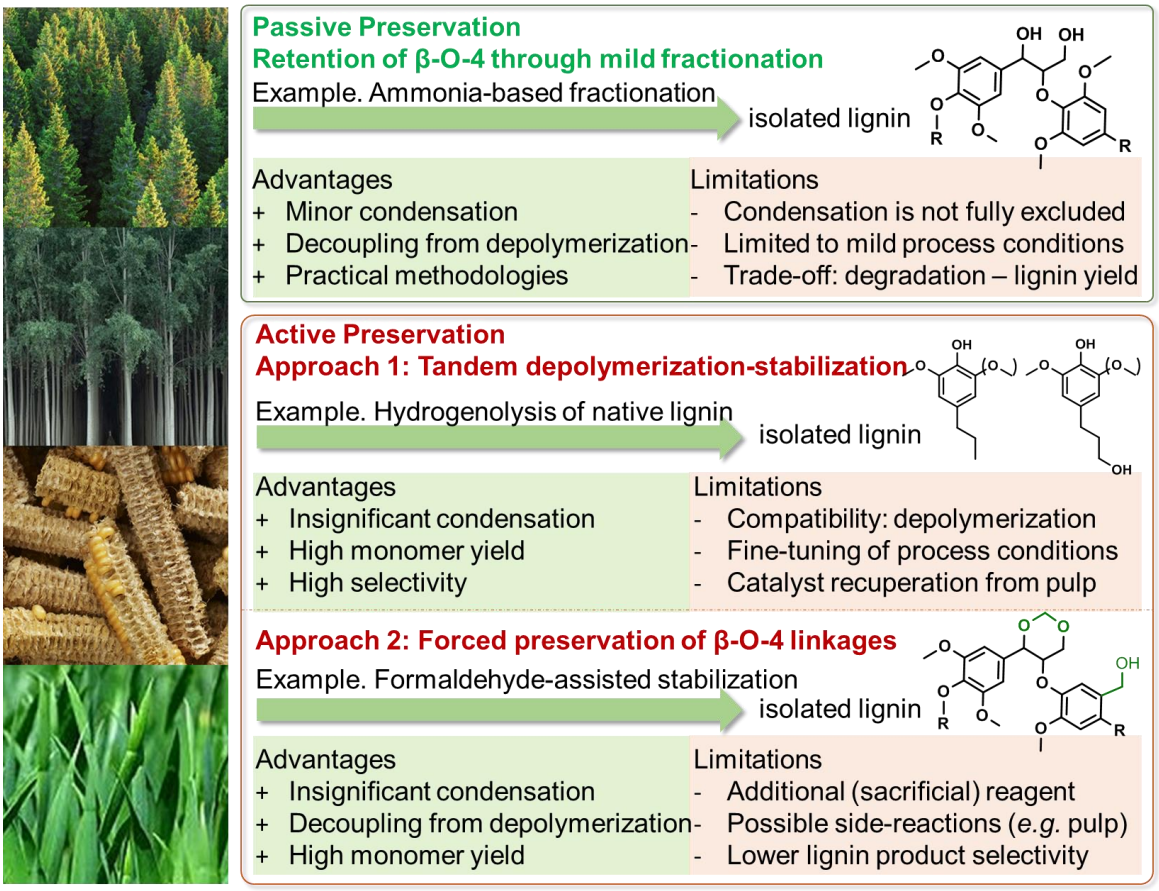

Figure 1.6 Schematic overview of passive β-O-4 preservation, active preservation (by approach 1: tandem depolymerization-stabilization; and approach 2: forced preservation of β-O-4 linkages) during biomass fractionation, displaying their main advantages and limitations. Adapted with premission from reference [6]. Copyright 2017 Royal Society of Chemistry.

Recently, some new lignin-first biomass fractionation concepts are emerging that subdue lignin condensation or degradation by employing mild operating conditions or active stabilization during biomass fractionation.[6] This new concept intentionally puts lignin valorization at the front stage of the biorefinery, which is feasible due to the rigid semi-crystalline structure of cellulose that is more resistant for degradation. Therefore, the cellulose can be valorized in a later stage.

One innovative strategy is implementation of alternative media (e.g., ammonia[93-96], ionic liquid[64, 97, 98], γ-valerolacetone[99, 100]) that uphold biomass decomposition under mild processing conditions[101-103] which lead to preserve more ether bonds and suppress the condensation and further facilitate the down-stream lignin depolymerization to low molecular weight chemicals (Figure 1.6). However, the milder condition for high ether bonds resulted in lower isolated lignin yield and *vice versa*.[104]

Another well-studied strategy is the catalytic hydrogenolysis of native lignin in lignocellulosic matrix is also extensively studied, in which lignin is extracted by solvolysis and then instantly depolymerized or reductively stabilized (shown in Figure 1.7). [105-114] This approach can produce depolymerized lignin oil with several monomers in high yields and some dimers and oligomers. The carbohydrates without lignin are ready for further treatment by traditional processes (e.g. enzymatic hydrolysis). A key challenge is how to balance the lignin removal from lignocellulose and conservation of carbohydrate in the pulp. Moreover, to separate the solid catalyst from the remining carbohydrate is an intrinsic challenge for heterogeneous catalysis. Luterbacher *et al*. unveiled another new fractionation strategy that applied formaldehyde to form relatively stable acetals with α- and γ-OH side-chain groups in β-O-4 linkages as well as to partially block reactive *meta*-groups by hydroxymethylation, which in turn suppress the formation of extra C-C bonds[115]. The separated lignin fractionation and the subsequent lignin depolymerization step enables more flexible lignin depolymerzation methods and independent optimization of the two steps. The sacrificial reagent, relatively harsh conditions, and organic solvents are necessary for this approach.[6]

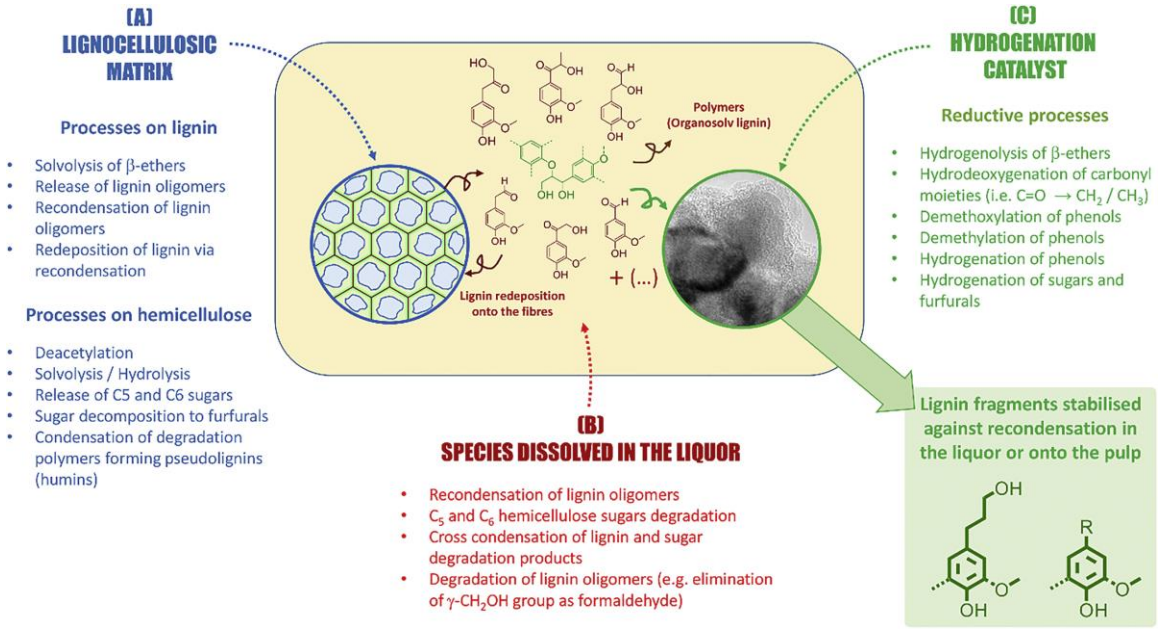

Figure 1.7 Schematic representation of chemical processes involved in the lignin-first biorefining via early-stage catalytic conversion of lignin. Reprinted with premission from reference [116]. Copyright 2017 Elsevier.

1.3.5 Electrocatalytic depolymerization

As previously introduced, thermal catalysis processes usually are employed at relatively high temperatures and pressures. However, catalyst recovery and aging under harsh conditions are often serious technical obstacles to achieve a practical, cost-effective process. Conversely, electrochemical depolymerization is a potential approach for highly sustainable conversion with electrons serving as the reagent. Therefore, the conversions can be considered as low cost, reagent free, environmentally friendly method, and can be performed at mild process conditions.

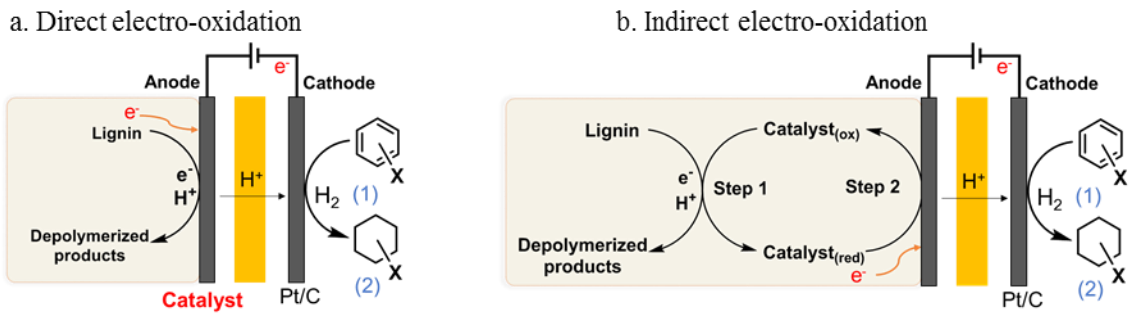

Figure 1.8 Schematic illustration of the electro-oxidation of lignin. a. Direct electro-oxidation of lignin with heterogeneous catalysts immobilized on the electrode surface. b. Indirect electro-oxidation of lignin with homogeneous catalysts as oxidants. The proton and electron can be used for (1) H_2 evolution or (2) hydrogenation of lignin oil at cathode.

There are two primary electro-oxidation strategies, namely indirect and direct. These chemistries are both conducted at the anode for lignin depolymerization (Figure 1.8). In direct electro-oxidation**,** a heterogeneous catalyst (Ni [117-121], PbO_2 [122, 123], RuO_2 [124, 125] etc.) is immobilized on the surface of the electrode, and the catalytic depolymerization process and electrolysis happen simultaneously on the electrode. The electrochemical processes are limited by surface catalysis [120], so the solubility of lignin, proton/electron conducting, and electrochemical stability of the electrolyte become key problems. Indirect electro-oxidation of lignin uses homogeneous catalysts (e.g. N-hydroxyphthalimide (NHPI)[126, 127]) as an oxidant and electron and/or proton reservoir [7, 128]. The catalyst is reduced when it oxidizes the lignin to products, and then is regenerated at the anode under an applied potential (Figure 1.8b). For this process, the lignin can be present as a slurry in the electrolyte reacts with the catalyst away from the anode. However, there are two key challenges for this process. One is the relatively harsh conditions for the reaction between lignin and catalyst. Second is the difficult separation of products from catalysts.

1.4 Polyoxometalate for the transformation of lignocellulose and lignin

1.4.1 POMs structure and properties

Polyoxometalates (POMs) are a class of a polyatomic ion with more than three transition metal oxyanions combined to form a closed 3-D framework. The most common structure of POMs are the Keggin, Dawson, and Anderson structures (Figure 1.9). The POM with Keggin structure (Figure 1.9a) is most widely used. It is approximately spherical shape with tetrahedral symmetry. POMs are promising catalysts due to some distinct properties. First, the high reactivity to oxidative degradation makes them a good electron reservoir. Second, the solubility can be tailored by the counter-cation type which is important for the liquid phase catalysis reaction. Thirdly, the redox properties also can be modified by changing the substituting metals or its structure. [129] Moreover, some POMs can be re-oxidized by oxygen or electrolysis indicating that POM can be a recycled catalyst.

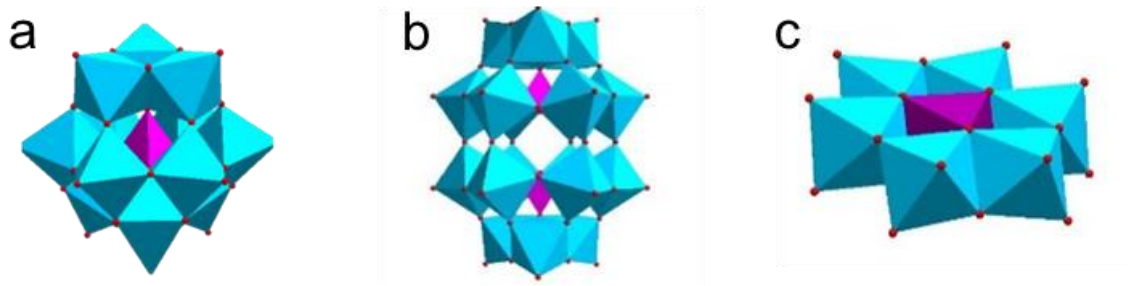

Figure 1.9 Structures of typical POMs: (a) Keggin structure, $XM_{12}O_{40}^{n-}$; (b) Dawson structure, $X_2M_{18}O_{62}^{n-}$; (c) Anderson structure, $XM_6O_{24}^{n-}$.

1.4.2 POMs for delignification and lignin depolymerization

POMs can be a potential oxidative catalyst for lignin depolymerization. If we consider the oxygen as the oxidant to reoxidize the POMs, there are two steps for the lignin oxidative degradation.

$$POM_{(ox)} + \text{lignin} \rightarrow POM_{(red)} + \text{lignin}_{(ox)} \quad (1.1)$$

$$POM_{(red)} + (m/4)O_2 + mH^+ \rightarrow POM_{(ox)} + (m/2)H_2O \quad (1.2)$$

in which $POM_{(ox)}$ and $POM_{(red)}$ are the oxidized and reduced POM, respectively. $\text{Lignin}_{(ox)}$ denotes the products from lignin oxidation, including both polymeric or low molecular weight products.

The thermodynamic conditions required for this achievement are as follows:

$$E(\text{lignin}) < E(\text{POM}) < E(O_2) = 1.22 - 0.059\ \text{pH} \quad (1.3)$$

Then, the POM can oxidize the lignin and it can be reoxidized by oxygen. Considering the different structure units of the lignin, the oxidation of phenolic units can happen at potential between 0.6 to 0.8 V and non-phenolic units can happen at around 1.0 V (vs. NHE at pH = 2).[130] Meanwhile, the redox potential of O_2/H_2O is 1.22V (vs. NHE at pH = 0). Thus, if the redox potential of POMs in the range of 0.6 - 1.2V, it can serve as potential catalyst with oxygen in lignin depolymerization.

POMs have been studied as a promising alternative for lignocellulosic pulp delignification processes to replace the environmental unfriendly chlorine-based reagents.[35] In these studies, a series of POMs show the ability to selectively breakdown the

residual lignin with oxygen and possibly fully convert the lignin.[131-133] The POMs were developed for lignin degradation rather than cellulose during pulping process, and finally leave a lignin free white pulp.

Using the POMs to selectively oxidize lignin into chemicals has also been reported.[134, 135] In the study of Voitl et al., $H_3PMo_{12}O_{40}$ was used to oxidize Kraft lignin from spruce wood to produce vanillin and other aromatics.[134] Zhao et al. performed a similar study using another POM, $H_5PMo_{10}V_2O_{40}$, to produce aromatics and tried to optimize the conditions (temperature, time, and catalyst concentration, etc.).[135] Gaspar et al. studied the delignification process catalyzed by Mn(II)-substituted molybdovanadophosphate polyanion, where several aromatics were also detected in the products solution.[136]

To degrade lignin into small molecular-weight chemicals, cleavage of the interunit linkages including the carbon-carbon (C-C) and carbon-oxygen (C-O) bonds is required. In the research of Weinstock et al., this cleavage is achieved by using POM to oxidize a lignin β-O-4 model compound (Figure 1.10).[131]

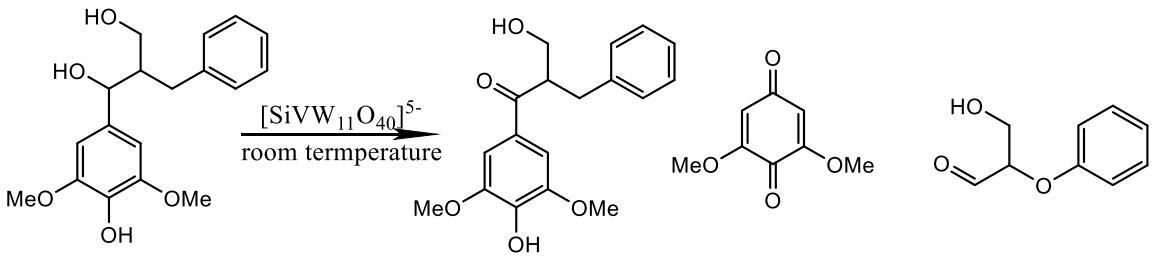

Figure 1.10 Products of the reaction of on excess of $[SiVW_{11}O_{40}]^{5-}$ with β-O-4 model compounds. [131]

The reaction mechanism is a fundamental aspect as in explaining the intermediates involved and the formation of products. Weinstock et al. conducted a study on the β-O-4 model compound of lignin with POM ($[AlVWO_{40}]^{-6}$) and showed its partial oxidation (Figure 1.11),[137] which inspired me to use POM selectively oxidize C_α-OH in β-O-4 moieties to suppress condensation in the following depolymerization process.

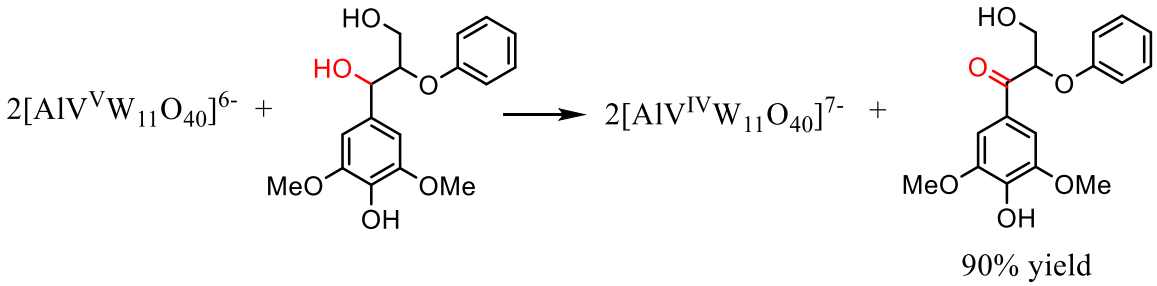

Figure 1.11 β-O-4 model compound of lignin partial oxidation by POM ($[AlVW_{11}O_{40}]^{-6}$). Adapted with permission from reference [137]. Copyright 2001 Nature.

Besides the mechanism, the kinetic studies of lignin (model compounds) oxidation by POMs helped us further understand the chemistry in lignin oxidation and optimization of process operation. Yokoyama et al. revealed that the reaction between non-phenolic model compounds and POMs has a kinetic isotope effect. The results indicated that the oxidation of benzylic hydrogen is the rate-determining step in POM oxidation of non-phenolic lignin model compounds. [138, 139]

1.5 Problem analysis and objectives

1.5.1 Problem statement

Lignin is a promising renewable aromatic chemicals resource due to its rich aromatic structure and huge production volume. Developing techniques to produce aromatics from lignin is not only urgent and challenging, but also a visible long-term opportunity. As indicated in literature review, numerous efforts have focused on depolymerizing the lignin to small molecules as bio-fuel or bio-chemicals. The abundant ether bonds (β-O-4, α-O-4, 4-O-5), especially the β-O-4 aryl linkage, are the major targets for cleaving during lignin depolymerization. Acid/base catalyzed/hydrolysis, pyrolysis, reduction, chemical oxidation, and biodegradation have been used to cleave these lignin linkages. However, most of the reported methods have some inevitable limitations such as high reaction temperature, high hydrogen pressure, safety concerns, or low products yield. There is still no efficient way to depolymerize lignin, especially from current industrial processes.

1.5.2 Problem analysis

There are three major concerns for effective lignin valorization. First, the condensation of the lignin fragments during depolymerization process increases the recalcitrance of the lignin and limits product yields. Second, the intensive use of acid or alkali results in the variation of the lignin structure and lignin condensation during lignin fractionation. This can reduce the amount of ether bonds and suppresses depolymerization of the isolated lignin in subsequent processes. Third, current studies only focus on the production of chemicals from lignin but ignore the possibilities to make extra value.

1.5.3 Hypothesis

To respond these three concerns, my PhD study focused on the following three parts, (1) suppress lignin condensation by selective oxidation of active benzyl alcohol to facilitate lignin depolymerization; (2) fractionate lignin from biomass for *in situ* depolymerization to prevent lignin condensation towards complete biomass valorization; and (3) combine lignin depolymerization to chemicals and hydrogen evolution together in one novel electrolysis process to maximize lignin valorization.

1.5.4 Objectives

Objective 1. Effective lignin depolymerization by blocking active benzyl alcohols

The key to suppressing condensation of lignin fragments during depolymerization is to block or modify the active α-OH in β-O-4 from forming the active C_α^+, which can react to form additional C-C linkages. My study will employ a preoxidation step before depolymerization. In the preoxidation process, the secondary benzylic alcohol (C_α-OH) in the lignin structure is oxidized to a ketone (C_α=O) at a low temperature. Then the stabilized lignin can be further depolymerized via oxidative cleavage to aromatic chemicals at an elevated temperature.

Objective 2. Lignin-first biomass fractionation towards complete biomass valorization

Besides the condensation during lignin depolymerization, the recalcitrant condensed lignin structure that is formed during biomass fractionation is another barrier for further lignin depolymerization. In this part, the POM catalyst will be employed to extract lignin from wood sawdust directly, while avoiding structural lignin condensation.

Then the extracted lignin will be further oxidized to small aromatic molecules, and the remaining cellulose can be further used to produce paper, bio-ethanol or chemicals for complete biomass valorization.

Objective 3. Electrolysis for simultaneously H_2 evolution and lignin depolymerization

The last part of my study will focus on developing a novel electrolysis process to combine lignin depolymerization and hydrogen evolution together, instead of only focusing on the production of aromatics, as in many current studies.

All the approaches used in this dissertation are summarized in Figure 1.12.

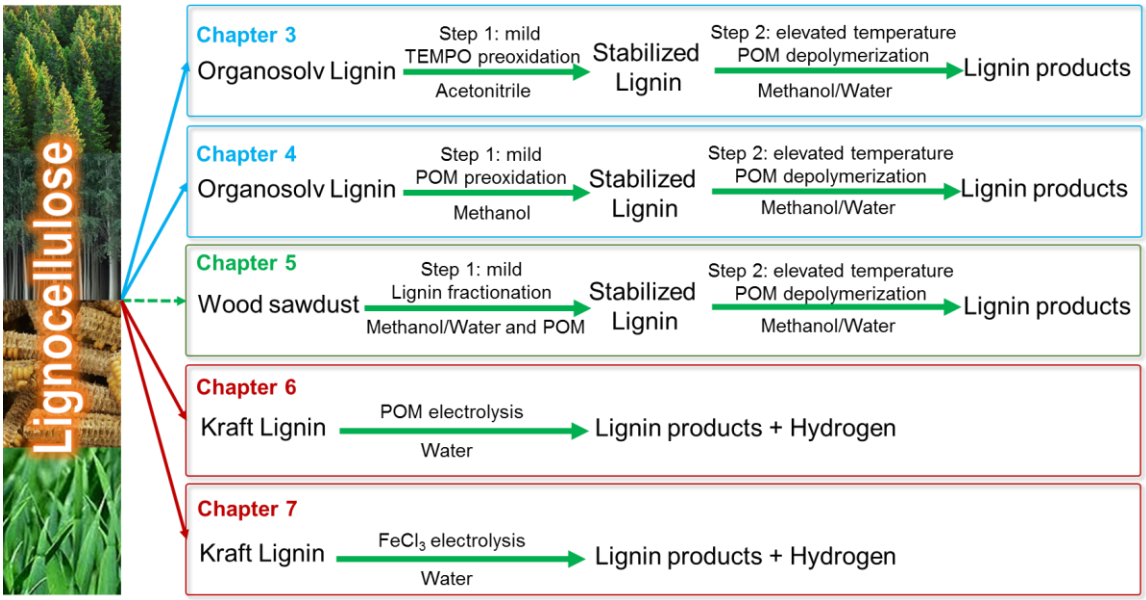

Figure 1.12 The overall approaches used in this dissertation.

CHAPTER 2. EXPERIMENTAL MATERIALS AND PROCEDURES

2.1 Materials

2.1.1 Chemicals

All chemicals and solvents used in this study were purchased from VWR International, Sigma-Aldrich (St. Louis, MO) or Tokyo Chemical Industry (TCI America) and used as received. All gases were purchased from Airgas. (South region, Atlanta, GA).

2.1.2 Lignin

The Kraft lignin (KLignin) was isolated from the black liquor in a commercial softwood (pine) Kraft pulping process by Domtar. Ethanol organosolv lignin (ELignin) was isolated from hardwood a commercial organosolv lignin process by American Process (ELignin). The feedstock is mixed northern hardwood that primarily is maple and aspen. Supercritical water extracted lignin (RLignin) was isolated from hardwood (birch) by Renmatix. The novel supercritical water instead of organic solvent was employed to deconstruct cellulose and lignin streams in its two-stage Plantrose Process. Alkline lignin (AL) and sulfonated lignin (SL) was purchased from Sigma Aldrich.

2.1.3 Biomass

Wood chips used in this study were acquired from a poplar, birch or loblolly pine tree from Georgia, USA. The wood chips were refined by a Wiley mill through a 0.13 cm screen and oven dried at 50 °C for 48 h.

2.2 Procedure of experiments

2.2.1 Lignin model compounds synthesis

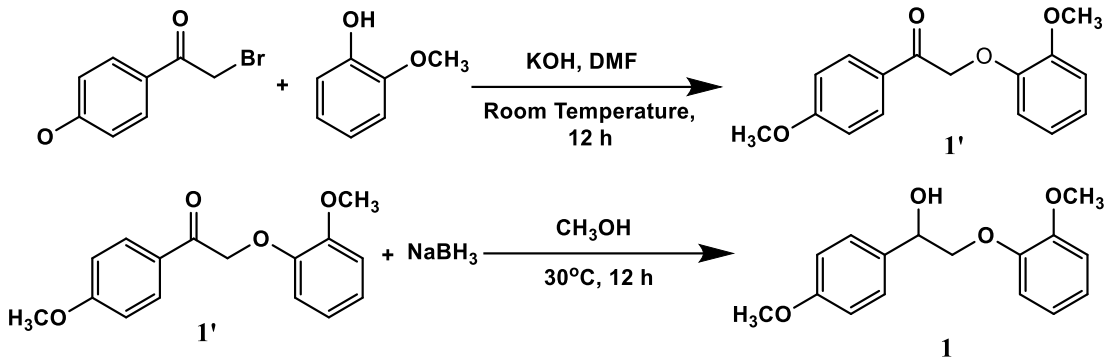

Figure 2.1 Synthesis of 2-(2-methoxyphenoxy)-1-(4-methoxyphenyl) ethanone (β-O-4 dimer 1)

To synthesize 2-(2-methoxyphenoxy)-1-(4-methoxyphenyl) ethanone (dimer **1′**), 2-Bromo-4'-methoxyacetophenone, Guaiacol (1.1 g) and potassium hydroxide (0.5 g) were dissolved in 35 mL of DMF (dimethylformamide) and stirred at room temperature for 12 h. After reaction, the reaction mixture was poured into water and extracted with 2V ethyl ether for 3 times. After drying of ethyl ether phase with sodium sulfate, 2-(2-methoxyphenoxy)-1-(4-methoxyphenyl) ethanone was recrystallized from ethanol. Then the products were analyzed by GC-MS and ^{1}H-NMR.

To synthesize 2-(2-methoxyphenoxy)-1-(4-methoxyphenyl) ethanol (dimer **1**), a solution of 2-(2-methoxyphenoxy)-1-(4-methoxyphenyl) ethanone（0.49 g) in methanol (20 mL) was treated with sodium borohydride (0.07 g) and stirred 12 h. A saturated solution of ammonium sulphate (20 mL) followed by chloroform (20 mL) was added to the reaction

mixture. The organic layer was separated, and washed with water for three times. Organic phase was dried with sodium sulfate, then removing organic solvent via rotary evaporators to obtain residual products. Finally, the residual products were recrystallized from ethanol to obtain pure 2-(2-methoxyphenoxy)-1-(4-methoxyphenyl) ethanol (β-O-4 dimer **1**). Then the products were analyzed by GC-MS and ^{1}H-NMR (Figure 2.2).

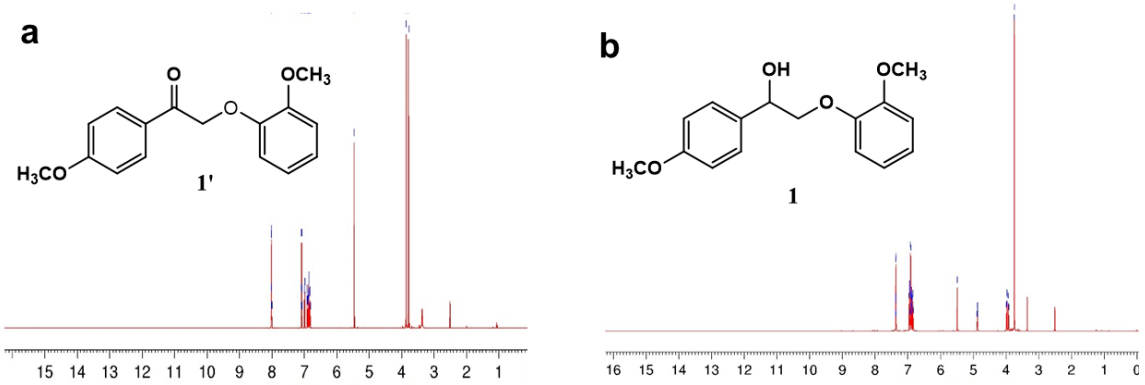

Figure 2.2 ^{1}H-NMR pattern of the dimers. **a.** 2-(2-methoxyphenoxy)-1-(4-methoxyphenyl) ethanone (β-O-4 dimer **1'**): ^{1}H-NMR (700 MHz, DMSO-d) δ = 8.03-7.99 (m, 2H), 7.09-6.81 (m, 6H), 5.45 (s, 2H), 3.86 (s, 3H), 3.78 (s, 3H). **b.** 2-(2-methoxyphenoxy)-1-(4-methoxyphenyl) ethanol (β-O-4 dimer **1**): ^{1}H-NMR (700 MHz, DMSO-d) δ = 7.37 (t, 2H), 7.37-6.84 (m, 6H), 5.49 (t, 1H), 4.87 (dd, 1H), 3.95 (ddd, 2H), 3.74 (t, 6H).

2.2.2 Procedure of thermal catalytic reactions of (modified) lignin with POM.

Lignin or modified lignin with solution was placed in a 100 ml Parr reactor. O_2 (or other gases) was flushed three times to remove air in the reaction system. Then, the reactor was pressurized with O_2 (or other gases), heated to determined temperature under stirring of, and maintained for different reaction times. After the reaction, the vessel was immediately cooled to room temperature by immersing in cold water. Gases in the reactor were exhausted to an inverted container vessel filled with water to determine the volume

and collected for GC analysis. The yield was calculated by effective carbon. The solid was filtered by qualitative filter paper, and washed with solvent. The solid was dried and weighed.

2.2.3 Procedure of lignin oxidation with POM/$FeCl_3$ for electrolysis process

POM and lignin (or other biomass) were added in deionized (DI) water in a conical flask to react under mild conditions (e.g. 100°C heating under N_2 protection). Electromagnetic stirring was used to obtain a homogeneous system. After reaction, the gas was collected by purging nitrogen. The solid lignin (or other biomass) residual was filtered by 40 μm filter paper, and then drying it under 80°C after washed by pure water. The liquid samples were diluted to 1 or 10 mmol/L for ultraviolet-visible (UV-Vis) absorbance determination at 700 nm by spectrophotometer (Agilent 8453). The absorbance of reduced PMo_{12} at the wavelength of 700 is linearly related to the reduction degree, so a linear reference curve for determine reducing degree of POM was obtained (Figure 2.3a).[140]

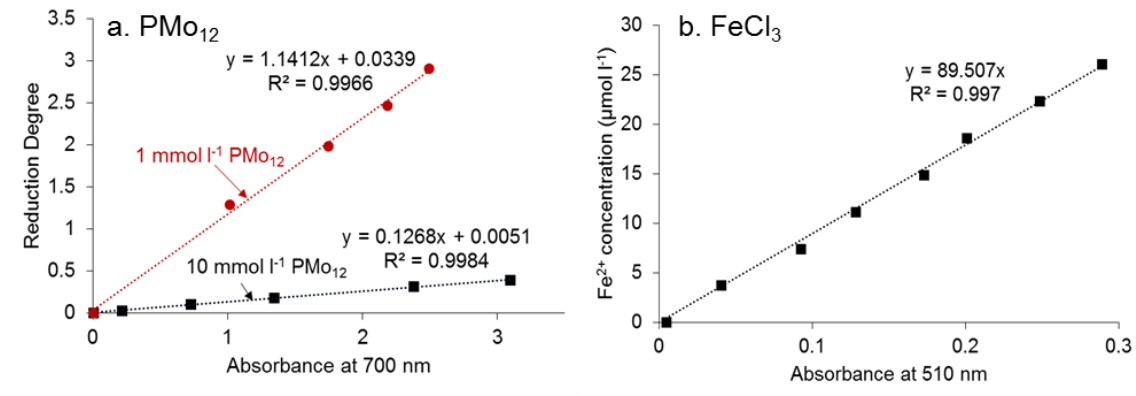

Figure 2.3 **a.** Calibration curve for 1 mmol/L (red) and 10 mmol/L (black) PMo_{12} solution with different reduction degrees at wavelength at 700 nm. **b.** Calibration curve for different concentration (in ppm) of Fe^{2+} solution at wavelength at 510 nm

Similarly, $FeCl_3$ and lignin were reacted in DI water in a homogenous system under mild at different temperatures and reaction times. The amount of soluble iron (II) in the solution was determined by reacting Fe^{2+} with 1, 10-phenanthroline to convert the solution to an intensively colored iron-complex that has a large absorb peak for 510 nm wavelength light. The UV-Vis spectrophotometer (Agilent 8453) was used to measure the absorbance. A different concentration of standards was used to obtain standard curve (Figure 2.3b).

2.2.4 Assembly of electrolysis cell and test methods

The bipolar plates of the electrolysis cell (Figure 2.4) were made of high-density graphite plates with a serpentine flow channel 2 mm wide, 5 mm deep, and 5 cm long (total geometry projected area of 1 cm^2). The graphite felt was purchased from Alfa Aesar, and was pretreated with concentrated sulphuric and nitric acids in a 3:1 volumetric ratio at 50 °C for 30 min. Then the graphite felt was washed with DI water until the pH of the wash became neutral, dried at 80 °C and cut to pieces with 2 mm width and 10 mm thick. These graphite electrodes were filled into the channel of anode plant. Nafion® 115 (127 micrometers thick, purchased from DuPont™) was used as proton exchange membrane in this direct biomass fuel cell. The membrane was pretreated in the boiling solution of 1 mol/L H_2SO_4 (Aldrich) and 3% H_2O_2 (Aldrich) for 30 min, then was washed and soaked in DI water.

The Nafion membrane was sandwiched between two graphite flow-field plates. The graphite-felts were filled into the channel of anode plant. A 5-layer gas diffusion electrode (FuelcellsEtc, US) was used as cathode electrode. The anode and cathode graphite flow-field plates were clamped between two acrylic plastic end plates. PTFE gaskets were included on the circumference of the graphite flow-field plates to prevent any leakage. PTFE tubing was used to connect the fuel cell and a pump that can transport electrolyte solutions into and out of the electrode cell.

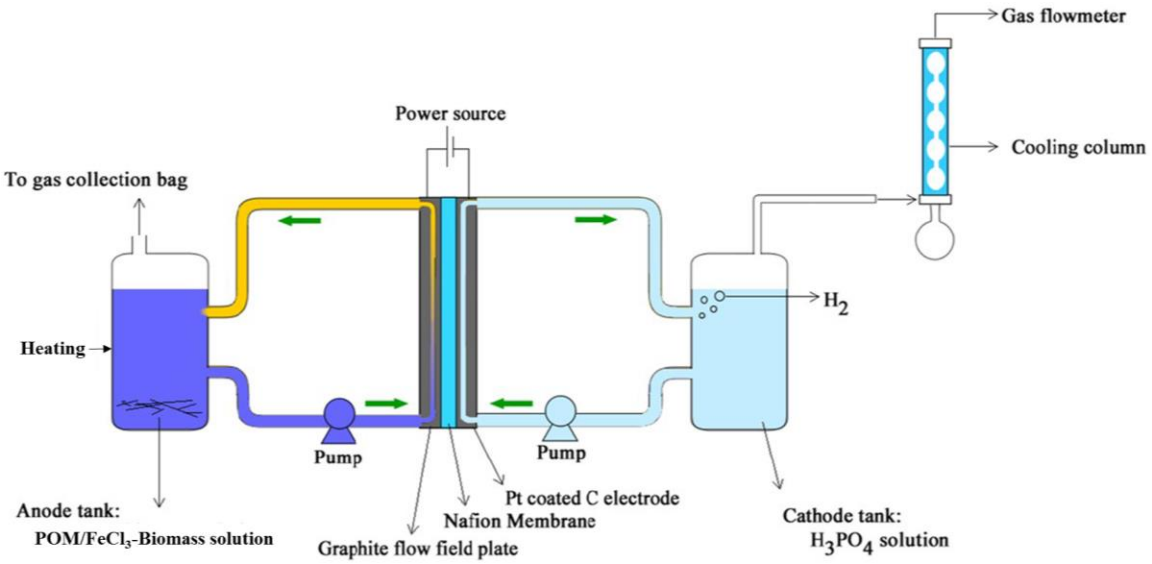

Figure 2.4 Experimental set-up for the study of direct biomass electrolysis in a proton exchange membrane (PEM) electrolysis cell. Reprinted with permission from reference[128]. Copyright 2016 Royal Society of Chemistry.

In the electrolysis experiments, obtained biomass-PMo_{12} or $FeCl_3$ solution (as shown in section 2.2.3) was stored in anode tank and H_3PO_4 solution (1 mol/L) was stored in cathode tank then pumped through the anode and cathode cell respectively. The temperature of the liquid in the cell was set at desired temperature. A Versa Stat 3 electrochemical working station (Princeton Applied Research) was used to examine the IV curves using the controlled potentiostatic method. The hydrogen evolution was conducted in a continuous test at constant-current densities of 100 mA cm^{-2}. In order to measure the produced hydrogen gas, the outlets of cathode cell passed through a cooling column (0°C) in order to separate water vapor and hydrogen. The rate of hydrogen production was followed by gas-volume measurements. Gas products from both anode and cathode were collected and analyzed by gas chromatograph (Agilent 490 micro-GC).

2.3 Procedures of characterization of lignin or lignin products

2.3.1 Characterization of lignin by NMR (^{1}H, HSQC and ^{31}P NMR)

All liquid NMR spectra data reported in my thesis were recorded with a Bruker BioSpin (Billerica, MA, USA) AVANCE 700MHz instrument equipped with a cryogenically cooled 5-mm triple-resonance $^{1}H/^{13}C/^{15}N$ TXI gradient probe with inverse geometry (^{1}H coils closest to the sample). All the NMR data processing and plots were carried out using MestReNova v11.0 software's default processing template (zero-filling is 32 K) and automatic phase and baseline correction.

2.3.1.1 ^{1}H-NMR

Quantitative ^{1}H-NMR was acquired with 32 transients and 1s pulse delay by employing a standard Bruker pulse sequence "zg" at room temperature.

2.3.1.2 HSQC-NMR

Phase-sensitive 2D $^{1}H–^{13}C$ HSQC spectra were performed with spectra widths of 12 ppm for ^{1}H (the acquisition time is 100 ms) and 220 ppm for ^{13}C with 620 increments (acquisition time is 8 ms) of 100 scans with a 500 ms interscan delay, 1K data points, 256 t_1 increments, and 64 transients. An adiabatic version of the HSQC experiment was used for all samples (hsqcetgpsisp.2.2 pulse sequence from the Bruker Library; phase-sensitive gradient-edited 2D HSQC using adiabatic pulses for inversion and refocusing).[141] Processing used typical matched Gaussian apodization in the ^{1}H dimension and squared cosine-bell apodization in the ^{13}C dimension. The volume integration of contours used

Bruker's Topspin 3.5 (Windows version) software, and was carried out on data that were not subjected to linear prediction.

Table 2.1 Assignments of the lignin $^{1}H–^{13}C$ correlation peaks in the 2D–HSQC spectra

Label	δC/δ H (ppm)	assignment
B_β	53.2/3.57	$C_\beta–H_\beta$ in phenylcoumaran substructures (B)
C_β	53.4/3.03	$C_\beta–H_\beta$ in β–β′ resinol substructures (C)
$-OCH_3$	55.3/3.67	C–H in methoxyls
A_γ	60.0/3.69 and 60.8/3.59	$C_\gamma–H_\gamma$ in γ-hydroxylated β-O-4′ substructures (A)
$X1_\gamma$	61.5/4.17	$C_\gamma–H_\gamma$ in cinnamyl alcohol end-groups (X1)
B_γ	62.8/3.74	$C_\gamma–H_\gamma$ in phenylcoumaran substructures (B)
C_γ	70.9/4.15	$C_\gamma–H_\gamma$ in β–β′ resinol substructures (C)
$A_{\alpha(S)}$	71.9/4.97	$C_\alpha–H_\alpha$ in β-O-4′ substructures (A) linked to a S-unit
$A_{\beta(H/G)}$	83.6/4.38	$C_\beta–H_\beta$ in β-O-4′ substructures (A) linked to a H-unit and G- unit
C_α	84.9/4.66	$C_\alpha–H_\alpha$ in β–β′ resinol substructures (C)
B_α	86.9/5.55	$C_\alpha–H_\alpha$ in phenylcoumaran substructures (B)

2.3.1.3 Quantitative ^{31}P-NMR

The contents of hydroxyl group in lignin were determined by qualitative Phosphorus-31 (^{31}P) as reported by Ben et al.[142] Typically, lignin samples (~10mg) were dissolved in 500μL of the mixture of pyridine/$CDCl_3$ (1.6:1, v/v) with chromium acetylacetonate (1.75mg) as relaxation agent and endo-N-hydroxy-5-norbornene-2,3-dicarboximide (NHND) (1.98mg) as internal standard. 100 μL of 2-chloro-4,4,5,5-

tetramethyl-1,3,2- dioxaphospholane (TMDP) was injected to react with lignin. The spectra were obtained by a Bruker Avance/DMX 400MHz NMR spectrometer with an inverse gated decoupling pulse sequence, 90^{o} pulse angle, 25s pulse delay, and 128 scans. The contents of hydroxyl group in different chemical environments were determined through their relative areas to the internal standard.

Table 2.2 Assignment of the ^{31}P NMR peaks for lignin

Chemical shift (ppm)	Assignment
150.0 – 145.5	Aliphatic OH
144.70 – 142.92	β-5
142.92 – 141.70	4-O-5
141.70 – 140.20	5-5
140.20 – 138.81	Guaiacyl
138.81 – 138.18	Catechol
138.18 – 137.30	*p*-hydroxyl-phenyl
136.60 – 133.60	Acid OH

2.3.2 Characterization of lignin and lignin oil by GPC

Before GPC was carried out, lignin samples were acetobrominated according to a slightly modified published procedure to facilitate complete dissolution in the chromatography solvent, tetrahydrofuran (THF). The dried lignin (10 mg) were dissolved in a 9:1 (v/v) glacial acetic acid/acetic bromide mixture (2.50 mL) and stirred at 50°C for two hours. The samples were then dried under vacuum at 40°C. The acetobrominated lignin

were then dissolved in THF (~10 mg/mL) and filtered through a 0.45-μm nylon membrane filter. For the lignin oil analysis, took 100μL of concentrated lignin oil solution in DCM (~5mg) in a vial and put it in fume hood for natural air dry. Then add 1 ml THF in vial to fully dissolve the lignin oil (5mg/ml). GPC analysis was carried out using an Agilent 1260 Infinity II HPLC with a refractive index detector on a two-column sequence of Agilent PLgel Mixed-B. THF was used as eluent, and the flow rate was 1.0 mL/min. Twelve narrow polystyrene standards (6570000, 3187000, 1044000, 482000, 217000, 70500, 19500, 9570, 4750, 1230, 580, and 162 Da) were used to construct a relative linear calibration curve.

2.3.3 Characterization of lignin by FTIR

Table 2.3 Assignment of the FTIR peaks of functional groups in Kraft softwood lignin [143, 144]

Peaks (cm^{-1})	Functional group
3375	O-H stretching vibration in aromatic and aliphatic structure
2934	C-H vibration sketch in the CH_2 group
2839	C-H vibration sketch in the CH_3 group
1705	C=O stretching of acetyl
1595	C=C aromatic skeletal vibration
1512	C=C aromatic skeletal vibration
1465, 1426	the stretching in the phenol-ether bonds
1366	Syringly ring breathing with C-O stretching
1265	C-O stretching and C-O linkage in guaiacyl aromatic $–OCH_3$ groups
1244	syringyl ring and C-O stretching
1215	ring breathing with C–C, C–O, and C=O stretching
1115	the aromatic in plane C–H bending deformation for S type lignin
1030	the aromatic in plane C–H bending deformation for G type lignin

The chemical structure of lignin and their residuals after the reaction are characterized by Bruker Vertex 80V attenuated total Reflectance-Fourier Transform Infrared Spectroscopy (ATR-FTIR). The scan range was 4,000 cm^{-1} to 600 cm^{-1} with a resolution of 4 cm^{-1}.

2.3.4 XPS analysis of surface structure of lignin

X-ray photoelectron spectroscopy (XPS) measurements were performed with a Kratos Analytical AXIS 165 electron spectrometer using a monochromated $Al_{K\alpha}$ X-ray source run at 100 W. Prior to the XPS analysis, the fine powder lignin samples were dried in freezer dryer for two days. Survey scans were taken with a 1.0 eV step and 80 eV analyzer pass energy while the high-resolution regional spectra were recorded with a 0.1 eV step and 20 eV pass energy. The base pressure was typically 1×10^{-9} Torr. During measurements, the pressure was not allowed to exceed 2×10^{-8} Torr, although normally the pressure remained much lower.

2.3.5 GC-MS/FID analysis of lignin oil

Gas Chromatography Mass Spectrometry (GC-MS) analysis was performed using a Varian (Agilent) 450-GC with a FactorFour™ VF-35ms capillary column (30m×0.25mm×0.25μm) coupled with a 300-MS Varian (Bruker) mass spectrometer (EI, 200°C). The carrier gas was helium at 1 ml min^{-1} with an autosampler injection volume of 1.0 μL using split ratio 50% in initial and 0.75 min. The injection temperature is 300°C and hold for 20 min. The GC oven was programmed to 50 °C for 2 min. Then, it was raised at the rate of 10 °C per min until the temperature reached 200 °C and was held at this temperature for 1 min. After that, the temperature was raised at the rate of 5 °C until the

temperature finally reached at 300 °C and held at the final temperature for 5 min. Eluting compounds were detected by an MS inert XL EI/ CI MSD with a triple axis detector and compared using NIST libraries.

GC-FID was performed using the same Varian (Agilent) 450-GC with a FactorFour™ VF-35ms capillary column (30m×0.25mm×0.25μm) coupled with a FID detector. The carrier gas was helium at 1.5 ml/min with an autosampler injection volume of 0.5 μL using split ratio 50% in initial and 0.75 min. The injection temperature is 300°C and hold for 5 min. The GC oven was programmed to 50 °C for 3 min. Then, it was raised at the rate of 10 °C per min until the temperature reached 200 °C. After that, the temperature was raised at the rate of 5 °C until the temperature finally reached at 300 °C and held at the final temperature for 22 min. Eluting compounds were detected by a front detector at 320°C (make up flow: 25 ml/min; H_2 flow: 30 ml/min; Air flow: 320 ml/min).

2.3.6 GC analysis of gases products from lignin depolymerization

The gases products after reaction are collected in FlexFoil™ sample bags. The collected gases were analyzed in a Varian 490 micro-GC with four channels consisting of four 10 m long columns (two Molecular Sieve 5 Å, one Plot column, and one Al_2O_3 column) and four TCD detectors with the lowest detection limit of 10 ppm for all calibrated gases. The gas yield was established by assuming a basis of nitrogen tie element and by calculating the yield of each gas component from the gas composition. The yield was verified by passing the contents of the gas bag through a Sierra Top-Trak 822 mass flow meter and totalizer that calculated the total volume of gas in the bag.

2.3.7 Lignin oil separation, identification and quantification

For the products in liquid phase, the solvent was evaporated and concentrated to 1 ml in a rotary evaporator. Then the organic products in the concentrated liquid phase were extracted three times by DCM (5 mL×3 times). Only low molecular weight (LMW) products from lignin (monomers and dimers/trimers) were extracted into DCM phase noted as extractable lignin oil and large molecular lignin fragments were remained in solution. Then the separated DCM layer was completely evaporated at room temperature to obtain lignin oil. The lignin oil was weighted and then dissolved in 2 ml DCM for further GC-FID and GC-MS analysis. 4-Ethyl-1,3-benzoldiol was added to the DCM as internal standard for quantitative analysis of monomers.

The lignin oil was quantified by weighing. The yield of lignin oil was calculated by comparing with the mass of lignin used. As mentioned, the monomers were identified using GC-MS and quantified using relative peak areas compared 4-Ethyl-1,3-benzoldiol to obtained from the GC-FID. The response factor for each component was calculated using the effective carbon number (ECN) method.[145]

The ECN rule has been widely accepted to quantify carbon-containing products by their peak areas in GC-FID. ECN is the sum contributions made by each carbon atoms in their functional groups contributions. The accuracy of this rule for lignin products was validated by Shuai and his co-workers [115]. The ECN of all detected products are listed in Appendix A. Monomers yield was calculated by the ECN approach following the equations below.[146, 147]

$$\text{Yield of lignin oil (wt\%)} = \frac{\text{Mass of DCM extracted lignin oil}}{\text{Mass of input lignin}} \times 100\%$$

$$\text{Mass of monomer}_x\text{(mg)} = \frac{Mass_{(\text{IS})}}{MW_{(\text{IS})}} \times \frac{Area_x/ECN_x}{Area_{\text{IS}}/ECN_{(\text{IS})}} \times MW_x$$

$$\text{Total monomers yield(wt\%)} = \frac{\sum_{x=1}^{n} Mass\ of\ monomer_x}{Mass\ of\ input\ lignin}$$

$$\text{Yield of dimers \& oligomers (wt\%)} = \text{Yield of lignin oil(wt\%)} - \text{Total monomers yield(wt\%)}$$

$$\text{Selectivitity}_x = \frac{\text{Yield of product x}}{\text{Total product yields}} \times 100\%$$

In these equations,

- *x*: the monomer detected by GC-MS and GC-FID
- $Mass_{i(IS)}$ (mg): the weight of internal standard (4-Ethyl-1,3-benzoldiol) in each analyzed sample;
- $MW_{(IS)}$ (mg/mmol): the molecular weight of internal standard (138.07 mg mmol-1);
- MW_x (mg/mmol): the molecular weight of monomer;
- $Area_{(IS)}$: the peak area of internal standard in the GC-FID chromatogram;
- $Area_x$: the peak area of monomer in the GC-FID chromatogram;
- ECN*x*: the effective carbon number of the lignin monomer molecule;
- $ECN_{(IS)}$: the effective carbon number (6) of internal standard;

CHAPTER 3. LIGNIN DEPOLYMERIZATION VIA EFFECTIVE INHIBITION OF CONDENSATION BY TEMPO OXIDATION*

3.1 Introduction

Due to the aromatic-rich structure of lignin, it is a promising renewable resource for aromatic chemicals production in future. Developing techniques to produce aromatics from lignin is not only urgent and challenging, but also a visible long-term opportunity. Numerous efforts have been put into depolymerizing lignin to small molecules as bio-fuel or bio-chemicals. [1, 16] The abundant ether bonds (β-O-4, α-O-4, 4-O-5), especially the β-O-4 aryl linkage, are the major targets for cleaving during lignin depolymerization. Acid/base catalyzed/hydrolysis[148, 149], pyrolysis[57], reduction[150], chemical oxidation[151], and biodegradation[152] have been used to cleave these lignin linkages. However, most of the reported methods have some inevitable limitations such as high reaction temperature, high hydrogen pressure, safety concerns and low products yield[153]. There is still no efficient way to treat lignin, especially from industrial processes.

A key issue is the condensation of lignin fragments during the lignin fractionation and the cleavage of lignin β-O-4 linkages in the present of an acid and high temperature. The condensed lignin structure can further trap the breakable ether linkages so that they cannot be accessed by catalysts, especially heterogeneous catalyst.[154] The mechanism of the formation of highly active lignin side-chain (benzylic) carbonations (A route) that

* This chapter is submitted to Chemical Engineering Journal for publication: X. Du, W Yang, W Liu, A Tricker, H Dai and Y Deng. High efficient lignin depolymerization via effective inhibition of condensation during polyoxometalate mediated oxidation.

reacts with the adjacent aromatic rings (G/H type) to form C-C bond in a benzofuran structure[155, 156] or (B route) condensates with electron-rich position of other aromatic ring (G/H type) in Figure 3.1 is widely accepted.[4, 115, 157] For industrial lignins from current biorefineries, we need to avoid their further condensation during lignin depolymerization and cleave the interunit C-O/C-C linkages.

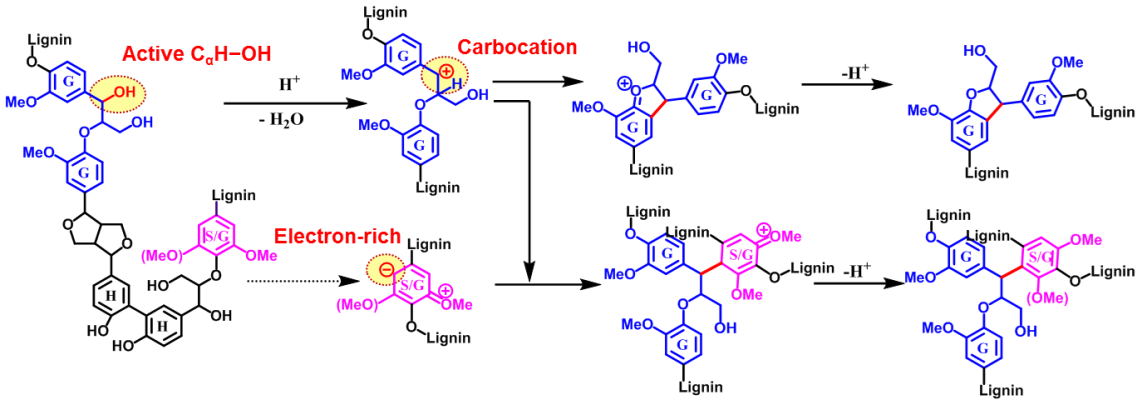

Figure 3.1 Possible condensation processes (A, B) during the reaction of lignin β-O-4 linkages. Condensation in the same β-O-4 linkage with a carbocation intermediate 1 (A, ref [155, 156]). Condensation caused by the condensation of β-O-4 carbocation intermediate 1 and G/S type of aromatic ring (B, ref [4, 115, 157]). Adapt with permission from reference [158]. Copyright 2017 American Chemistry Society.

Recently, several innovative two-step methodologies have been developed to effectively depolymerize lignin by selectively oxidize the secondary alcohol in β-O-4 linkage followed by ether bond cleavage. [2-5] By the calculations of density functional theory (DFT), the bond dissociation enthalpy (BDE) of C_β-O bond in β-O-4 linkage decrease after oxidation of C_αH−OH (68.2-71.8 kcal mol^{-1}) to C_α=O (55.9-57.1 kcal mol^{-1}) [91] thus making bond more labile (Figure 3.2). The stable C_α=O also can prevent the generation the reactive carbonations and further condensation. A feasible strategy to

overcome the recalcitrance of lignin is to weaken the C_β–O in β-O-4 linkage by oxidizing the C_αH–OH.

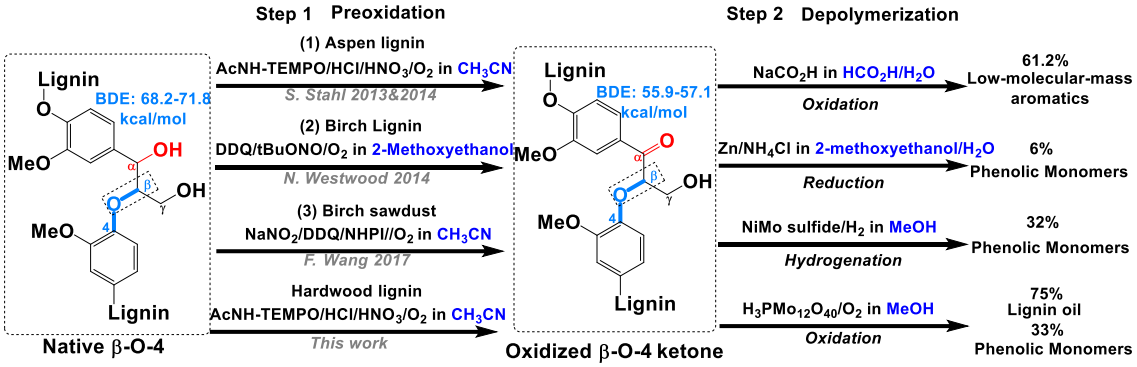

Figure 3.2 Previous studies to depolymerize lignin by benzylic oxidation methods to decrease C–O ether BDEs in the β–O–4 linkages (preoxidation step) and facilitate subsequent cleavages (depolymerization step). [2-5]

As shown in Figure 3.2, successful generation of oxidized β-O-4 ketone and further cleavage to aromatics has been studied by several routes including: (1) acetamido-TEMPO[2, 3] was applied to oxidize Aspen lignin and further depolymerized to 60wt% yield of low-molecular-weight (LMW) aromatics in aqueous formic acid by Stahl's lab[3]; (2) 2,3-dichloro-5,6-dicyano-1,4-benzoquinone (DDQ) was used to oxidize a Birch lignin and then reduced by Zn/NH_4Cl in aqueous solution to 6 wt% phenolic monomers by Westwood's lab;[5] (3) DDQ/ N-hydroxyphthalimide (NHPI)-mediated benzylic oxidation of the (C_αH–OH) moieties followed by further hydrogenation in a NiMo sulfide catalysis process resulting in the cleavage of ether bonds to aromatic monomers by Wang's lab.[4]

Polyoxometalate (POMs) is a green and high-efficiency catalyst that has been employed to remove residual lignin from unbleached pulp in the pulp industry[159]. Previous

studies have shown POMs are capable of degrading lignin into high-valued chemicals. [151, 160, 161] This study has focused on $H_3PMo_{12}O_{40}$ (PMo_{12}) as a reversible oxidant and is very stable at the temperatures and pH values used within this study. PMo_{12} is a commercially available POMs with a redox potential that it is higher than lignin subunits and lower than oxygen.[134] Figure 3.3 shows the lignin catalytic depolymerization process by POM — reduction of $POM_{(ox)}$ ($[PMo^{VI}_{12}O_{40}]^{3-}$) by lignin and oxidation of $H\text{-}POM_{(red)}$ ($[PMo^{V}_{12}O_{40}]^{4-}$) by O_2 spontaneously — sum to electron transfer from lignin to O_2. Further, the reduction of O_2 by $H\text{-}POM_{(red)}$ initially gives superoxide anion – O_2^- ($O_2 + e^- \rightarrow O_2^-$) and subsequently becomes H_2O_2 ($2O_2^- + 2H^+ \leftrightarrow O_2 + H_2O_2$) [129, 162] and hydroxyl radical – $OH\cdot$ ($H_2O_2 + e^- + H^+ \rightarrow H_2O + OH\cdot$)[163]. Therefore, the oxidation of $H\text{-}POM_{(red)}$ by O_2 can be achieved under specific conditions (time, temperature, and O_2 pressure) using these highly reactive intermediates of radical-chain oxidation (e.g. O_2^-, $HO\cdot$).[164] Moreover they can further oxidize the products of the substrate to CO_2 and H_2O. [132] Numerous studies reported the use of POMs for oxidative delignification processes with oxygen, but have low yields of monomers, primarily because of the condensation of lignin fragments (aldehyde and carboxylic)[134, 135, 165] and the over-oxidation of products to gases [35]. Voitl and co-workers found that methanol can both dissolve lignin and generate radical scavengers ($CH_3\cdot$ and $CH_3O\cdot$) to couple with aldehyde and carboxylic products to form stable methyl ester products[160]. This study will focus on effectively producing aromatic chemicals and suppressing over-oxidation to gases products using a simple system of POM in methanol.

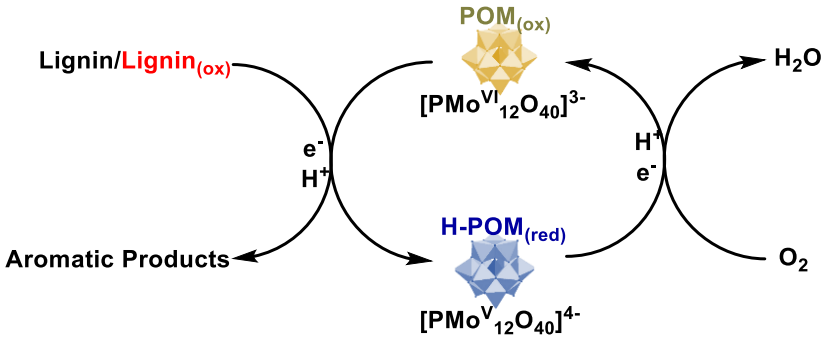

Figure 3.3 Proposed lignin catalytic depolymerization process by POM with oxygen.

Experimentally, a novel approach which includes two oxidation steps was developed. In the first oxidation process, TEMPO/O_2/HNO_3/HCl selectively oxidized C_α-OH to C_α=O (blocking active C_α-OH), which depressed the formation of the free radical, and significantly improved the lignin depolymerization. The second oxidation was conducted with a regenerable POM at 150 ^oC under 10 bar oxygen, which effectively degraded the pre-oxidized lignin into valuable chemicals. Methanol, as the main solvent in the depolymerization reaction, not only dissolved lignin but also reacted with aldehyde and carboxylic products to form stable intermediate products to prevent further condensation. Meanwhile, methanol, with a low boiling point (64.7 °C), could be separated with a simple distillation process[166]. In this study, a detailed analysis of the depolymerization products, including yield and compositions, were performed to elucidate the roles of blocking of active C_α-OH and the solvent (methanol). At optimal conditions, a depolymerization product yield of 74.53 % (based on total lignin) with a relatively low average molecular of 363 Da was obtained. Among this depolymerized low molecular weight products, 32.75 % (based on total lignin mass) was monomers (13.35 % aliphatics and 19.40 % aromatics),

and 41.78 % was oligomers (mainly lignin dimer and trimers). The results indicate that the novel two step oxidative depolymerization method reported here is superior to common oxidative depolymerization methods reported previously[160, 167, 168].

3.2 Experimental section

3.2.1 Materials

Lignin was isolated by supercritical water extraction from Renmatix. Further purification was conducted via dissolution and regeneration of lignin using 1,4 dioxane [169]. Details and other chemicals used in this study are shown in 2.1 section.

3.2.2 Modification of lignin by TEMPO oxidation

Dried lignin (200 mg) and TEMPO (6 mg) were added to a 50 mL bottle. 10 mL acetonitrile (containing 100 μL H_2O), 9 μL of hydrochloric acid (37%) in 1.5 mL acetonitrile, and 6 μL of nitric acid (67%) in 1.5 mL acetonitrile were injected. The reaction mixture was stirred at 65 °C under 1.2 atm oxygen gas for 24 h. After evaporation, the pre-oxidized lignin was obtained, which was directly used for depolymerization in a POM/O_2 oxidation system.

3.2.3 Procedure for catalytic reactions of lignin

See details in section 2.2.2.

3.2.4 Analysis and characterization of lignin oil

See section 2.3 for lignin oil separation, identification, quantification, GPC, GC, and GC-MS/FID analysis, along with yield calculation.

3.3 Results and discussion

3.3.1 Oxidative depolymerization of lignin using a regenerable POM system

Initial depolymerization reaction was conducted with regenerable polyoxometalates under aerobic conditions. The redox potential of POM_{ox} (POM in oxidation state) is high enough to oxidize lignin to low molecular products[170], accompanied by the formation of $H{-}POM_{red}$ (POM in reduction state). Hence, a re-oxidation of $H{-}POM_{red}$ to POM_{ox} is essential for sequentially degrading lignin with a high efficiency.

Briefly, in the depolymerization process, POM_{ox} oxidizes lignin at 150 °C while POM_{ox} is reduced to $H{-}POM_{red}$ as shown in Figure 3.3. Then, the $H{-}POM_{red}$ is re-oxidized to POM_{ox} with the O_2 as the oxidant at 150 °C. In other words, the POM should be completely regenerated without consumption. To demonstrate that POM is regenerated by oxygen in the lignin degradation processes, pure POM_{ox} aqueous solution (with a similar concentration as used in actual lignin depolymerization reaction) was studied. POM was first reduced by electrochemically for 60 minutes by exposing the POM solution to a 1 V electric field. The POM solution gradually changed the color from yellow to dark blue, indicating the POM was reduced to $H{-}POM_{red}$. The reduced $H{-}POM_{red}$ solution was then oxidized by O_2 under 10 bar gas pressure at 150 °C (similar condition as that will be used in lignin depolymerization process). After ~30 minutes, the color of the solution changed from dark blue to yellow (typical color of POM_{ox}). The UV-vis spectral curve showed no obvious absorbance at 790 nm wavelength, indicating $H{-}POM_{red}$ was reoxidized back to POM_{ox}. These results clearly verify that the POM is regenerated at 150 °C and 10 bar O_2, which is the condition used for lignin depolymerization.

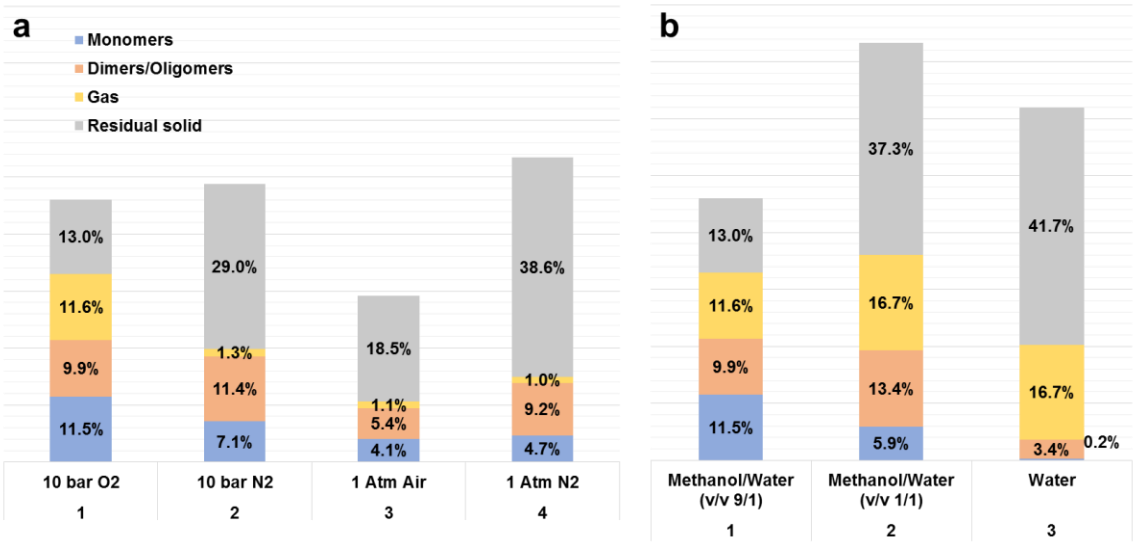

Figure 3.4 Oxidative depolymerization of lignin under: **a.** varying gases and pressures **b.** varying solvent systems. (Lignin oil: the sum of monomers and dimers/oligomers) Reaction conditions: 0.2 g lignin (without C_α-OH preoxidation), 0.9125 g POM (0.05 mol/L), methanol (18 mL)/H_2O (2 mL), 150 °C for 4 h.

Figure 3.4a summarizes the amount of products obtained from the oxidative depolymerization of original lignin (in contrary to the lignin after blocking the active C_α-OH groups) under varying gases and pressures. Entry 1 and 2 were conducted to compare the results for reactions in O_2 and N_2 with 10 bar gas pressure. For the reaction conducted under O_2, the yield of total monomer was 11.5 wt%, and the residual solid was 13.0 wt%. For this reaction, a high gas production (mainly CO_2 and CO) of 11.6 wt% was observed. It was also noted that, for the reaction under 10 bar oxygen (Entry 1), the final solution showed a yellow-green color (typical color of POM_{ox}) which indicated that majority of POM was regenerated to its original oxidation state in depolymerization process. However, when oxygen was replaced by nitrogen (N_2) (Entry 2), the $H-POM_{red}$ could not be regenerated to $POM_{ox,}$ leading to a lower monomer yield of 7.1 wt% and a higher residual

solid yield of 29.0 wt%. After reaction, the resulting solution showed a deep blue color (typical color of POM_{red} in reduction state), which clearly indicated that POM_{ox} was reduced to $H{-}POM_{red}$ by lignin but could not be regenerated back to POM_{ox} under nitrogen[171]. Entry 3 and 4 compared the results of lignin degradation at atmospheric pressure with air and nitrogen respectively. Although lignin could be partially depolymerized by POM oxidation in these conditions, the solid residue was high, and the solution color was changed from yellow to dark blue, indicating that resulted $H{-}POM_{red}$ could not be regenerated back by air or nitrogen at atmospheric pressure. In summary, the use of O_2 at 10 bar and 150 ^{o}C results in a complete regeneration of POM during the depolymerization processes, leading to higher efficiency of lignin degradation than that without POM regeneration.

3.3.2 Effect of methanol during lignin depolymerisation

It has been known that lignin has a higher dissolubility or dispersibility in methanol than in water, which could improve the reaction kinetics of lignin with POM[172]. Methanol can also be used as a radical scavenger. Previous researches indicate that the formation of the aldehyde and carboxylic fragments within the lignin depolymerization process will induce condensation[158]. Voitl *et al.* found experimental evidence that the radical coupling reactions with radicals generated from methanol ($CH_3\cdot$ and $CH_3O\cdot$) will inhibit lignin fragments condensation reactions[160].

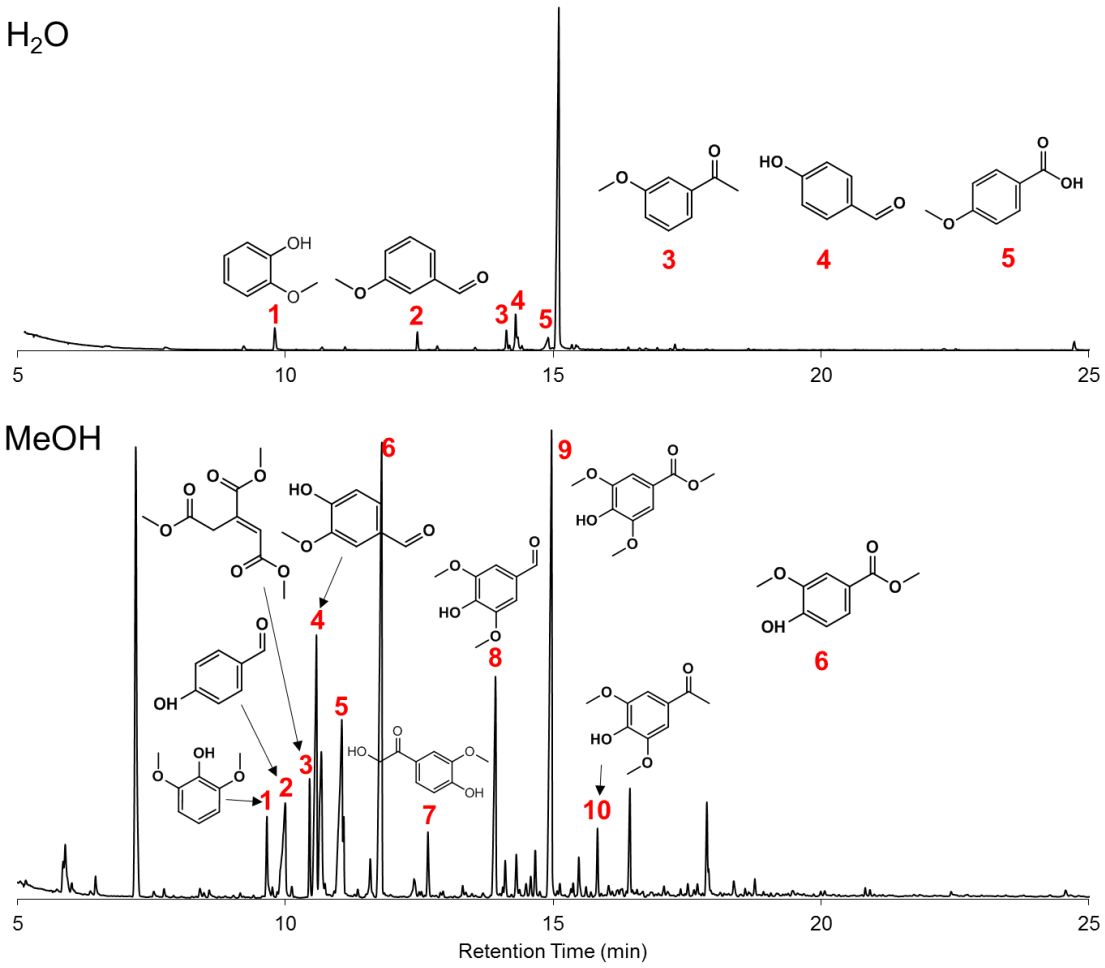

Figure 3.5 GC-MS analysis of products obtained from the oxidation depolymerization lignin (without blocking active C_α-OH) in methanol/water mixtures (v/v: 18/2) or water under 10 bar O_2 at 150 °C for 4 h.

In above study shown in Figure 3.4a, instead of water, methanol was used as the main solvent. In order to further understand the role of methanol, reactions using water as the solvent were conducted and were compared to reactions in a methanol/water mixture (Figure 3.4b). In the pure water system, only some aldehyde and carboxylic products were observed (Figure 3.5). However, when methanol was added as the main solvent, some carboxylic esters (methyl vanillate) or acetovanillone occurred, which suggests that methanol was incorporated into lignin-derived products (Figure 3.5). The yields of the

lignin degradation products in water or methanol/water mixtures are shown in Figure 3.4b. Entries 1, 2, and 3 compare the results for reactions in methanol/water mixtures (v/v: 18/2 and 10/10) and water only, illustrating the role of methanol. The results indicate that the more ratio of methanol in solvent led to higher yields of both extractable lignin oil and monomers. With pure water, more than 41.7 wt% residual solid was remained, and a lowest extractable lignin oil yield of 3.6 wt% and monomer yield of 0.2 wt% were observed. However, in the methanol/water mixtures a lower residual solid of 13.0 wt% and higher extractable lignin oil of 21.4 wt% and monomer yields of 11.5 wt% were obtained. In summary, methanol plays a significant role in lignin depolymerization reactions due to the excellent solubility of lignin and the limitation for the condensation of depolymerization products.

3.3.3 Effect of active C_α-OH preoxidation

Blocking of the active C_α-OH plays a significant role in depressing condensation of lignin fragments and improving lignin degradation efficiency. In this study, the active C_α-OH was blocked via selective oxidation of the C_α-OH to a ketone. According to previous reports, Rahimi found that TEMPO/HNO_3/HCl oxidation system could efficiently catalyze the selective oxidation of Cα-OH to ketone with O_2.[3] To achieve a better understanding of the reaction, a model lignin compound, 2-(2-methoxyphenoxy)-1-(4-methoxyphenyl) ethanol (β-O-4-A) was synthesized according to previous studies[173]. The detailed procedures of lignin model compounds synthesis and selective oxidation of lignin model compounds over the TEMPO/HNO_3/HCl oxidation system are shown in section 2.2.1. GC-FID data shows that a very effective and high selective oxidation of C_α-OH to ketone was achieved, with conversion up to 88 %.

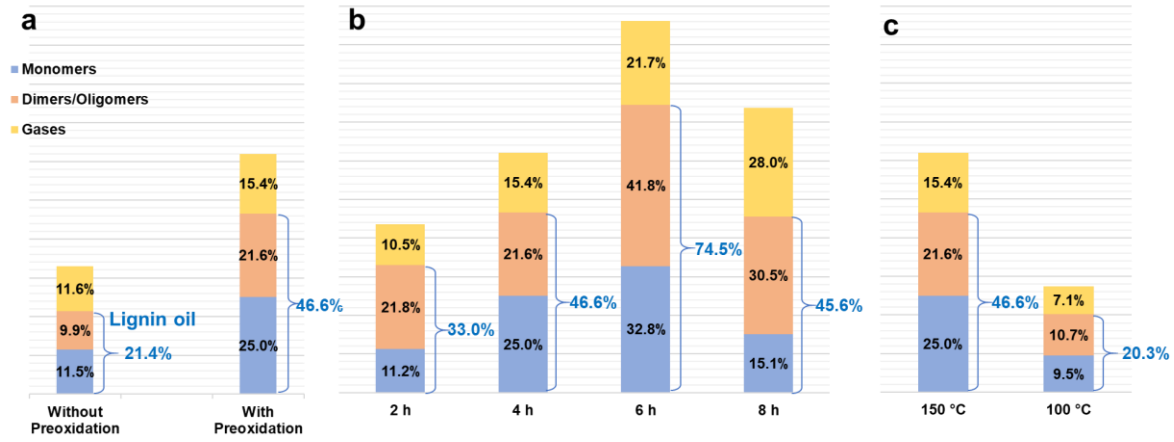

Figure 3.6 Oxidative depolymerization of lignin under varying conditions. a. Effect of with vs. without TEMPO preoxidation (4 h reaction time). b. Effect of reaction time (with TEMPO preoxidation). b. Effect of reaction temperature (with TEMPO preoxidation for 4 h). Reaction conditions: 0.2 g lignin (with or without blocking C_α-OH), 0.9125 g POM (0.05 mol/L), 10 bar O_2, methanol (18 mL)/H_2O (2 mL).

The essential role of blockage of the active C_α-OH via selective oxidation is illustrated in Figure 3.6 a. With the blocking treatment, the lignin was effectively degraded into a total extractable lignin oil with a 46.6 wt% yield, with a monomer yield of 25.0 wt% (based on total lignin added). Without blocking, a lower extractable lignin oil yield of 21.4 wt% and a monomer yield of 11.5 wt% were observed with the same degradation conditions. These results demonstrate the importance of C_α-OH oxidation in promoting lignin depolymerization and restraining the condensation reactions. It was clearly demonstrated from this study that blocking active C_α-OH plays a key role in improving the yield of low molecular compounds.

It was expected that higher efficiency of lignin depolymerization may be obtained by raising the reaction temperature and using longer reaction time (Figure 3.6 b,c)[174]. In this study, a highly efficient depolymerization of lignin via combined strategy of blocking active C_α-OH and POM oxidative depolymerization under relatively mild reaction

conditions was observed. To conclude, various conditions (reaction temperature and time) were tested to optimize the extractable lignin oil and monomer yields. The above results indicate that a higher degradation of lignin could be achieved by pre-converting of the C_α-OH to C_α=O and weakening the β-O-4 bond even at a relatively mild condition (150 °C and 10 bar O_2). Lowering the reaction temperature to 100 °C (Figure 3.6 c) resulted in a lower extractable lignin oil yield of 20.3 wt%, and lower monomer conversion yield of 9.5 wt%. However, the lower temperature avoided over oxidation of depolymerization products and led to a lower gas product yield (CO and CO_2) of 7.1 wt%. Reaction time also plays a significant role in lignin depolymerization. Reaction times of 2, 4, 6, 8 h were conducted to degrade lignin, as shown in Figure 3.6 b. Long reaction time led to a higher yield of depolymerization products. While too long of a reaction time caused over-oxidation and degradation of low molecular products and produced large amount of gas products including CO and CO_2. With the increasing of reaction time, both the extractable lignin oil and monomer yield increased initially but declined later, and a large amount of CO and CO_2 gas products ranged from 10.5 wt% to 28.0 wt% was observed. When the depolymerization time reached 6 h, the optimal extractable lignin oil yield of 74.5 wt% and monomer yield of 32.8 wt% were achieved. The detailed analysis of extractable lignin oil and gas products compositions will be discussed later.

3.3.4 Chemical composition of lignin oil and gaseous products

Gaseous products generated from oxidative depolymerization of lignin were analyzed by GC-TCD-FID. From GC results, it was found that CO_2 and CO are the major components of gaseous products. In oxidative depolymerization processes, over oxidation sequentially converts low molecular depolymerization products to CO, CO_2 and H_2O[175].

As a result, higher reaction temperature, longer reaction time and higher O_2 gas pressure caused over oxidation of lignin and generate more CO and CO_2 gas, which is consistent with GC results. The average molecular weight (M_W) of the original lignin is about 7424 Da. Through effective oxidative depolymerization, the molecular weight of lignin decreased sharply, and a large amount of low molecular compounds was obtained. The molecular weights obtained from the depolymerization of lignin with or without blocking active C_α-OH were very similar (321 and 299 Da). After converting active C_α-OH to ketone, the neighbor β-O-4 bond in lignin structure was weaken, which resulted in a highly efficient degradation of lignin. While the conversion of secondary benzylic alcohols (C_α-OH) to C_α=O also made ring opening easier aliphatic products were also obtained. The lignin ring opening reaction was presented in Figure 3.7, including 1) oxidation, depolymerization, and demethylation and 2) ring opening processes[176]. During the oxidative depolymerization of lignin, the products of the aromatic monomers were further converted into quinone intermediaries which rapidly undergo ring-cleavage to yield unsaturated aliphatic carboxylic acids[177, 178]. These aliphatic carboxylic acids will react with methanol to form corresponding esters.

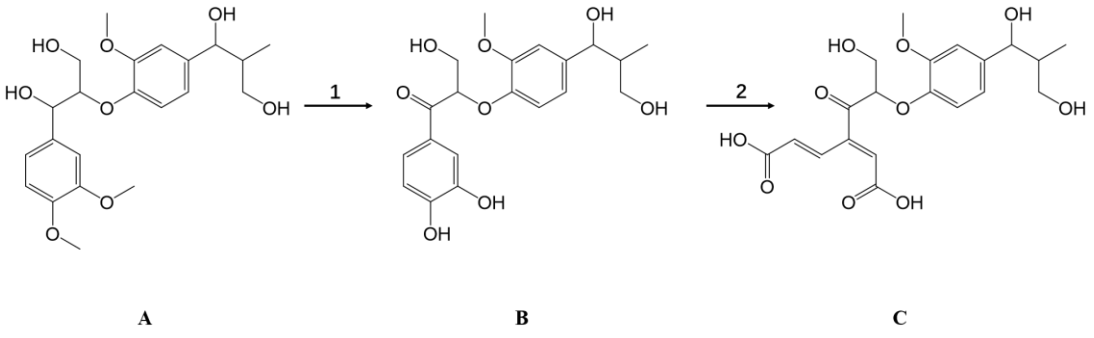

Figure 3.7 Scheme representing 1) oxidation, depolymerization, and demethylation and 2) ring opening, leading to unsaturated aliphatic and hydroxylated carboxylic acid containing structure C [179, 180].

GC-MS and GPC were utilized to analyze the extractable lignin oil obtained from the oxidative degradation of modified lignin (blocking active C_α-OH) with varying times and temperatures. The lignin oil (average molecular weight of 296-363 Da) mainly consists of a set of oligomers (dimer, trimer et.), aliphatic monomers, and aromatic monomers. The aliphatic and aromatic monomeric chemicals with relatively low boiling points were detected with GC-MS and the main product structures are shown in Figure 3.8. These can also be observed from the GPC results in Figure 3.9 (vary reaction times), which show two main peaks around 125 to 144 Da (monomer) and 441 to 540 Da (oligomer).

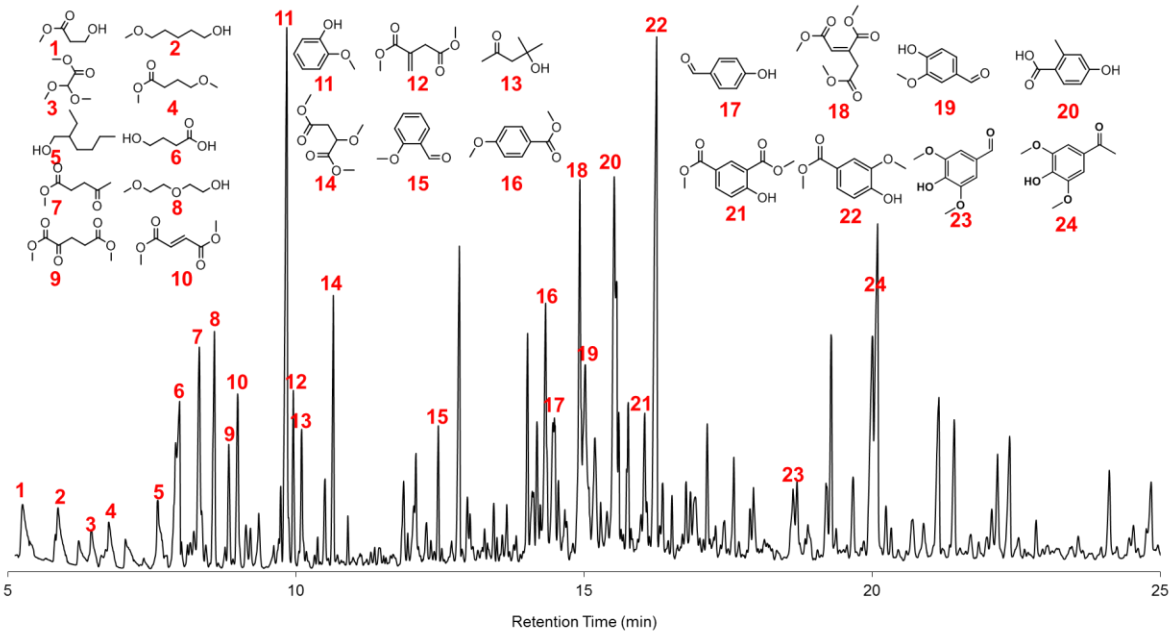

Figure 3.8 GC-MS analysis of products obtained from the oxidation depolymerization of lignin (by C_α-OH preoxidation) for 6 h.

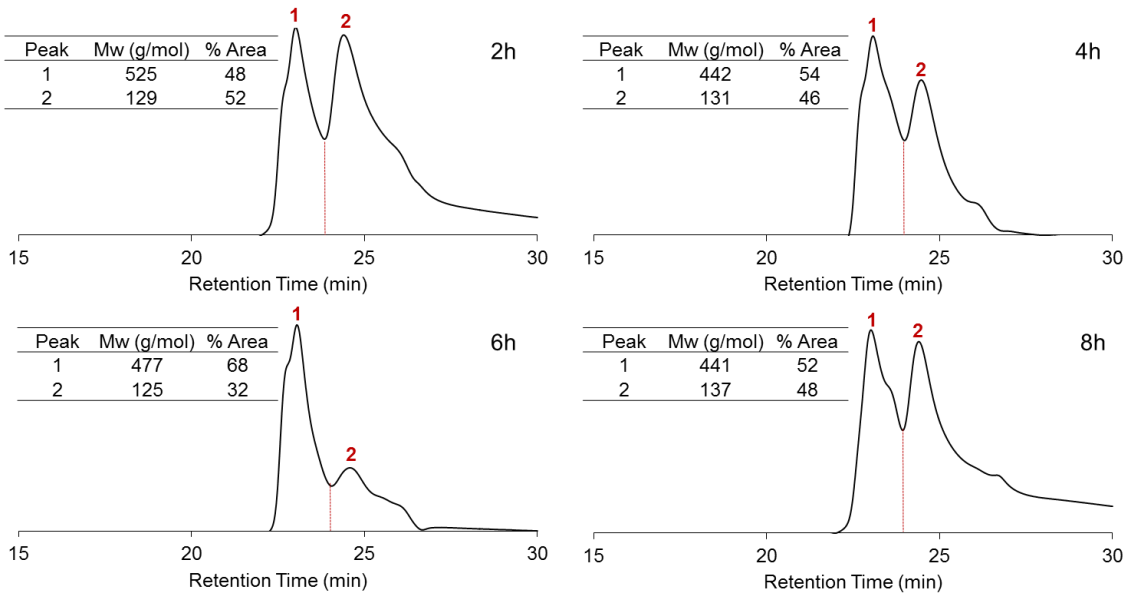

Figure 3.9 GPC analysis of products obtained from the oxidation depolymerization of lignin (with C_α-OH preoxidation) for 2 h, 4 h, 6 h, 8 h.

Table 3.1 shows the yields and distribution of oligomer, aliphatic monomer, and aromatic monomer. Lowering the reaction temperature to 100 °C (entry 5, Table 3.1) resulted in a lower extractable lignin oil and monomer yield. However, the low temperature avoids the ring-opening reaction, which leads to the lowest aliphatic chemicals (0.2 wt%) in extractable lignin oil. Both the lignin conversion and product distribution could be influenced by the reaction time. For instance, the extractable lignin oil and monomer yield gradually increased with increasing time, and 74.5 wt% of extractable lignin oil (average molecular weight of 363 Da) was generated after 6 h degradation, and monomer yield (based on total lignin) reached 32.8 wt%. However, more aliphatic chemicals were detected. While sequentially increasing the reaction time to 8 h, extractable lignin oil and monomer yield decreased, and more gas products of CO and CO_2 were generated. In

summary, combined two step oxidization strategies was demonstrated to effectively depolymerizing lignin to extractable lignin oil (optimal yield of 74.5 % with average molecular weight of 363 Da and monomer of 32.8 %) under a relatively mild condition.

Table 3.1 Detailed products distribution of the lignin oil obtained from the oxidative degradation of lignin with vary times and temperatures.[a]

Entry	t (h)	T (°C)	Lignin oil (%)	Mw (Da)	Oligomer (%)	Aliphatic Monomer (%)	Aromatic Monomer (%)
1	2	150	33.0	319	21.8	1.5	9.7
2	4	150	46.6	299	21.6	6.5	18.5
3	6	150	74.5	363	41.8	13.4	19.4
4	8	150	45.6	296	30.5	3.3	11.7
5	4	100	20.3	355	10.7	0.2	9.3

[a] Reaction conditions: 0.2 g lignin (with blocking C_α-OH), 0.9125 g POM (0.05 mol/L), 10 bar O_2, Methanol (18 mL)/H_2O (2 mL)

3.4 Conclusion

In summary, a combined strategy of preoxidation of C_α-OH to ketone followed by POM oxidation has been adopted to depolymerization of lignin at mild condition. Results showed that the blocking of C_α-OH position of lignin *via* selective oxidation significantly depressed condensation reactions and promotes lignin depolymerization. Further oxidative degradation was performed under a relatively mild condition (150 °C, 10 bar O_2) using regenerable POM oxidation system. In addition, when methanol was added into reaction

mixture, positive effects on the stabilization of oxidation depolymerization products (aldehyde and carboxylic products) were obtained and further condensation was avoided. As shown in GC-MS data, a relatively large amount of methyl ester was observed. Under optimal conditions, extractable lignin oil of 74.5 % with average molecular weight of 363 Da and the total monomer yield up to 32.8 % were obtained at 150 °C and 10 bar O_2 for 6 h.

CHAPTER 4. HIGH YIELD INDUSTRIAL LIGNIN CONVERSION BY A TWO-STEP POLYOXOMETALATE CATALYTIC OXIDATION STRATEGY IN ONE-POT[†]

4.1 Introduction

As introduced in Chapter 3, several innovative two-step methodologies have been developed to effectively depolymerize lignin by selectively oxidize the secondary alcohol in β-O-4 linkage followed by ether bond cleavage (Figure 3.2). [2-5] However, all the current two-step processes were conducted in two different catalytic systems (*i.e.* solvents, catalysts in Figure 3.2), which becomes an important challenge for practical industrial application. Herein, for the first time we report a two-step oxidation protocol that can be achieved in one-pot by the same polyoxometalate (POM) catalytic system. The benzylic alcohol ($C_\alpha H{-}OH$) of industrial ethanol lignin is oxidized to ketone ($C_\alpha{=}O$) at low temperature in preoxidation step, and then further oxidized to low molecular weight aromatics at an elevated temperature with high yield. The present work realize the lignin preoxidation and depolymerization in the same pot with POM as only catalyst to suppress condensation and overoxidation in methanol, which will provide a knowledgebase for lignin chemistry and overall biorefinery concept in general.

[†] This chapter will be submitted for publication: X Du, W Yang, A Tricker,a W Liu, S Aluri, T Kwok, Z Geng, P Gogoi, and Y Deng*

4.2 Experimental section

4.2.1 Materials

Lignin is isolated by ethanol from American Process without further purification. Details and other chemicals used in this study was shown in 2.1 section of this dissertation.

4.2.2 Modification of lignin by POM oxidation under mild condition

In preoxidation step, 200 mg of lignin, 1.825 g (0.05 mol/L) PMo_{12} and 20 ml of solvent (methanol, water) were taken in a 50 ml round-bottom flask. After flushing the reaction mixture with nitrogen, the flask was sealed and placed into a preheating water bath at ~ 60°C with magnetic stirring.

4.2.3 Procedure for catalytic reactions of lignin

See details in section 2.2.2.

4.2.4 Analysis and characterization of lignin oil

Lignin oil separation, identification and quantification. GPC, GC, GC-MS/FID analysis, and yield calculation (see section 2.3)

4.3 Results and discussion

4.3.1 Selective oxidation of lignin model compound over POM

For initial tests, we used a β-O-4 dimer (**1**), representing the predominant ether linkage units with their characteristics and available methoxy groups. For the preoxidation of targeted benzyl alcohols, we found that the PMo_{12} oxidation system could effectively oxidize **1** to **2** under mild conditions (Figure 4.1). 100% conversion (**1** was not detected after preoxidation) was obtained in 2 h at 60 °C, as was consistent with prior reports using different Keggin structure POMs in water. [137, 181] CO_2 was not detected, as is expected at the low temperature.

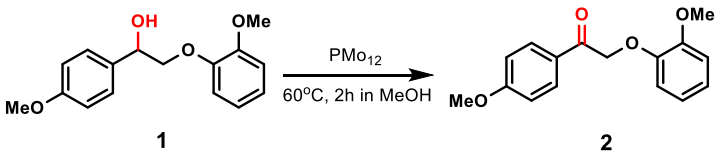

Figure 4.1 Preoxidation of C_α-OH in lignin model compound (β-O-4 dimer **1**) to C_α=O and subsequent depolymerization at elevated temperature with oxygen.

4.3.2 Selective oxidation of lignin by POM at mild condition

In this work, in addition to the model compounds of β-O-4 dimers, we also investigated the application of the two-step preoxidation -oxidation strategy in the conversion of industrially available organosolv lignin extracted by an ethanol isolation method (noted as EtOH lignin). The EtOH lignin (particle size <0.45 mm; moisture content 2.3%; ash content 1.18%) was used to study the effect of pre-oxidation for the real lignin under similar reaction conditions.

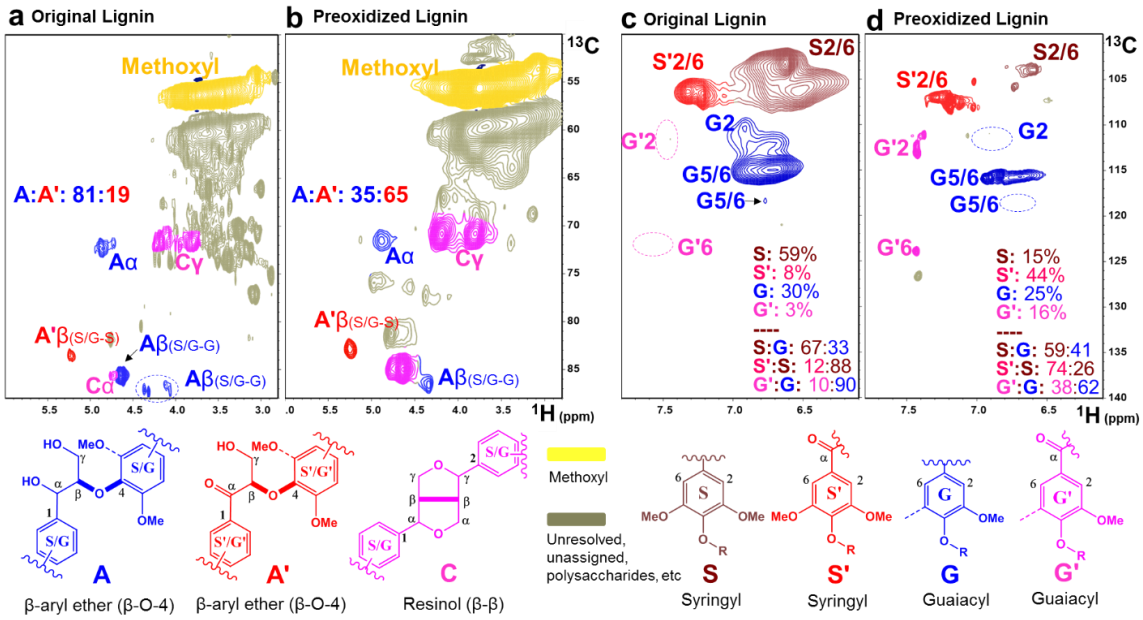

Figure 4.2 Partial 2D HSQC NMR spectra of an EtOH lignin (in DMSO-d_6) before and after preoxidation. The aliphatic regions of (**a**) original EtOH lignin and (**b**) lignin after PMo_{12} preoxidation at 60°C for 2 h. The aromatic regions of (**c**) original EtOH lignin and (**d**) lignin after PMo_{12} preoxidation at 60°C for 2 h. Contours are color-coded to the structures responsible. Percentages are from volume integrals.

The 2D HSQC NMR results showed that the preoxidation method also has good reactivity with real lignin. Figure 4.2 shows HSQC spectra of EtOH lignin before and after preoxidation (60°C, 2h in methanol). The aliphatic region (Figure 4.2a,b) shows that most of the α-OH groups in the **S** and **G** units were oxidized to benzylic ketones **S′** and **G′**. Most of the β-aryl ether units **A** (81%) in the original lignin (Figure 4.2a) were oxidized to their analogues **A′** (65% in Fig. 3B). The data suggest that the remaining unoxidized ether units in **A** is 35%. The aromatic regions (Figure 4.2c,d) further support the conversion of benzylic alcohols to their analogues ketones. The data unveil that most of benzylic alcohol units (59% **S**; 30% **G**) in original lignin were oxidized to ketones (44% **S′**; 16% **G′**). The

assignments of β-aryl ether (**A**, **A′**), resinol (**C**), **S** (**S′**) and **G** (**G′**) units are based on the previous studies. [2, 182-184] These preliminary studies show that the preoxodation of more than half of the benzylic alcohols in industrial lignin that is similar with the results in the model compounds.

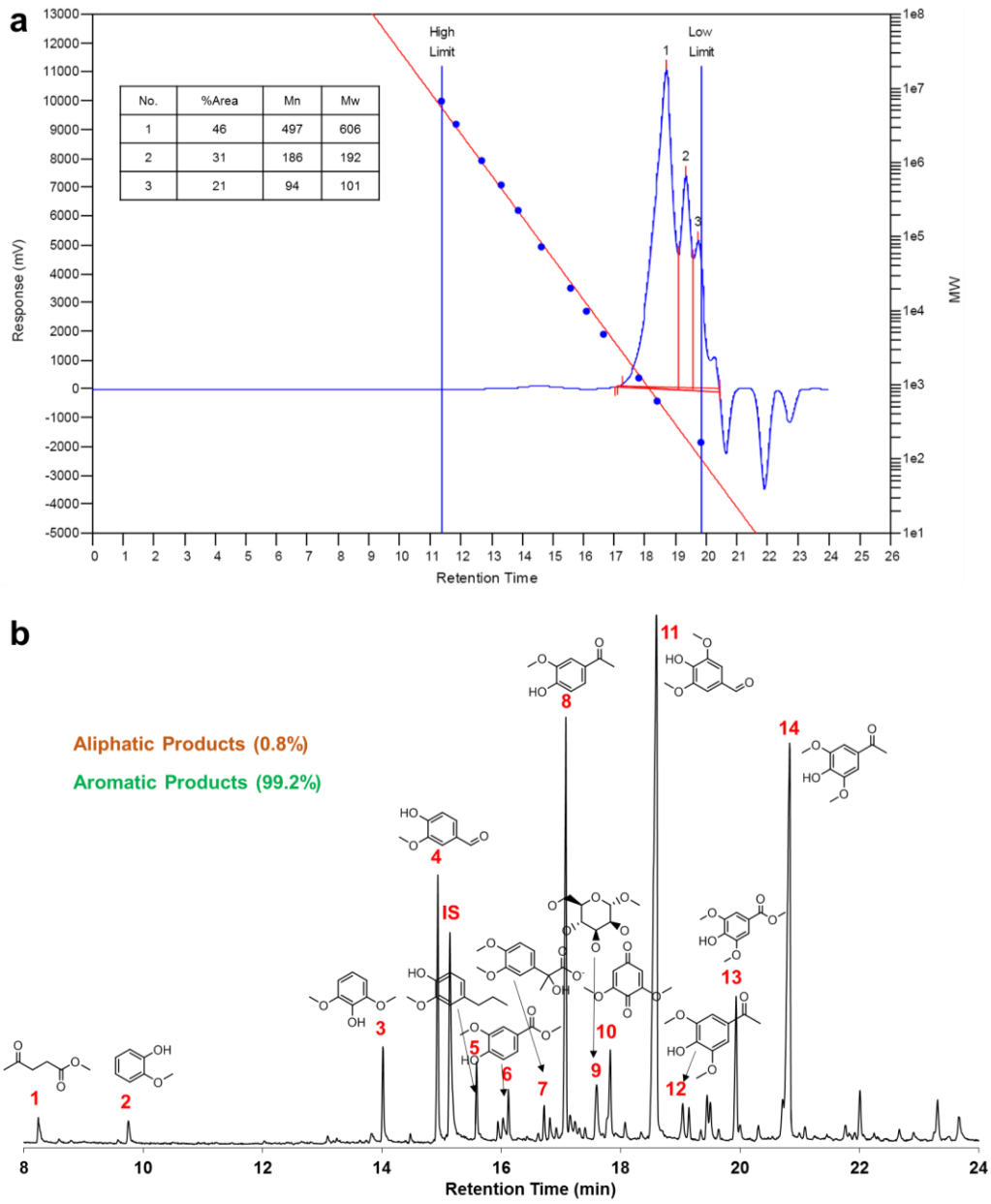

Figure 4.3 a). GPC Spectrum of lignin oil after preoxidation; b). GC-MS spectrum of lignin oil after preoxodation (60˚C, 2h in methanol with N_2 protection)

After preoxidation of lignin (60°C, 2h in methanol with N_2 protection), only a small amount of depolymerized products (3.8wt% lignin oil) was detected in the liquid phase, in which 36% are monomers (including both small molecular aliphatic and single-ring aromatic products in this study), with the remaining as dimers and oligomers (Figure 4.3a). Small amount of aromatic products were detected (Figure 4.3b) that indicated some ether bonds were cleavage under the mild conditions.

4.3.3 The effect of with and without preoxidation

Without the preoxidation, only 23.8 wt% of lignin was converted to lignin oil (monomers: 13wt% yield; dimers & oligomers: 10.8 wt%) by PMo_{12} oxidation. However, the yield of lignin oil increased to 58.0 wt% with the preoxidation process (monomers: 30.0 wt% yield; dimers & oligomers: 28.0 wt%) (Figure 4.4a). Lignin monomers identification (by GC-MS) and quantification (by GC-FID) are extensively introduced in the supplementary materials. Total 85% of the detected monomers are aromatics with preoxidation, in which three aromatic chemicals, including methyl syringe (**13**) from S unit and methyl vanillate (**8**) and vanillin (**7**) from G unit, accounted for 64% of all monomers. Otherwise, two major products are aliphatic chemicals (**5** and **6**) that are from ring opening of aromatics. We detected intermediate of ring opening product after preoxidation (**10** in Figure 4.3b). The GC-FID spectrum (Figure 4.4a) roughly showed three regions of detected products, aliphatic (RT<18.5 min), aromatic (18.5 min<RT<24.5 min) products and dimers (>24.5 min). It suggests a possible way to separate the products mixture by distillation. Because more than 70% of the products are **13**, **8**, **7**, **5** and **6**, it has the potential to separate them.

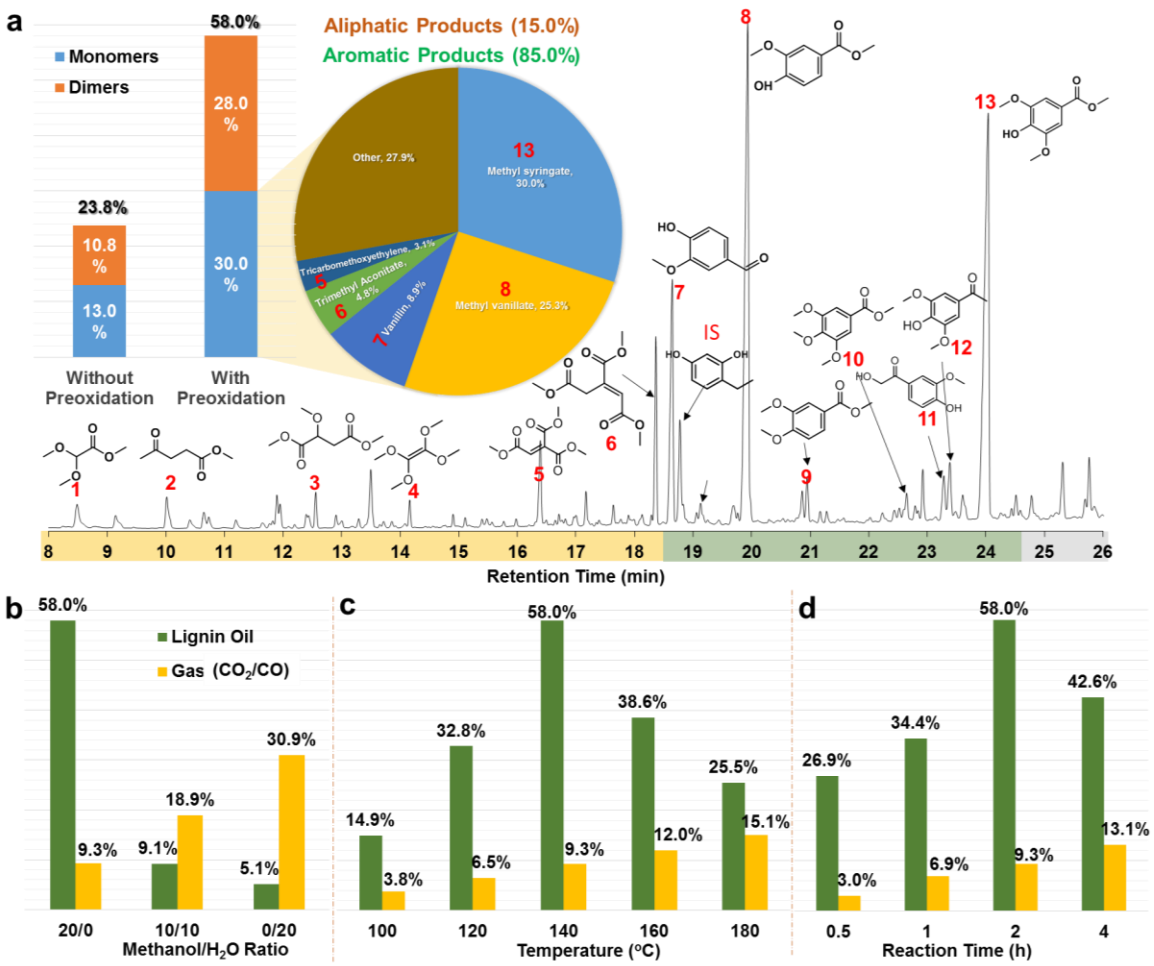

Figure 4.4 **a.** The GC-FID spectrum of with the yield of lignin oil and monomers by two-step (preoxidation-oxiation) strategy. The effects of **b.** solvent (methanol/water ratio), **c.** temperature (100-180 ˚C) and **d.** reaction time (0.5-4 h) for the yield of lignin oil and gases products (CO_2, CO). Reaction conditions for two-step reaction. Preoxidation: 0.2 g EtOH lignin, 0.05 mol/L PMo_{12}, 60˚C, 2h in methanol with N_2 protection; Oxidation: 140˚C (vary in **c**), 2h (vary in **d**), in 20 mL methanol (vary in **a**) with 10bar O_2. Reaction conditions for one-step reaction. Preparation: 0.2 g EtOH lignin, 60˚C, 2h in methanol with N_2 protection; 0.05 mol/L PMo_{12}, 140˚C, 2h, in 20 mL methanol with 10bar O_2.

4.3.4 Suppressing gases products formation during the oxidation reaction.

POMs have been applied in the delignification process in pulping, where POMs were employed to remove residual lignin. Some of these studies reported that a series of

POMs is capable to selectively break down of residual lignin in pressurized oxygen and that is possible to fully oxidize the lignin into CO_2 and H_2O in water.[137] However, the over-oxidation of the substrate to gaseous products is not in favored in our case. It is always a big issue to avoid by using oxidative methods. In our study, we found that the CO_2 production can be greatly reduced from 30.9% based on effective carbon amount of lignin in pure water solution to 9.3% by using pure alcohol as solvent (Figure 4.4b). There are two possible reasons for it. First, CH_3OH can react with carboxyl group in lignin fragments by esterification and avoid its decarboxylation to CO_2. It was confirmed by that many methyl esters only were found in depolymerized products from methanol as solvent but not water (Figure 4.5), which is consistent with previous study[134]. Second, CH_3OH can serve as radical scavenger to capture the emerged ·OH and avoid lignin fragments to further oxidation. CH_3OH can generate small radicals like $\cdot CH_3$ or $CH_3O\cdot$ that can be considered as a coupling agent to integrate with radicals from reduction of O_2 by $H\text{-}POM_{(red)}$.[134] Then it would limit the radical-chain oxidation reaction with the lignin fragments to gases products. If it is in water, the hydroxyl radical will rapidly diffuse in water via a hydrogen exchange reaction ($\cdot OH + H_2O \rightarrow H_2O + \cdot OH$)[185] and further react with lignin fragments to CO_2 and H_2O.

Methanol also greatly suppressed the repolymerization of lignin fragment radicals by competitive coupling with radical scavenger and improved the efficiency of lignin depolymerization. [134] The oxidation of lignin in methanol yields around ten times the lignin oil (58.0 wt%) compared to that in pure water (5.1 wt%). The solvent recovery and products separation is another issue need to consider. It is worth to note that methanol solvent can

be easily recovered due to its volatility and leave lignin oil and PMo_{12} remaining. Then the lignin oil is easily separated from PMo_{12} by organic solvent (e.g. DCM[111, 114]) extraction.

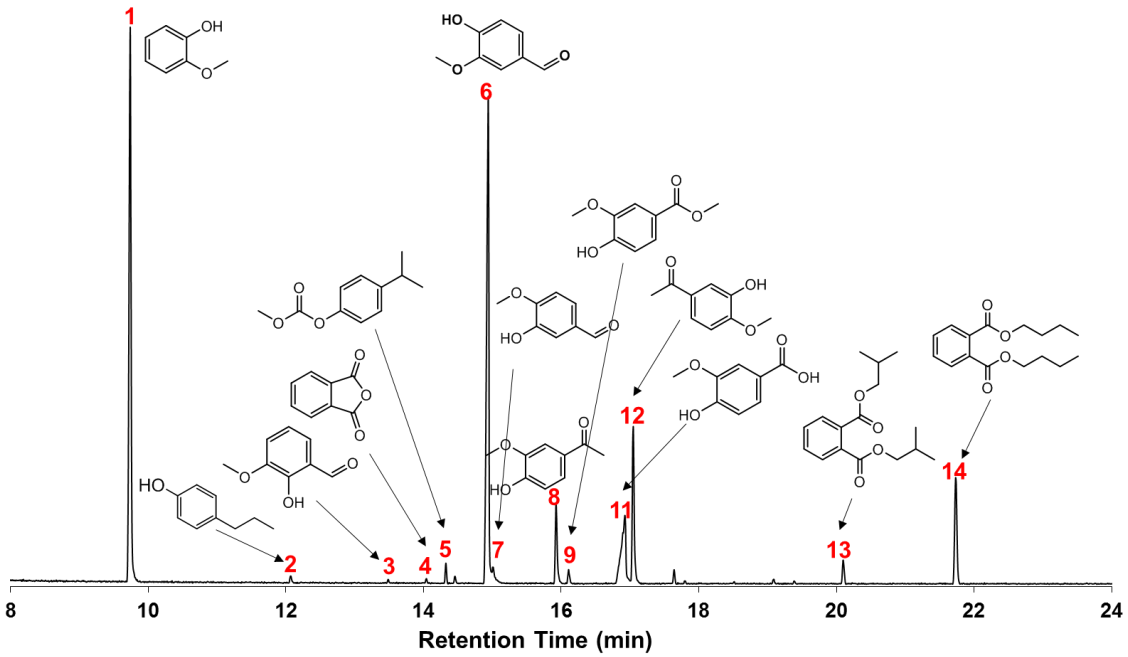

Figure 4.5 GC-MS spectrum of lignin oil after two-step (preoxodation-oxidation) in water. Reaction conditions: Preoxidation 60˚C, 2h in water with N_2 protection; Oxidation 140˚C, 2h, in water with 10bar O_2.

Besides solvent, both PMo_{12} and oxygen also play vital roles for the production of gases (CO_2 and CO) from lignin. Without PMo_{12}, only traces lignin (0.6 wt%) is mineralized to gases products which is probably because oxygen cannot oxidize lignin to CO_2 at relatively low temperature (140^{o}C). Without oxygen, only small amount of lignin (3.6 wt%) is converted to gases since PMo_{12} only acted as stoichiometric oxidant to oxidize lignin and without regeneration.

4.3.5 The effect of temperature and reaction time

The mild conditions (140 ˚C, 2 h in methanol) in this study gave a considerable yield of lignin oil (58.0 wt%). The yield increases along with the increasing temperature until to 140 ˚C and then decreases with further elevated temperature, which probably because the higher temperature can facilitate the large lignin molecules depolymerize to small fragments at first and then the small fragments are further oxidized to CO_2 (Figure 4.4c). The reaction time has the similar effect for the lignin depolymerization (Figure 4.4d). Furthermore, the longer reaction time can produce more aliphatic products due to the constant ring opening reaction (Figure 4.6). Ideally, oxidation methods should enable efficient depolymerization and avoid over-oxidation of the lignin to gases products, so the optimum reaction condition for our case was set at 140 ˚C for 2 h.

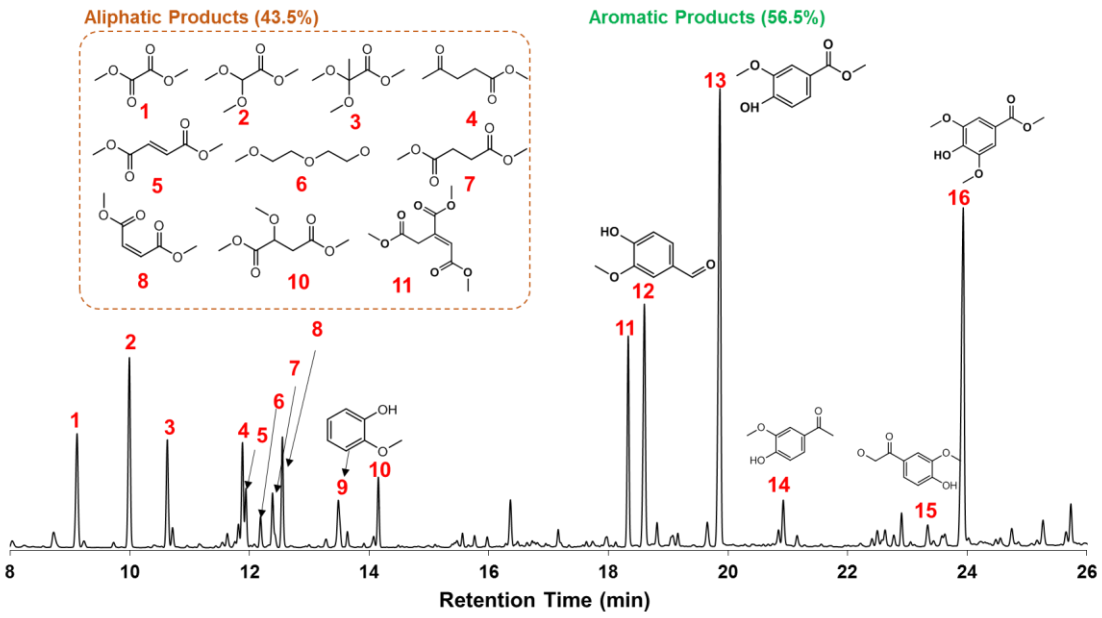

Figure 4.6 GC-FID spectrum of lignin oil after two-step (preoxodation-oxidation). Reaction conditions: Preoxidation 60˚C, 2h in methanol with N_2 protection; Oxidation 140˚C, 4h, in methanol with 10bar O_2.

4.3.6 For other lignin feedstock

We also employed this two-step strategy to other industrial lignins, including lignin isolated from supercritical water (R-lignin) and Kraft process (K-lignin). As showed in Figure 4.7, the improvement of yield of lignin oil with the preoxidation process was also observed for R-lignin (without preoxidation: 32.2 wt% vs. with preoxidation: 49.1 wt%) and K-lignin (without preoxidation: 22.7 wt% vs. with preoxidation: 31 wt%). The results suggest that the simple two-step strategy can be applied in a wide range of lignin depolymerization practices. Due the inevitable condensation during industrial lignin fractionation that restrains the lignin depolymerization, this strategy probably can perform better for native lignin.

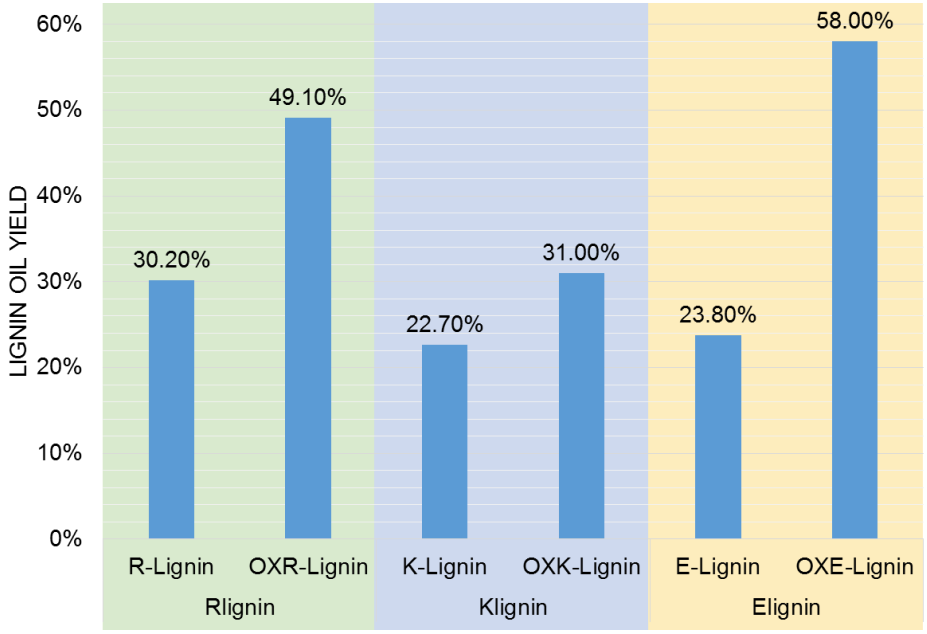

Figure 4.7 The lignin oil yield with and without preoxidation for different lignin resources. RLignin: The lignin is isolated by supercritical water extraction from hard wood, which is provided by Renmatix Inc. KLignin: The lignin is isolated by Kraft process from softwood, which is provided by Domtar Inc. ELignin is the lignin used in our study. It is isolated by ethanol extraction from hardwood, which is provided by American Process Inc.

4.4 Conclusion

In summary, we firstly developed a simple and effective two-step (preoxidation-oxidation) strategy to stabilize the active benzyl alcohols to ketones in the preoxidation process under mild condition and then further oxidize it to low molecular weight aromatics (and aliphatic products) at an elevated temperature with POM as only catalyst. The mechanism was initially studied for the lignin model compounds (β-O-4 dimer), and is further confirmed by applied in an ethanol extracted hardwood lignin. The yield of lignin oil (monomers, dimers) is more than twice with the preoxidation as without preoxidation. Only a few of dominant chemicals are present in products mixture that can enable the potential downstream purification. The solvent also plays an important role in the lignin depolymerzation. The methanol can greatly suppress the overoxidation to gases products and improve the yield of lignin oil comparing with in water. This strategy was successfully applied to different lignin feedstocks to pave an efficient and simple way for lignin depolymerization.

CHAPTER 5. LIGNIN FIRST FRACTIONATION OF WOOD TO AROMATICS BY A TWO-STEP OXIDATION METHODS‡

5.1 Introduction

In traditional lignocellulosic biorefineries, the ultimate objective is to isolate valuable products from the carbohydrate fractions, especially from cellulose. The lignin is fractionated by harsh processing conditions (e.g., Kraft, lignosulfonate, alkali pulping) in industrial delignification to avoid lignin residues in the carbohydrate. However, the lignin undergoes irreversible condensation and structural changes in such severe environment is the root reason for ineffective depolymerization of lignin.

Recently, new lignin-first concepts have been emerging out that subdue lignin condensation or degradation by employing mild operating conditions or active stabilization during biomass fractionation. [6] These new concepts intentionally put lignin valorization at the front stage of the biorefinery, which is feasible due to the rigid semi-crystalline structure of cellulose that is more resistant to degradation. Consequently, the cellulose can be valorized in a subsequent stage. One innovative strategy is the implementation of alternative media (e.g., ammonia[93-96], ionic liquid[64, 97, 98], γ-valerolacetone[99, 100]) that supports biomass decomposition under mild processing conditions. [101-103] The improved preservation of ether bonds and decreased extent of condensation further facilitates down-stream lignin depolymerization to low molecular weight chemicals. However, the milder condition needed for high ether bonds retention results in a lower yield in lignin

‡ This chapter will be submitted for publication: X Du, A Tricker, W Liu, W Yang, P Gogoi, and Y Deng*

isolation.[104] The other well-studied strategy is the simultaneous fractionation and catalytic hydrogenolysis of the native wood lignin. The lignin is extracted by solvolysis followed by immediate lignin depolymerization and reductive stabilization of reactive intermediates. [105-114] This approach can produce depolymerized lignin oil with handful monomers, dimers and short oligomers in high yield. The lignin free carbohydrates are further treated by traditional processes (e.g. enzymatic hydrolysis) to produce water soluble sugar. The key challenge is how to balance the lignin removal and keep as much as carbohydrate in the pulp. Moreover, separation of solid catalyst from the pulp is another intrinsic challenge for heterogeneous catalysis. Luterbacher *et al*. demonstrated another new fractionation strategy which applied formaldehyde to form relatively stable acetals with α- and γ-OH side-chain groups in β-O-4 linkages as well as to partially block reactive *meta*-groups by hydroxymethylation, which in turn suppress the formation of extra C-C bonds[115]. The separated lignin fractionation and the subsequent lignin depolymerization step enables more flexible lignin depolymerization methods and independent optimization of the two steps. However, a sacrificial reagent, relative harsh conditions, and organic solvents are necessary for this approach.[6]

Polyoxometalates (POMs), as chlorine-free oxidizing reagents, have been extensively studied for delignification in the pulping process due to the low redox potential of lignin compared with polysaccharides.[132, 136, 137, 181, 186-192] However, most of these studies aimed to extract and completely oxidize the lignin to CO_2 and H_2O (not chemicals) in aqueous solution, [35, 186]. Accordingly, their efforts focused on synthesizing specific POMs that **a)** possess high redox potential (with vanadium, manganese substituted) to fully oxidize lignin, **b)** can be re-oxidized by oxygen in aqueous media (the limiting step) to

adapt to the industrial pulping process, and **c)** can work in neutral pH to avoid carbohydrate hydrolysis.

To enable efficient lignin fractionation and depolymerization to chemicals, we devised a distinct two-step (fractionation-depolymerization) oxidative catalysis strategy that employs a low concentration of POM. The lignin is stabilized and fractionated from the lignocellulose at mild conditions and then further deconstructed to lignin oil in a subsequent depolymerization step. In this study, the application of the POM in this two-step manner offers several distinct advantages over previous POMs delignification studies including a) POMs can be used to remove lignin without over oxidation and easily re-oxidized by oxygen in an alcohol solvent at low temperature, b) the isolated lignin in solution can be further oxidized to chemicals at an elevated temperature with oxygen, and c) separation of the lignin fractionation and depolymerization steps enables broader POMs choices and independent optimization. The first two advantages of POM use in lignin treatment have been verified in Chapter 4. Importantly, two-step POM oxidation provides a lignin-first organosolv fractionation methodology to extract, stabilize, and disperse native lignin in alcohol without suffering condensation. This approach differs from current delignification processes (e.g. Kraft, lignosulfonate, organosolv) by achieving effective lignin separation and depolymerization while preserving the carbohydrate pulp.

5.2 Experimental section

5.2.1 Materials

Wood chips used in this study were acquired from a poplar, birch or loblolly pine tree from Georgia, USA. The sawdust was obtained by a Wiley mill with a 0.13 cm screen, and then dried 50 °C for 48 h in an oven.

5.2.2 Lignin fractionation and depolymerization.

For the lignin fractionation step, a Parr reactor (100 ml) was charged with 1 g wood sawdust (40 mesh), 0.1825 g (0.0025 mol/l) PMo_{12}, and 40 ml of methanol. The reactor was sealed and pressurized with 10 bar oxygen at room temperature. The reactor was heated to 100 °C for a predetermined time with 300 rpm stirring. A benchmark experiment was carried out by using 0.0025 mol/L H_2SO_4 in the same conditions[193]. The vessel was cooled to room temperature by put in cold water after reaction. Gases were collected and measured by water displacement for GC analysis. The yield of gases was calculated by effective carbon number. The solid was filtered by qualitative filter paper (Whatman filter paper, 1004-027 Quantitative), and washed with methanol. The solid was air dried and weighed for the determination of carbohydrates and lignin. The collected mixture solution was directly analyzed or treated with a lignin depolymerization step. For analysis, the solvent was removed with a rotary evaporator at 50°C. The dried residue was then dissolved in 25 ml of THF to extract lignin, leaving the catalyst and carbohydrates as precipitates. Then the THF solution was completely evaporated at 50°C overnight under vacuum to complete dryness. The extracted lignin was weighed and 100 μL of internal standard naphthalene was subsequently added. 5 mg of the extracted lignin were dissolved

in 1mL of THF for GPC analysis and 10 mg were dissolved in 1 mL DCM for GC-MS and GC-FID analysis.

When the mixture solution was used for the lignin depolymerization, the solution was moved to Parr reactor (100 ml) and pressurized by 10 bar of oxygen at room temperature. Then the reactor was heated to determined temperature (e.g. 140 °C) and time with 300 rpm stirring. Similarly, the reactor was cooled to room temperature, and the gases were collected for GC analysis. The solution was evaporated in a rotary evaporator at 50°C. Then the dried residual was extracted three times by DCM (10 mL×3 times). Lignin products (monomers and dimers/trimers) were extracted into DCM phase noted as extractable lignin oil. Then the separated DCM solution was completely evaporated at 50°C overnight under vacuum to obtain lignin oil. The lignin oil was weighed and then dissolved in 2 ml of DCM with the internal standard naphthalene for further GC-FID and GC-MS analysis.

5.2.3 Determination of structural carbohydrates and lignin in biomass.

The Klason lignin and carbohydrates (cellulose and hemicellulose) contents in sawdust are determined by the NREL laboratory analytical procedures for standard biomass analysis.[194] The method is summarized as following:

Prepare clean and dry filtering crucibles with constant weight. Weigh 300.0 mg of the sample or QA standard into a tared pressure tube. Add 3.00 mL of 72% sulfuric acid to each tube. Use a Teflon stir rod to mix until the sample is thoroughly mixed. Place the pressure tube in a water bath set at 30 °C and incubate the sample for 60 minutes. Using the stir rod, stir the sample every 5 to 10 minutes without removing the sample from the

bath. After 60 minutes hydrolysis, dilute the acid to 4% concentration by adding 84 mL of deionized water. Mix the sample by inverting the tube several times. Autoclave the sealed samples for one hour at 121°C. After completion of the autoclave cycle, allow the hydrolyzates to slowly cool to near room temperature before removing the caps.

Vacuum filter the autoclaved hydrolysis solution through the previously weighed filtering crucible and collect the filtrate in a filtering flask. Transfer 50 mL of the filtrate into a sample storage bottle. This sample will be used to determine acid soluble lignin and carbohydrates. Use deionized water to quantitatively transfer all remaining solids out of the pressure tube into the filtering crucible and rinse the solids. Dry the crucible containing acid insoluble residue at 105 °C for 6 hours. Remove the samples from the oven and cooled in a desiccator. Record the weight of the crucible and dried residue to the nearest 0.1 mg.

5.2.4 Analysis and characterization of isolated lignin and lignin oil.

Isolated lignins were characterized by NMR and GPC. (see section 2.3) Lignin oil separation, identification, and quantification were performed using GPC, GC, GC-MS/FID analysis, and yield calculation (see section 2.3)

5.3 Results and discussion

5.3.1 The catalytic strategy for lignin fractionation and depolymerization

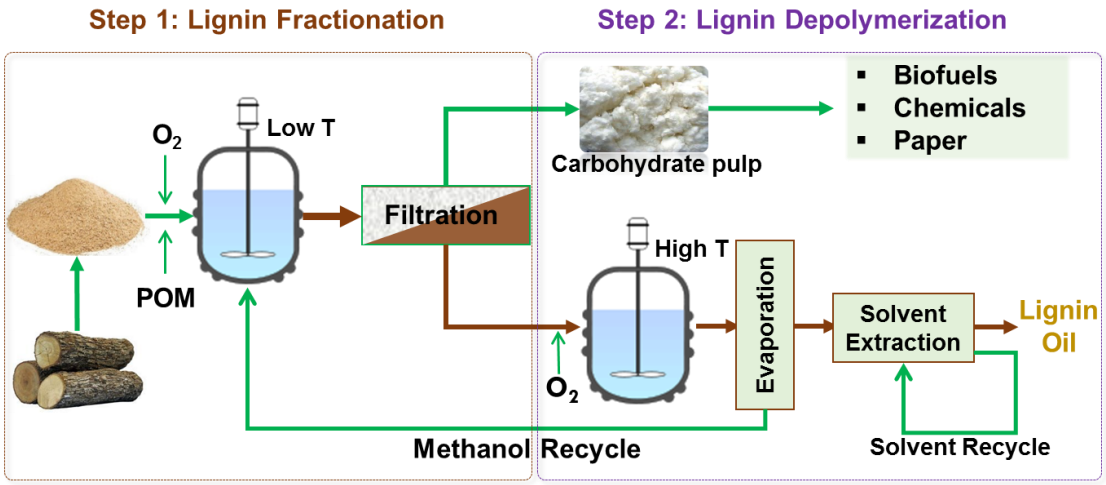

Figure 5.1 Comprehensive catalytic strategy for lignin fractionation and depolymerization towards complete lignocellulose utilization. Lignocellulose is used without pretreatment and is fractionated to lignin and carbohydrate pulp streams for further conversion. Step 1: The lignin and some lignin products are fractionated from lignocellulose under mild conditions. Step 2: the isolated lignin is further depolymerized to lignin oil and filtered carbohydrate pulp can be moved for further utilization.

The full picture of catalytic strategy established here consists of two steps (Figure 5.1). To obtain a high phenolic monomer yield, requires the fulfillment of two conditions: lignin fractionation from the lignocellulosic matrix followed by dissolution of the lignin fragments without condensation (step 1) and lignin depolymerization by ether or carbon-carbon bond cleavage without condensation (step 2). At the core of this strategy is the flexible use of polyoxometalates (POM) in these two distinct steps. In first step (lignin fractionation), the POM can isolate the lignin (and part of hemicellulose fraction) into methanol from lignocellulose under mild conditions. The POM also can selectively oxidize

the benzyl alcohols in lignin to ketones to avoid their condensation, as shown by my previous study and other studies[137, 181]. In the second step, the carbohydrate pulp can be easily filtered out for further treatment to make biofuels, chemicals, and paper. The remaining lignin will be further depolymerized by POM in methanol with oxygen at an elevated temperature. To verify the effect of our process, each step was fully examined by employing a set of reactions.

5.3.2 Step 1: Lignin fractionation by using PMo_{12} as a catalyst at mild condition

The composition of raw poplar sawdust (40 mesh) was analyzed according to the procedure described in above (section 5.2.3). The mass percentages of (hemi)cellulose, lignin and extractives in raw poplar sawdust were 76.4 wt%, 22.0 wt%, and 1.6 wt%, respectively (entry "original" in Figure 5.2). The results are consistent with a previous study.[18] Figure 5.2 shows the yield of (hemi)cellulose and lignin in solid fraction and in the liquid fraction from different fractionation conditions. The compositional analysis of the solid fraction was conducted using the same procedure as the poplar sawdust. The (hemi)cellulose pulp yield and delignification degree were calculated by following equations:

$$(Hemi)cellulose\ pulp\ yield\ (wt\%) = \frac{m_P}{m_0} \times 100\%$$

$$Delignification\ (\%) = \left(1 - \frac{m_{L_s}}{m_{L_o}}\right) \times 100\%$$

in which, m_P and m_0 are the mass (g) of recovered (hemi)cellulose pulp and raw poplar sawdust, respectively, and m_{Ls} and m_{Lo} are the mass (g) of lignin in solid fraction and in original poplar sawdust, respectively.

Isolation of the lignin (or its fragments) from the lignocellulose matrix requires (i) either breaking the ester linkages in lignin-carbohydrate complexes [195, 196] or (ii) partially cleaving the ether linkages in lignin to depolymerize the native lignin.[114] Then the native lignin will be disentangled and released into the solvent. Different fractionation conditions were explored, such as different catalysts (PMo_{12}, H_2SO_4), different solvents (methanol, water and their mixture) and reaction conditions (gas pressure, concentration of catalyst).

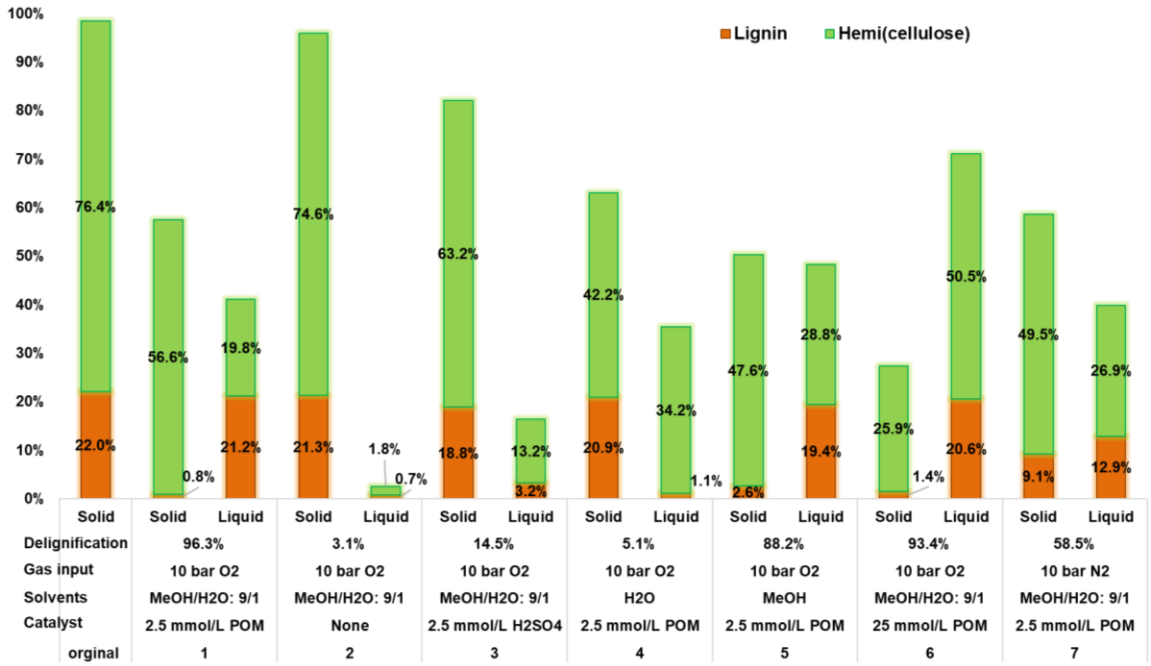

Figure 5.2 The fractionation of lignin from poplar sawdust under different conditions (100 ˚C, 2h)

PMo_{12}, H_2SO_4 and without catalyst were tested to study their efficiency for fractionation of poplar sawdust. Without catalyst (Figure 5.2, entry 2), the poplar sawdust was treated in methanol/water (v/v: 9:1) at 100 ˚C with oxygen for 2 hours. The lignin and (hemi)cellulose in liquid fraction was only 2.5 wt% (with 1.8 wt% (hemi)cellulose and 0.7 wt% lignin). The delignification was as low as 3.1%. H_2SO_4 (2.5 mmol/L), a commonly used catalyst in organosolv pulping process, showed a slightly higher delignification degree (14.5%) and liquid fraction (16.4 wt%) (Figure 5.2, entry 3). When PMo_{12} (2.5 mmol/L) was used, the delignification degree further increased to 96.3%, with a (hemi)cellulose pulp yield of 56.6 wt% (Figure 5.2, entry 1). This result is comparable with ethanol organosolv pulping process (54.3% pulp yield, 195 ˚C, 210 min in ethanol/water (v/v: 6:4))[197]. Due to the acidic property of PMo_{12}, its concentration has a significant effect on pulp yield. With a PMo_{12} concentration of 25 mmol/L (Figure 5.2, entry 6), 10 times higher than in entry 1, a good delignification degree was obtained (93.4%) but with a much lower pulp yield (25.9%) due to the severe hydrolysis of the cellulose and hemicellulose. The results indicated that low concentration of PMo_{12} can give a high pulp yield and high delignification degree at the same time.

After treatment in pure water (Figure 5.2, entry 4), the delignification degree was only 5.1%. Pure water is not a good solvent for the delignification process under mild conditions. Moreover, oxygen was not able to reoxidize PMo_{12} at 100 ˚C in water (as shown in my previous study), and so the PMo_{12} could only be used as a stoichiometric oxidant; similar as when the oxygen is replaced by nitrogen (Figure 5.2, in entry 7). Pure methanol as a solvent gave better results for delignification (88.2%) with good pulp yield (47.6 wt%), but still performed worse than the mixture of methanol and water (v/v: 9:1) (Figure 5.2,

entry 1). The alcohol concentration applied during pulping was found to have a major effect on the pulp yield in previous studies. [197, 198 197, 198 197, 198197, 198] Lower alcohol concentration leads to more extensive hemicellulose hydrolysis and dissolution under the increasing acidity.

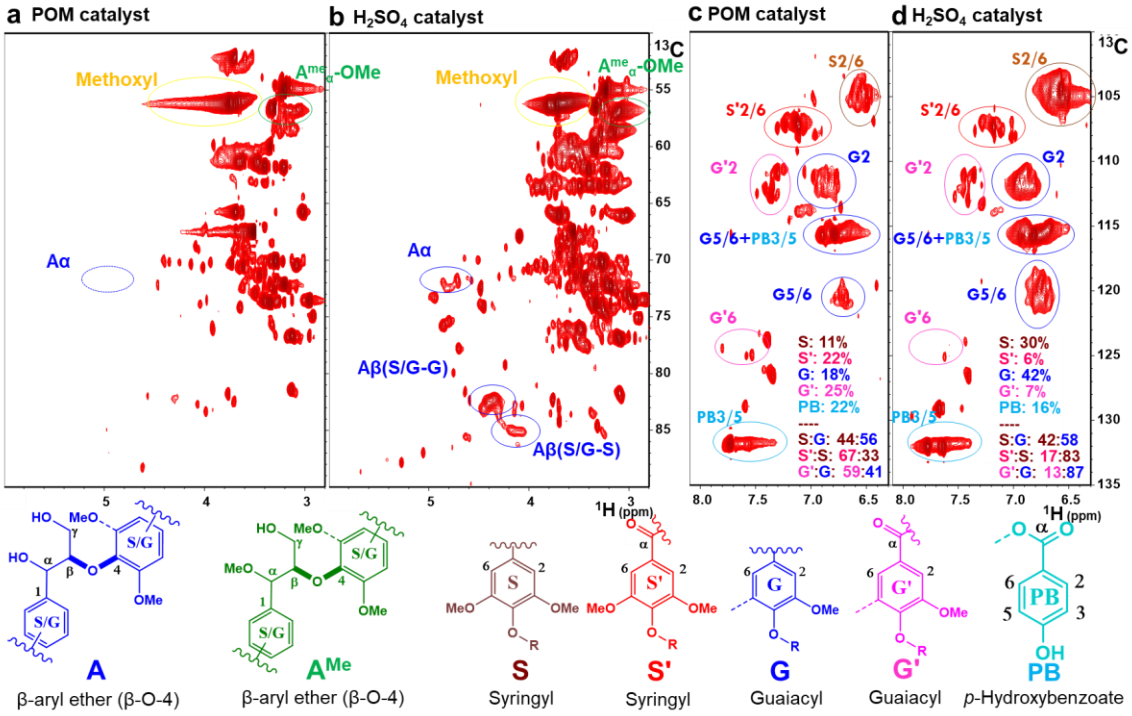

Figure 5.3 2D HSQC NMR analysis (700 MHz, d_6-DMSO) of: a) aliphatic region and c) aromatic region of isolated lignin from poplar using PMo_{12} as catalyst; b) aliphatic region and d) aromatic region of isolated lignin form poplar using H_2SO_4 as catalyst. Contours are cycled by color according to the structures to which they have been assigned.

Methanol can be used as etherification reagent to modify the C_α–OH group in β-O-4 linkages with water assistance during the lignin fractionation process, as shown in a previous study by Liu et al.[199] This facilitates the lignin depolymerization by avoiding condensation. The esterification of lignin structure was confirmed by 2D HSQC NMR (Figure 5.3) by the appearance of the C_α–OH methylated β-O-4 (**A^{Me}**) signals. The methyl

group in $\mathbf{A^{Me}}$ was observed at δC/δH 56.5:3.15 (Figure 5.3 a,b). As discussed in my previous study (chapter 4), the PMo_{12} can also oxidize the C_α–OH group to C_α=O under mild conditions to suppress condensation. The aromatic regions (Figure 5.3c,d) supported the conversion of benzylic alcohols to their analogues ketones. The data unveil that more benzylic alcohols units in native lignin were oxidized to ketones (22% **S′**; 25% **G′**) using PMo_{12} as a catalyst compared with the distribution (6% **S′**; 7% **G′**) using H_2SO_4 as a catalyst. Similarly, the assignments of β-aryl ether (**A**, **A′**), resinol (**C**), **S** (**S′**) and **G** (**G′**) units are based on previous studies. [2, 182-184] With both the methanol esterification and PMo_{12} oxidation of C_α–OH effects, the isolated lignin was released and stabilized in methanol for further depolymerization. Due to the higher temperature (100 ˚C) than in the preoxidation step of chapter 4 (60 ˚C), a small part of lignin was depolymerized to some smaller fragments (shown in Figure 5.4), including some monomers and dimers. The block units of hemicellulose (product 3 and 6 in Figure 5.4) were observed since part of hemicellulose was hydrolyzed and degraded by acid PMo_{12}.

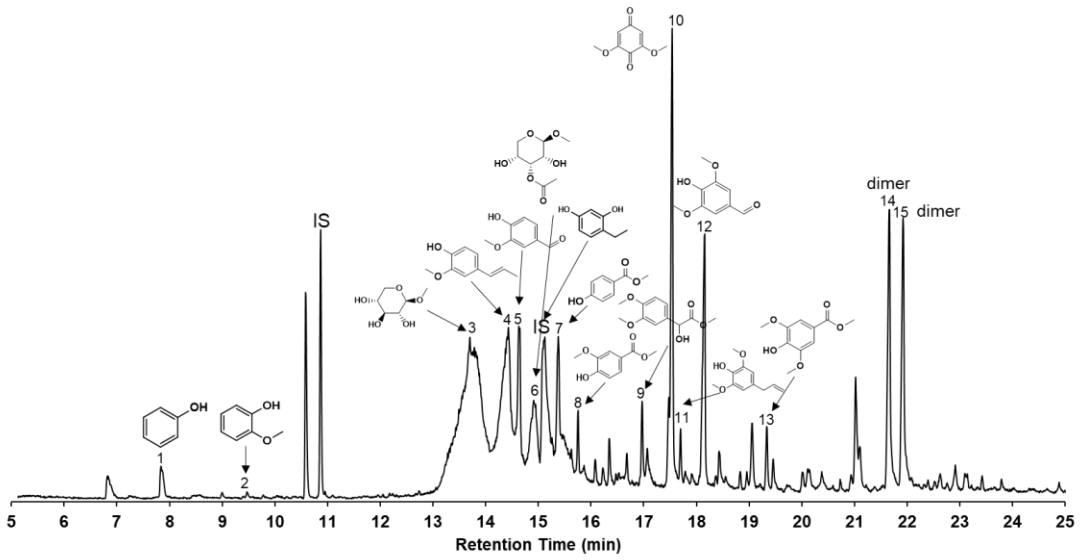

Figure 5.4 GC-MS spectrum of lignin fragments in isolated lignin after fractionation (100˚C, 2h in methanol/water (9:1) with 10 bar O_2)

5.3.3 Step 2: Fractionated lignin depolymerization by PMo_{12} as catalyst at elevated temperature

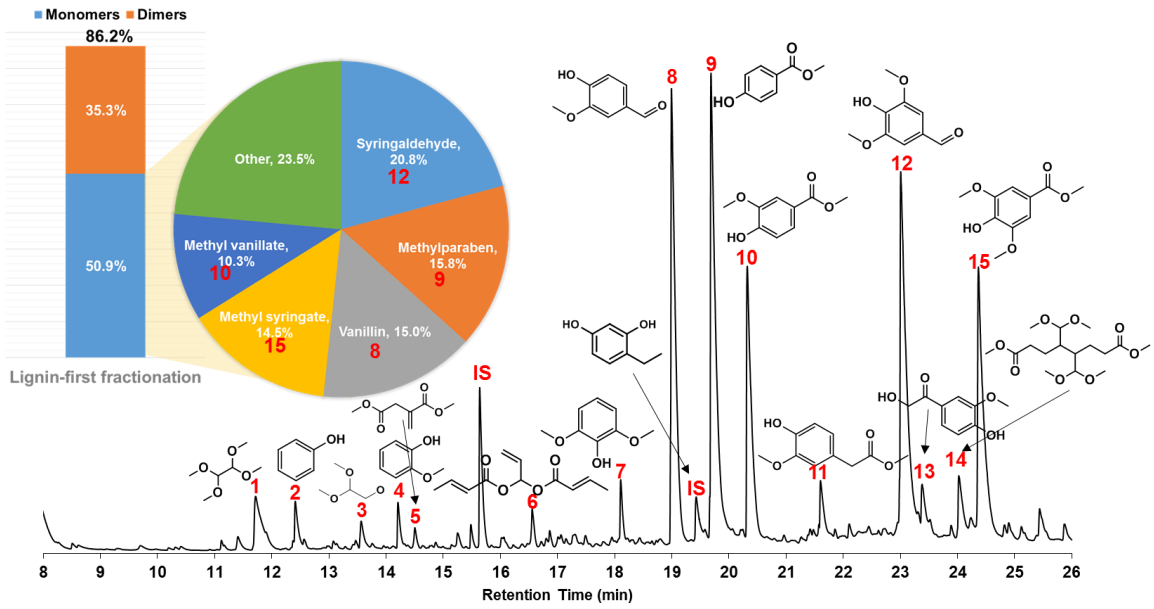

Figure 5.5 The GC-FID spectrum of lignin oil by lignin-first strategy with yields of monomers & dimers and its 5 major monomers. Lignin fractionation: 1 g poplar sawdust, 2.5 mmol/L PMo_{12}, 100˚C, 2h in methanol/water (9:1) with 10 bar oxygen; Lignin depolymerization: 140˚C, 2h, in methanol/water (9:1) with 10 bar oxygen.

As elaborated in the discussion of step 1, the lignin was effectively fractionated from the lignocellulosic matrix in a methanol/water mixture by low concentration of PMo_{12} with oxygen at low temperature (Figure 5.2, entry 1). The solid (hemi)cellulose pulp and liquid lignin (with some hemicellulose) fractions can be easily separated by filtration. The solid stream can be further used for paper making, bio-ethanol production by fermentation or other biochemicals production. The liquid stream will be further treatment by the PMo_{12}

inside under an evaluated temperature with oxygen. As studied in chapter 4, the fractionated lignin was treated at 140 ˚C for 2 hours for depolymerization to low-molecular-weight (LMW) products (lignin oil). As shown in Figure 5.5, the yield of lignin oil is 86.2 wt% (monomers yield: 50.9 wt%; dimers yield: 35.3 wt%). This is much higher than the best result (58%) using ethanol lignin in Chapter 4. Total 86.8 wt% of the detected monomers are aromatics, in which five aromatic chemicals, including syringaldehyde (**12**), methyl syringe (**14**) from S unit, methyl vanillate (**10**) and vanillin (**8**) from G unit and methylparaben (**9**) from H unit, accounted for 76.5% of all monomers.

The overall catalytic approach and the mass balance obtained with poplar lignocellulose are shown in Figure 5.6. Our results suggest that the PMo_{12} fractionated lignin can be further depolymerized to LMW products by PMo_{12} at elevated temperature with high yield without a solvent or catalyst separation step.

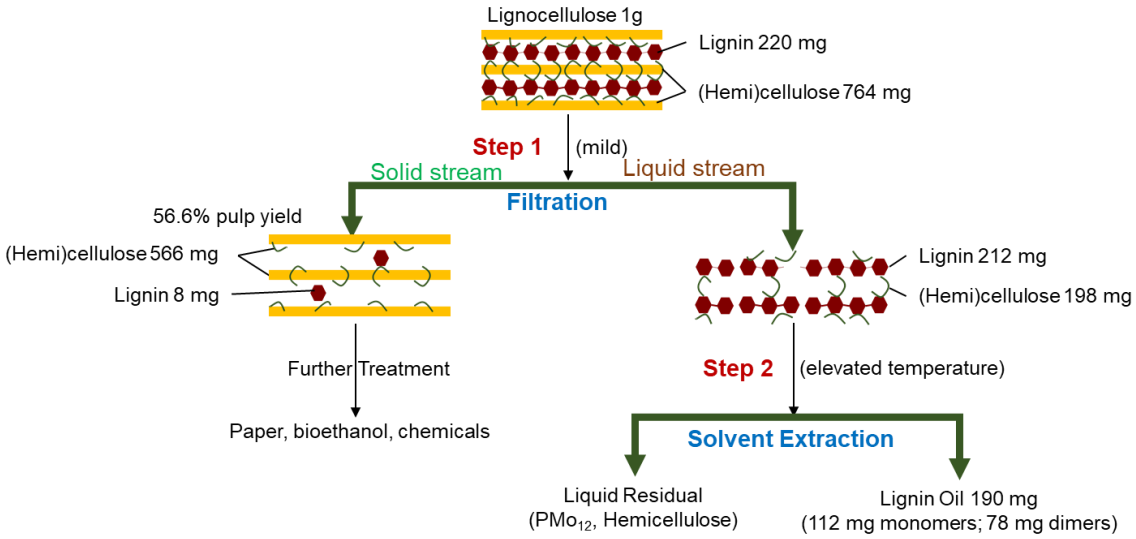

Figure 5.6 Schematic representation of the overall catalytic approach and mass balances obtained with poplar lignocellulose. This strategy includes lignin fractionation (step 1) and depolymerization (step 2).

5.4 Conclusion

A lignin-first fractionation and depolymerization strategy towards complete utilization of lignocellulose has been developed by using PMo_{12} as the only catalyst. In this study, a low concentration of PMo_{12} catalyst is employed to fractionate lignin (and lignin fragments) from wood sawdust under mild conditions (100 °C) in mixture of methanol and water. A high delignification degree (96.2%) while avoiding structural lignin condensation by methanol esterification and POM oxidation of C_{α}–OH groups in the β-O-4 linkages. Then extracted lignin was further oxidized to low molecular weight products with an 86.2 wt% yield. The remaining cellulose can be further used to produce bio-ethanol, allowing complete biomass valorization. Finally, the approach described here will inspire the development of novel biorefineries for effective lignin isolation and utilization in industry.

CHAPTER 6. POM-MEDIATED ELECTROLYSIS FOR SIMULTANEOUSLY LIGNIN DEPOLYMERIZATION AND HYDROGEN EVOLUTION [§]

6.1 Introduction

As introduced, lignin has great potential to be a renewable source of aromatic chemicals in the future. Usually, the widely used thermal catalytic depolymerization processes are employed at relatively high temperatures and pressures. Catalyst recovery and aging under harsh conditions are often serious technical obstacles to achieve a practical, cost-effective process. Conversely, electrochemical depolymerization is a potential approach for highly sustainable conversion with electrons serving as the reagent. Therefore, the conversions can be considered as low cost, reagent free, environmentally friendly method, and are possibly performed at mild process conditions.

Moreover, with high hydrogen content, lignin is also a potential renewable resource for the sustainable generation of the cleanest fuel – hydrogen. Unfortunately, the current technologies either completely degrade biomass or lignin to syngas (no lignin chemicals are produced) or depolymerize lignin to chemicals but not produce hydrogen. Therefore, simultaneously depolymerize lignin to value added chemicals and produce hydrogen will be a great pathway for biorefinery industry. Hydrogen as the most promising energy carrier in future has attracted considerable interests in recent years. Currently, around 95% (~15

[§] The full data of this research were accepted for publication in ChemSusChem, 2017. Reprinted with permission from "X Du, W Liu, Z Zhang, A Mulyadi, A Brittain and YL Deng. Low energy catalytic electrolysis for simultaneously hydrogen evolution and lignin depolymerization to valuable chemicals. *ChemSusChem*. 2017, 10:847-854." Copyright 2017 WILEY-VCH. Part content of this chapter was accepted for publication in Energy & Environmental Science. Reprinted with permission from "W. Liu, Y. Cui, X. Du, Z. Zhang, Z. S. Chao, Y. L. Deng, High efficiency hydrogen evolution from native biomass electrolysis Energy & Environmental Science 2016, 9, 467-472." Copyright 2016 The Royal Society of Chemistry.

trillion mol per year) of the world's supply of H_2 is obtained by petroleum reforming and coal gasification.[200] Because biomass is one of few currently available renewable energy sources, a biomass based route for sustainable hydrogen generation is highly attractive.[201]

Hydrogen production from biomasses includes a variety of developing technologies, including thermo-conversion, photoelectrochemical conversion, fermentation, and electrolysis.[202] Biomass thermo-conversion (e.g., gasification, pyrolysis and water/steam treatment etc.) presents a possible large-scale hydrogen production route from agricultural or forestry residues,[203] but there are also some technical barriers including low heat efficiency, poor catalyst durability, and impurities in the product etc.[204] The photoelectrochemical (PEC) process and fermentation are promising approaches for hydrogen production from biomasses and derivatives.[205, 206] However, the low hydrogen generation rate of the PEC process and fermentation has still not been overcome yet so they are difficult to be practically adopted.[204] The electrolysis process provides a quick and convenient approach to produce pure hydrogen. The PEM electrolyzers are commonly used for electrolysis of water, which is a mature and scalable technology for sustainably producing H_2 with only water and an energy input. Water is oxidized to produce oxygen and proton (H^+) at anode ($H_2O \rightarrow ½\ O_2 + 2H^+ + 2e^-$), and H^+ combined with electron (e^-) from external circuit to produce hydrogen at cathode ($2H^+ + 2e^- \rightarrow H_2$). However, PEM water electrolysis cannot be efficiently performed in a PEM electrolyzer without using noble-metal catalysts (such as iridium or platinum) at both anode and cathode. Besides, in order to split water into H_2 and O_2, the applied potential must be higher than the standard potential of 1.23 V. Practically, the cell potential usually ranges from 1.6 V to 2.0 V to obtain current density 1 A cm^{-2} even with noble-metal catalysts.[207] Therefore, replacing anodic oxygen evolution with the oxidation of much more easily oxidizable species leads to a great reduction of the potential required to produce hydrogen. With this strategy, different biomass derivatives including methanol[208-210], ethanol[211-213] and glycerol[214] were

oxidized to substitute water. Chen *et al.* designed a catalyst by coating palladium nanoparticles on a 3D nanostructured titanium dioxide nanotube arrays, which greatly improved the performance of the PEM electrolyzer using ethanol.[215] However, the noble-metal catalyst is only effective for alcohol electro-oxidation, but not for native biomass.

Polyoxometalates are water-soluble molecular metal-oxide clusters that have been used in photocatalytic water splitting.[216] In some advanced research studies, POMs were used as the electron-coupled-proton buffer in water electrolysis for decoupling hydrogen and oxygen evolution.[200, 217] Herein, we present a novel chemical-electrolysis conversion (CEC) process utilizing polyoxometalates as both a catalyst and an electron–proton carrier for hydrogen generation directly from lignin. In this process, lignin can be effectively decomposed *via* a chemical conversion by aqueous POM at low temperature and followed by electrolysis with very low electric energy input to generate hydrogen.

6.2 Experimental section

6.2.1 Materials

The lignin used in the experiments included: (1) pine Kraft lignin (KL) was donated from a North American kraft pulp company, (2) alkline lignin (AL) was purchased from Sigma Aldrich, and (3) sulfonated lignin (SL) was purchased from Sigma Aldrich. Details and other chemicals used in this study was shown in 2.1 section of this dissertation.

6.2.2 Lignin oxidation with POM

See section 2.2.3 for details.

6.2.3 POM-mediated electrolysis process

See section 2.2.4 for details.

6.3 Results and discussion

6.3.1 The POM-mediated PEM electrolysis process

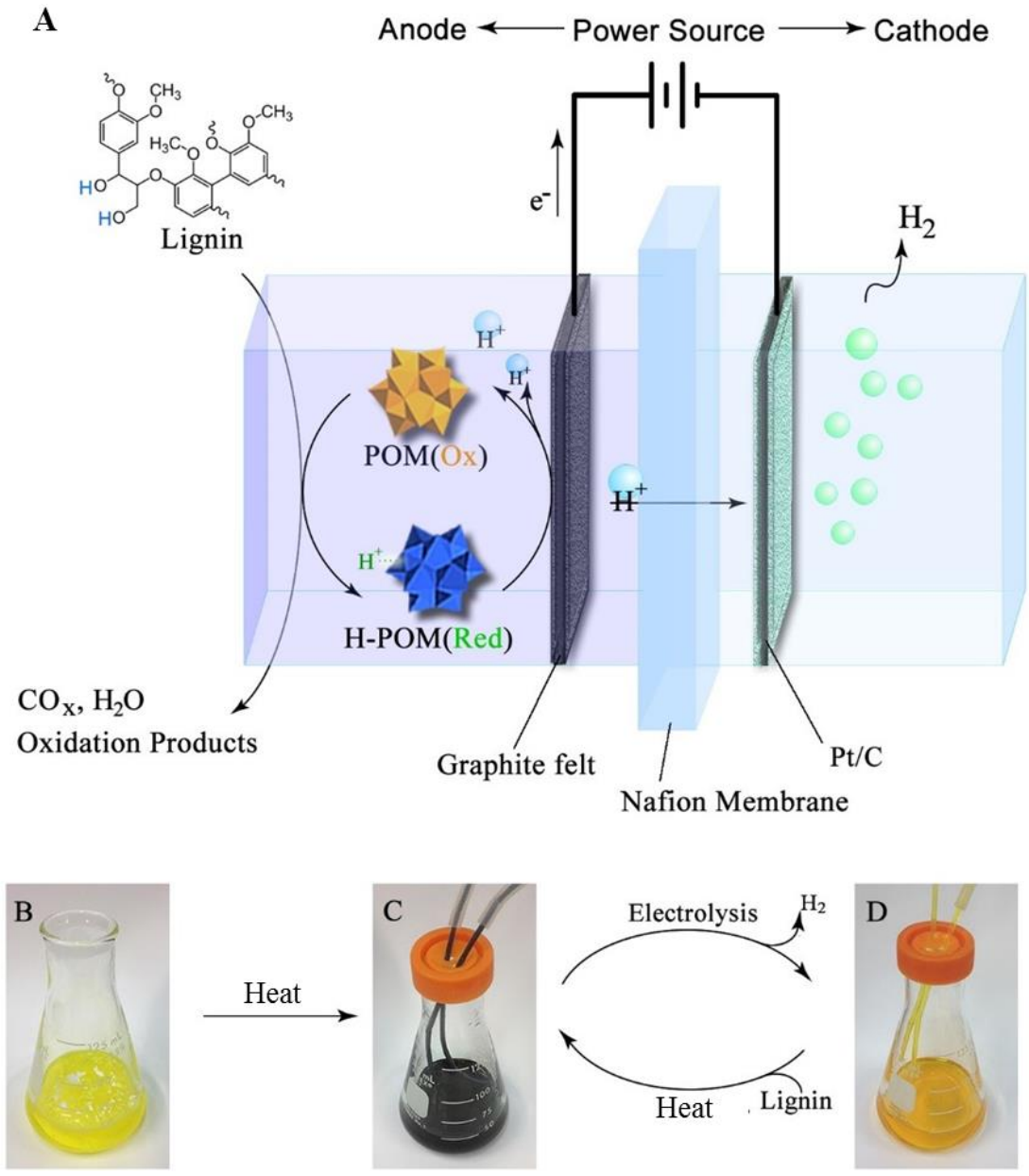

Figure 6.1 (A) Schematic illustration of the chemical-electric conversion process. The anode is a simple graphite-felt electrode; the cathode is a gas-diffusion electrode loaded with the Pt black catalyst (4 mg cm^{-2}). (B) Solution of POM–lignin before heating. (C) The color change of lignin–POM mixture after heating. (D) The lignin–POM solution after the electrolysis for hydrogen production.

The chemical-electrolysis conversion process was conducted in a common PEM electrolysis cell, which is schematically illustrated in Figure 6.1. The proton exchange membrane was sandwiched between a simple graphite-felt anode without coating any catalyst and a carbon cathode coated with a Pt black catalyst (4 mg cm^{-2}) for hydrogen evolution. In POM-lignin system, this conversion process can be realized by two steps.[128] At the first step, the lignin–PMo_{12} (PMo_{12}: 0.1 mol/L) mixture gradually changed the color from initial yellow to dark blue (shown in Figure 6.1C), indicating the reduction of POM and the oxidation of lignin under heating due to the redox potential of POM (0.8-1 V vs. NHE) is high enough to oxidize lignin [35] (eqn 6.1). At the second step, the electrolysis carried out by applying an electric potential to the anode and the cathode (shown in Figure 6.1A). At the same time, the obtained lignin–POM solution was pumped into the anode and the phosphoric acid aqueous solution (1 mol/L) was pumped into the cathode side of the electrolysis cell. During the electrolysis, the reduced POM was gradually electro-oxidized, and turned back to yellow (eqn 6.2); hydrogen bubbles released from the cathode outlet and was collected (eqn 6.3). When the reduced POM blue completely turned to yellow at the anode side (shown in Figure 6.1D), a chemical-electrolysis conversion cycle was completed. Experimentally, the lignin–POM solution could be heated *in situ* with the circulation in the electrolyzer to generate hydrogen.

$$POM_{Ox} + H_2O + \text{Lignin} \xrightarrow{\Delta} \text{H-}POM_{Red} + CO_2 + \text{Oxidized products} \quad (6.1)$$

$$\text{H-}POM_{Red} \xrightarrow{\text{Anode}} POM_{Ox} + H^+ + e^- \quad (6.2)$$

$$H^+ + e^- \xrightarrow{\text{Cathode}} 1/2\ H_2 \quad (6.3)$$

This electrolyte pair mediated PEM electrolyzer has several advantages than traditional electrolysis, including (1) the lignin feedstock can be directly oxidized to small molecules by POM under mild conditions (100^{o}C heating in this study) at the anode side; (2) POM can replace the noble metal catalyst (e.g. Platinum, Iridium) at the anode

electrode; (3) energy consumption is greatly reduced because the anodic oxygen reduction was replaced by low oxidation stage POM_{red} ions; and (4) POM are chemically and thermally stable, and are completely regenerated during the electrolysis process.

6.3.2 The POM reduction by oxidation of lignin

Several commercial lignins including Kraft softwood lignin, alkali lignin and sulfonated lignin were used as the feedstock. PMo_{12} at a concentration of 0.1 mol/L was used to oxidize the three lignins at 10 g/L under 100℃ with N_2 protection. The PMo_{12} acted as a stoichiometric oxidant when the reaction carried out under an inert atmosphere, so the oxidation of lignin was accompanied by the reduction of the PMo_{12}. The reduction degree of PMo_{12} was defined as the average number of electrons (in moles) that were transferred from the lignin to one mole of the PMo_{12} anion.[128] Because the light absorbance of reduced PMo_{12} at the wavelength of 700 nm is linearly related to the reduction degree, it can be used to determine the reduction degree of POM (Figure 2.3).[140] As shown in Figure 6.2, the reduction degree of PMo_{12} suddenly increased in the first 3 hours, and then slowly increased to 2.18, 2.17 and 2.10 for KL, AL and SL after 28 hour reaction, respectively. It should be noted that the reduction degree of PMo_{12} in the SL solution increased faster than KL and AL in the first hour, but finally lower than KL and AL after 28 h reaction. It is probably because the SL can easily dissolve into PMo_{12} -water solution, so the good mixing of SL and oxidant benefited the reaction firstly. For the KL and AL, they both were particle suspensions during the reaction at first and gradually dissolved into the mixture solution along with the reaction.

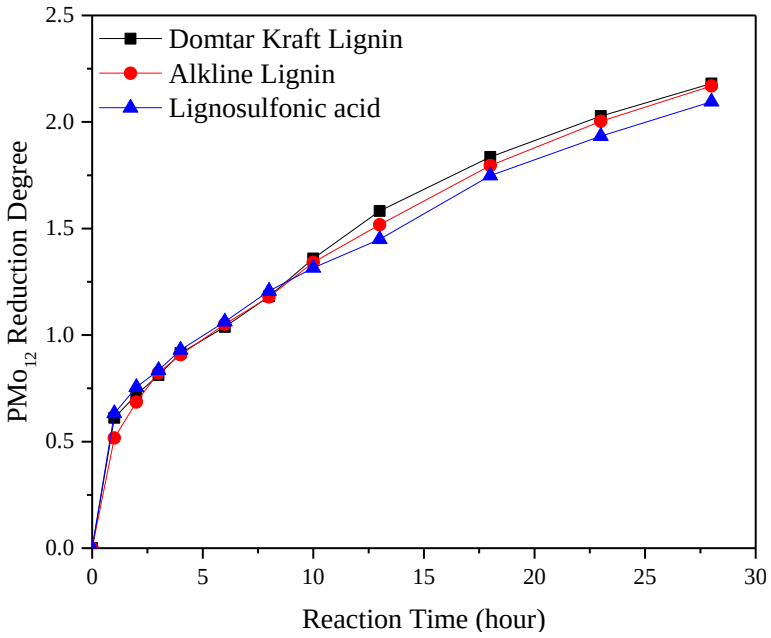

Figure 6.2 The PMo_{12} reduction degree along with the PMo_{12} (0.1 mol/L) reacted with KL, AL and SL under mild conditions. Reaction conditions: KL/AL/SL (10 g/L), PMo_{12} (0.1 mol/L), 100℃ under N_2 protection.

6.3.3 The performance of POM-mediated electrolysis

To verify the role of PMo_{12} in lignin PEM electrolyzer, two control tests were conducted with phosphoric acid (H_3PO_4, 1 mol/L) or H_3PO_4 with KL (10g/L lignin in 1 mol/L H_3PO_4) without PMo_{12} in anode respectively. As shown in Figure 6.3a, no obvious current was detected in both control tests even when the applied potential was 1.2 V which is lower than the standard potential of water electrolysis (1.23 V). Moreover, the graphite electrode at anode possess large over-potential for oxygen evolution reaction in both H_3PO_4 solution and KL suspension without POM. Therefore, the lignin alone cannot be directly used as feedstock to produce hydrogen in a PEM electrolyzer if the applied potential is lower than 1.23 V with a carbon anode.

In this electrolysis system, the reduction degree of PMo_{12} is the key factor determining the performance of the electrolysis because the actual anode discharge ion is

PMo_{12} anions. There is no obvious difference in electrolysis performance using different lignin feedstock (Figure 6.3a). The longer reaction time in the preoxidation process can increase the reduction degree of PMo_{12}, which is positively related to the PEM electrolysis performance (Figure 6.3b). The high KL concentration can benefit the PEM electrolysis performance, but no further improvement was observed if the KL concentration was higher than 10 g/L (Figure 6.3c). The onsite potential of PMo_{12} solution was ~0.6 V (Figure 6.3a).

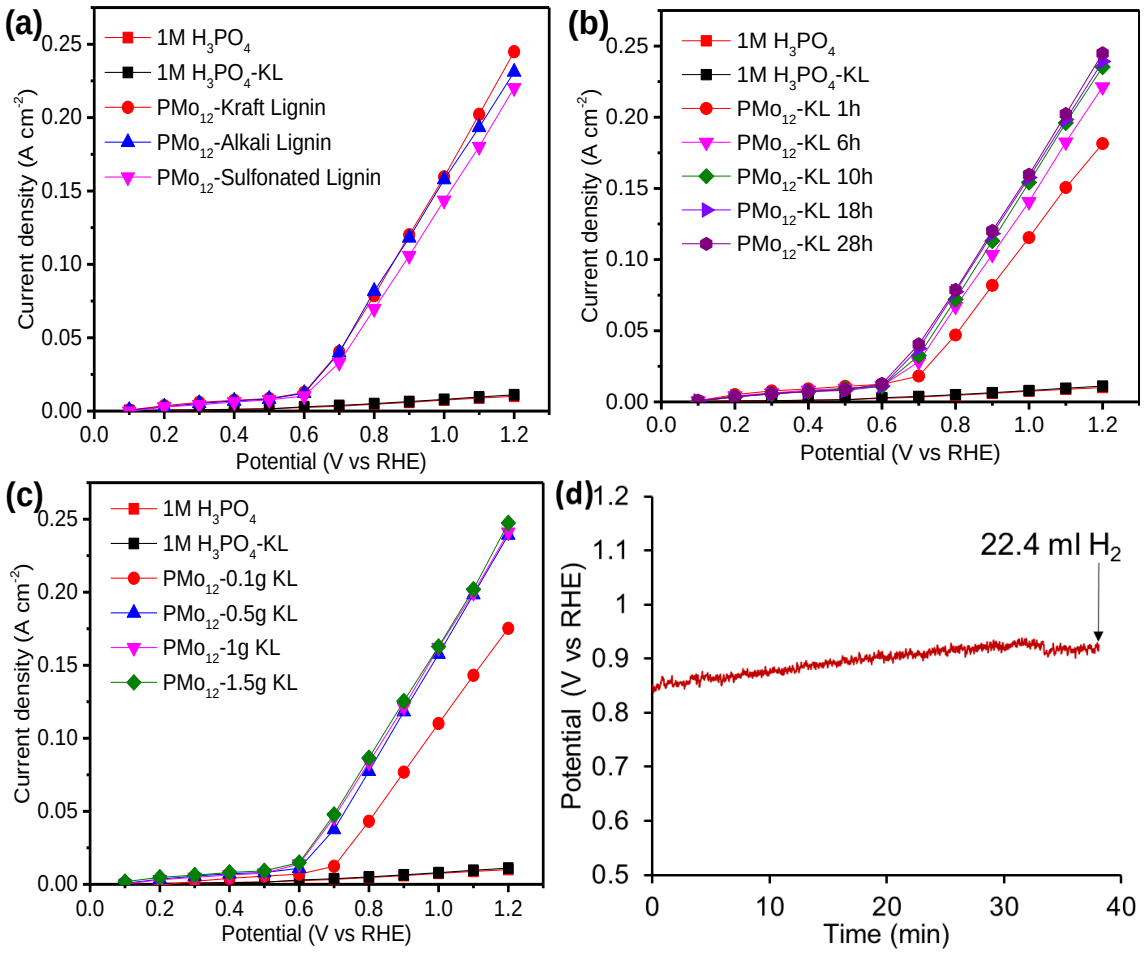

Figure 6.3 The effects for polarization curves of lignin and PMo_{12} solution. **a)** PMo_{12} (0.1 mol/L) reacted with different kinds of lignin (KL, AL and SL), **b)** Different reaction time with KL to obtain different reduction degree of PMo_{12}, **c)** Different amount of KL with 0.1 mol/L $FeCl_3$, and **d)** hydrogen evolution during constant current density electrolysis. Applied potential *vs.* time during 0.1 A cm^{-2} constant current density electrolysis of PMo_{12}-KL (electrode area 1 cm^2).

The energy consumption and Faraday efficiency of the HER by the lignin-PMo_{12} based PEM electrolyzer are other important factors affecting the hydrogen evolution. In a continuous electrolysis test, a constant current density of 100 mA cm^{-2} was applied, and the volume of produced H_2 was measured. As shown in Figure 6.3d, the potential is almost stable during the process of 24 ml H_2 generation. According to Faraday's law, theoretical yield of 26.52 ml H_2 gas during the constant-current electrolysis was calculated (Figure 6.3d). The average Faraday efficiency is 90.48% for 0.1 mol/L PMo_{12}-KL, which suggest a high electron transfer efficiency in our PEM electrolyzer. At current density 0.1 A cm^{-2}, the electric energy consumption was 2.54 kW h Nm^{-3} for PMo_{12}-KL, which suggests 39.5% electric energy was saved compared to the reported best PEM water electrolysis (4.2 kW h Nm^{-3})[207].

6.3.4 The products of lignin depolymerization by POM oxidation

In our electrolysis process, electrolysis can not only produce hydrogen from lignin with much lower energy consumption compared to pure water electrolysis system, but also depolymerize lignin into aromatic low molecular weight chemicals by the oxidative reaction between lignin and POM during the entire electrolysis process. Because over 95% of the world lignin product is Kraft lignin,[13] the depolymerization of Kraft lignin in our electrolysis system was focused. As introduced, a series of POMs is capable to break lignin polymer down low molecular weight segments and possible to further convert residual lignin into CO_2 and H_2O by wet oxidation.[35, 132, 134, 181] In this study, the oxidation of lignin by aqueous PMo_{12} was studied under mild conditions (100^oC with N_2 protection).

The oxidation of lignin is accompanied by reduction of the catalyst (PMo_{12}). The catalyst from oxidized state to reduced state without regeneration is noted as an oxidation cycle in this study. Then the reduced PMo_{12} is reoxidized at anode under electric field, and the regenerated PMo_{12} can be reused in the next oxidation cycle. In order to obtain a

significant change of lignin depolymerization, 3 oxidation-cycle heating (3 cycles × 6 hours/cycle = 18 hours) at 100°C was employed. After reaction, 82.2% of residual lignin still remain for PMo_{12} (0.1 mol/L). The GC (Agilent 490 Micro GC) results showed carbon dioxide is the major component (91%) in the gas phase with small amount of methane (9%). It probably can be ascribed to the cleavage of C-C bond and C-O bond of methoxyl group (-O-CH_3) by oxidation. In aqueous phase, the total organic carbon analysis (Shimadzu TOC-VCPH-155B) results showed 0.77 g/L organic materials were present in filtrated reaction solutions for PMo_{12}-KL reaction system. Based on the weight percentage of carbon content in original pine lignin (54.9%)[218], the amounts of lignin oxidized products dissolved in the aqueous solution after 3 reaction cycles with PMo_{12} were calculated from TOC analysis results. The KL in the solid residual, liquid, gas and other part after reacted with PMo_{12} are shown in Figure 6.4a.

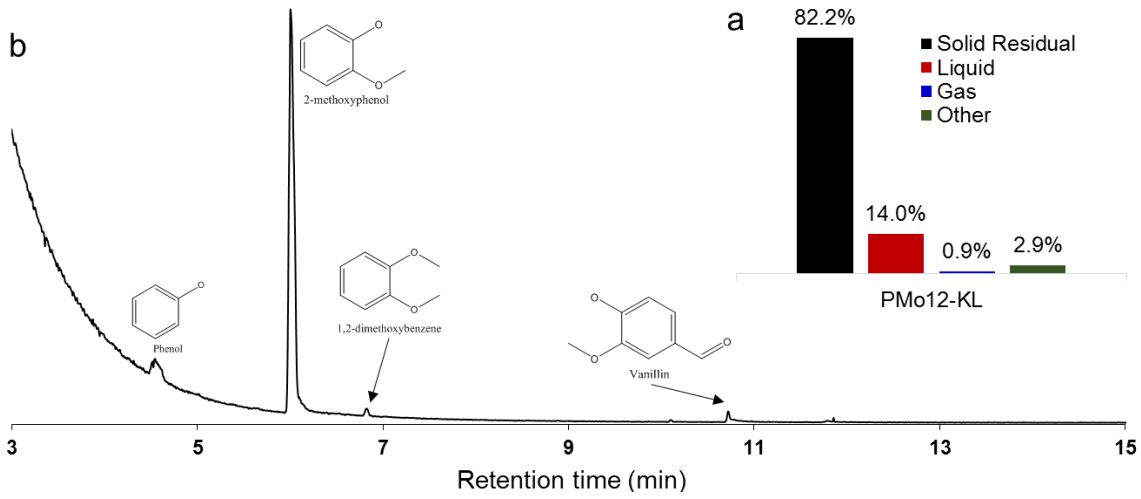

Figure 6.4 **a.** The solid, liquid and gas fractions after 3 oxidation-cycle reaction with PMo_{12}. **b.** GC-MS analysis of Kraft lignin (KL) reaction with PMo_{12} (PMo_{12}-KL) mixture. Reaction conditions: KL (10 g/L), PMo_{12} (0.1 mol/L), 100°C, 18 h under N_2 protection.

Besides employing more oxidation cycles, increasing the reaction temperature will also improve the conversion degree of lignin. For example, 26.6% of solid lignin was

oxidized to low molecular weight water soluble lignin segments when the reaction temperature increased to 190^{o}C for 1 h, which is significantly higher than that obtained at 100^{o}C for 18 h (14.0%).

The oxidized products from lignin in the liquid were extracted by 30 ml diethyl ether from 50 ml reacted solution and were then analyzed by GC-MS. As shown in Figure 6.4b, phenol, guaiacol, 1,2-dimethoxybenzene, vanillin and 3,4-dimethoxybenzaldhyde were identified in solution after lignin reacted with PMo_{12}. The major depolymerized products of AL and SL also are similar as KL after PMo_{12} oxidation. Besides these small monomers were detected by GC-MS, the molar mass distribution of dissolved lignin products analyzed by the gel permeation chromatography (GPC) showed that the dissolved lignin products included monomers and oligomers. Therefore, the PMo_{12} can depolymerize the lignin to small aromatics under mild conditions.

6.3.5 The functional groups and structure changes during POM depolymerization

To further elucidate the functional groups and structure changes during PMo_{12} catalyzed lignin depolymerization process, the KL solid residual was analyzed by solution-state 2D-NMR (Bruker Avance 700MHz), phosphorus-31 (^{31}P) NMR (Bruker Avance/DMX 400MHz), attenuated total reflectance-Fourier transform infrared spectroscopy (ATR-FTIR, Bruker Vertex 80V) and X-ray photoelectron spectroscopy (XPS, Kratos Analytical AXIS 165). Figure 6.5a shows the side chain (δC/δH 48-91/2.0-6.0) regions of the HSQC NMR spectra of the original KL, and KL residuals after reacted with PMo_{12} (KL-PMo_{12}). The KL-PMo_{12} spectrum indicated that most of the ether linkages (β-O-4, β-5, β-β) were broken with only a tiny amount of resinol (β-β) detected. PMo_{12} can effectively break the ether bonds in lignin structure. In the ^{31}P NMR spectra (Figure 6.5b), peaks in the range of 133-150 ppm are assigned to specific hydrogen atom in different chemical environments (Table 2.2). According to the spectra, hydroxyl group contents in

lignin reacted with PMo_{12} reduced compared with original lignin. Briefly, all the aliphatic –OH were consumed and only a small amount of –OH in catechol structures left after the reactions.

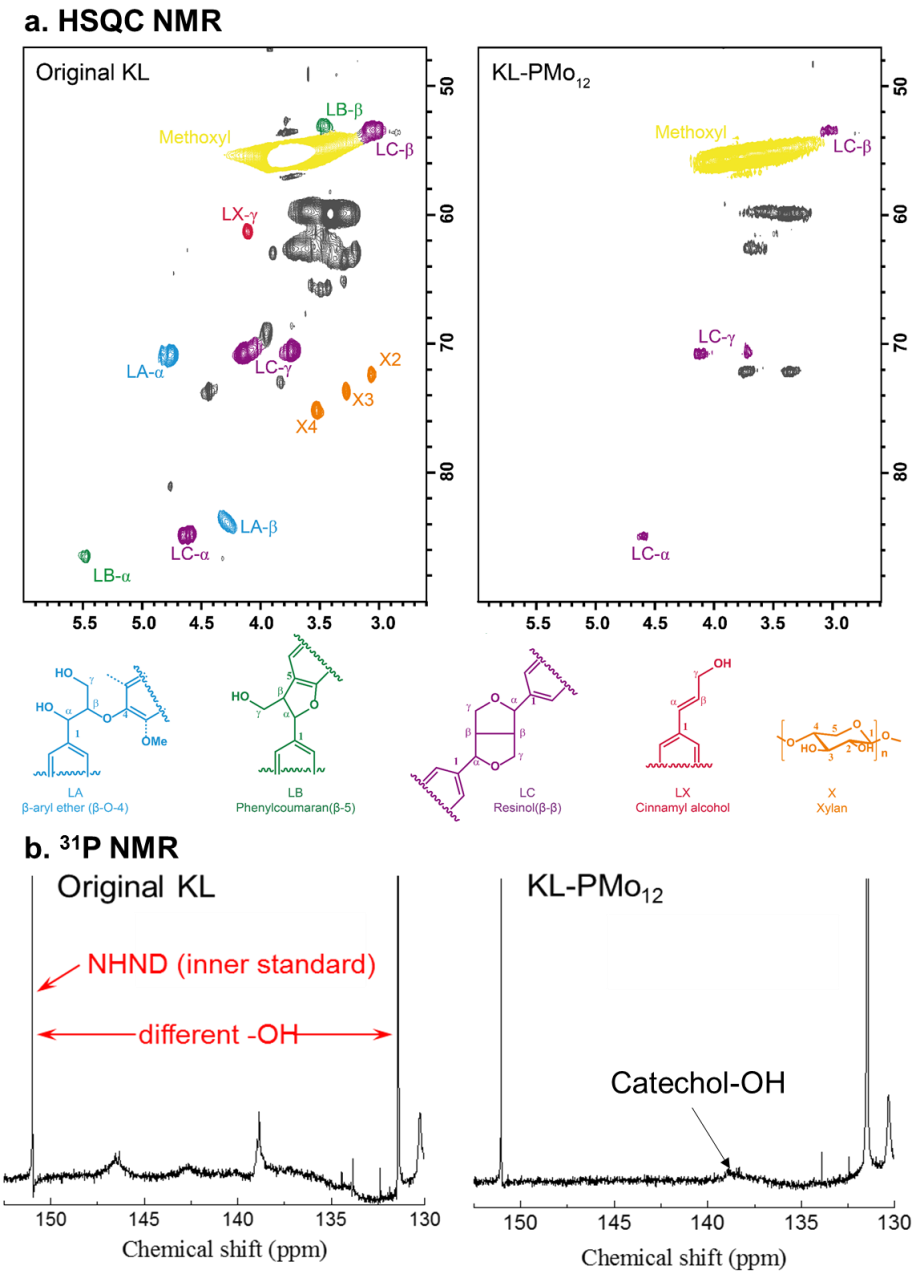

Figure 6.5 a). Side chain (*d*C/*d*H 48–91/2.0–6.0) regions in the 2D HSQC NMR spectra of original KL, and KL residuals after reaction with PMo12 (KL–PMo12). b) 31P NMR spectra of original Kraft lignin (KL), lignin residual after reacted with PMo_{12} (KL-PMo_{12})

Figure 6.6a shows the ATR-FTIR spectra of original KL, and lignin residuals after reacted with PMo_{12}. The assignments of FTIR peaks for the functional groups in KL were summarized in Table 2.3. [143, 144] A decrease in the intensity of the hydroxyl group (–OH) absorption band around 3,375 cm^{-1} was observed, indicating that the –OH content in KL was decreased after the oxidation reaction which also confirmed by ^{31}P NMR results. The higher content of C=O in PMo_{12}-KL was evidenced by a stronger band around 1,705 cm^{-1}. The reacted lignin was shifted to a higher wavenumber values (1738 cm^{-1}), which is probably attributed to the new formed C=O (ketone, aldehyde, carboxylic acid, etc.) in different environments. The peak around 1,512 cm^{-1} is probably due to one of the substituted aromatics. The decrease in the relative peak intensity probably means substitution reaction occurring, which could change the frequency of the ring vibration. The peak intensity of aromatic –OH deformation vibration around 1,366 cm^{-1} increased probably due to the oxidation reaction. Decreasing in the intensities around peaks 1,265 cm^{-1} and 1030 cm^{-1} for C-O and C-H in the lignin's guaiacyl (G) units (Table 2.3) was observed, which can be attributed to that the G units were removed from KL structure. The detected vanillin and guaiacol from G units in liquid solution by GC-MS also confirmed this conclusion. The surface chemistry of KL, PMo_{12} modified KL was examined by XPS (Figure 4). Among all samples, the peaks of carbon (C 1s) and oxygen (O 1s) were observed at 286 and 533 eV, respectively (Figure 6.6b). The oxygen/carbon (O/C) ratio of original KL (0.294) is much lower than the KL after PMo_{12} oxidation (0.380). It is probably because the oxidation reaction introduced more oxygen in lignin structure. The Gaussian peaks obtained through deconvolution of the C 1s peaks are shown in Figure 6.6c,d. These peaks are carbon-related functional groups and can be differentiated by distinct binding energies. The C1s A (284.6 eV), B (286.3 eV), C (289.0 eV) peaks are assigned to no bond to oxygen carbon (C-C, C=C), one bond to oxygen (C-O) and two bonds to oxygen (C=O, O-C-O), respectively. The estimations of the amount of these three functional groups based on relative peak areas are also shown in Figure 6.6. The results indicated a significant decrease

in C-O bonds and an increase in C=O bonds from original KL to PMo_{12}-KL, which confirmed that the degree of lignin oxidation increased. The oxidation of C-O can be partially ascribed to -OH oxidation and cleavage of the β-O-4 linkages that is the major linkage in lignin structure.[1, 17] In addition, the oxidation of C-O and the formation of C=O were independently confirmed by FTIR spectra before.

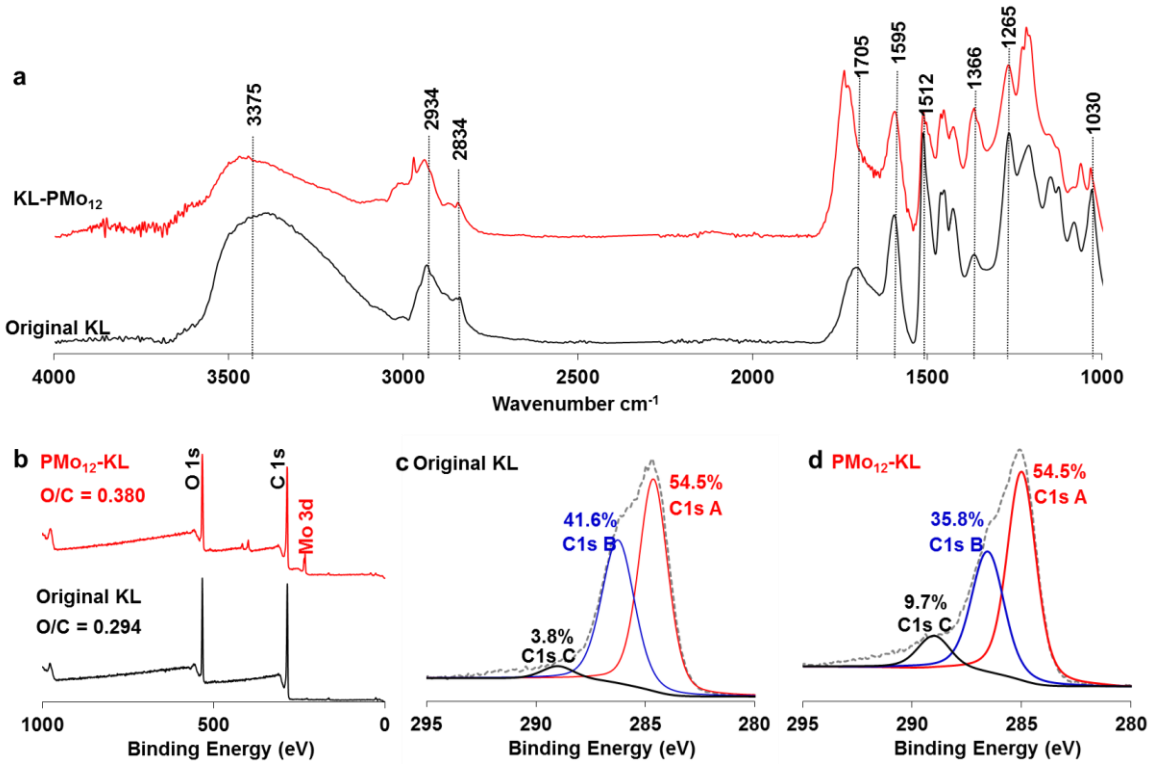

Figure 6.6 a) Analysis of KL before and after PMo_{12}-mediated oxidation by FTIR (scan range 4000–600 cm^{-1} with a resolution of 4 cm^{-1}). b) XPS widescan spectra of KL c) before, d) after PMo12-mediated oxidation (scans taken with a 1.0 eV step and 80 eV pass energy; the high resolution regional spectra c), d) were recorded with a 0.1 eV step and 20 eV pass energy). Reaction conditions: KL (10 g/L), PMo12 (0.1 mol/L) 100 ^{o}C, 18 h, under N_2 protection.

The HSQC NMR, ^{31}P NMR, ATR-FTIR and XPS results indicated that PMo_{12} not only have the potential to oxidize the –OH group on the surface of lignin structure, but also can cleave most ether bonds (eg. β-O-4, β-5, β-β). The aromatic products in liquid further

confirmed the ability of PMo_{12} as catalyst in lignin depolymerization under mild condition. The companied reduction of PMo_{12} can be used in PEM electrolyzer to facilitate the electrolysis for hydrogen production. In a continuous operation process, the anode reaction can be implemented in a thermal insulation reactor. Therefore, the heat energy input can be maintained at a very low stage. The lignin as only feedstock can be depolymerized to small molecules.

6.4 Conclusion

In conclusion, lignin as feedstock in the novel PEM electrolyzer was directly oxidized by POM under mild conditions at the anode side, and reduced POM_{red} could be completely regenerated to POM during the electrolysis. 14.0% of lignin was oxidized to small aromatic molecules in 3 oxidation-discharge cycles (total 18 h) at 100^{o}C. The conversion yield could be further improved by more oxidation cycles or optimization of reaction conditions. The functional groups and structure changes of lignin during depolymerization process were characterized by HSQC NMR, ^{31}P NMR, ATR-FTIR, and XPS. Moreover, the noble metal at the anode electrode was replaced by carbon-based material (graphite felt) in the electrolyzer because no catalytic reaction on the anode surface is needed if POM is used as the soluble catalysts and electron carriers. The average Faraday efficiency is over 90%. The electrolysis at fixed current density of 0.1 A cm^{-2}, the electric energy saving could be as high as 39.5% comparing to the reported best alkaline water electrolysis. This study provided a way to produce the aromatic monomers as well as hydrogen in one process.

CHAPTER 7. FERRIC CHLORIDE-MEDIATED ELECTROLYSIS FOR SIMULTANEOUSLY LIGNIN DEPOLYMERIZATION AND HYDROGEN EVOLUTION [**]

7.1 Introduction

A novel biomass PEM electrolysis approach was described in chapter 6, in which the hydrogen evolution reaction (HER) could be conducted directly from lignin with low energy consumption. Aqueous polyoxometalate (POM) solution served as a catalyst to replace the noble-metal at the anode, the raw biomass (e.g. lignin) is oxidized and electrons are transferred to POM by heating. These exciting results provide a way to combine lignin depolymerization and HER in one process (Figure 7.1a). POM is chemically stable and an effective mediator and charge transfer catalyst, the high molecular weight of POM (molecular weight of $H_3PMo_{12}O_{40}$ is 1,825.25 g mol^{-1}) reduces the diffusibility and dischargeability on the anode. For such extremely high molecular weight catalyst, it is also difficult to obtain a high molar concentration that is necessary for increasing both lignin oxidation and anode discharge rate. Clearly, if a low cost and small ion pair can be identified, the electrolysis performance will be improved. Herein, as shown in Figure 7.1b, this chapter reports that the Fe^{3+}/Fe^{2+} ion pair is an excellent candidate to realize the lignin oxidation and anode discharge circle. The standard potential of Fe^{3+}/Fe^{2+} is 0.77 V vs. NHE. It has been reported that the oxidation degradation of phenolic units of lignin can take place by Fe^{3+} oxidation.[35, 219] After oxidation, the reduced Fe^{2+} can be regenerated to Fe^{3+} during the PEM electrolysis process.

[**] The full data of this research were accepted for publication in ChemSusChem, 2017. Reprinted with permission from "X Du, W Liu, Z Zhang, A Mulyadi, A Brittain and YL Deng. Low energy catalytic electrolysis for simultaneously hydrogen evolution and lignin depolymerization to valuable chemicals. *ChemSusChem*. 2017, 10:847-854." Copyright 2017 WILEY-VCH.

In this study, we demonstrate the PEM electrochemical oxidation of lignin into small molecules as well as hydrogen evolution using $FeCl_3$ as a catalyst and charge carrier. Since the Fe^{2+} after lignin oxidation can release the electron to carbon anode under electric field without any noble metal catalyst, the simple graphite-felt was used as electrolysis anode. The results show that the novel electrolysis method can not only produce hydrogen under very low electric potential but also convert lignin to low molecular weight value-added chemicals simultaneously.

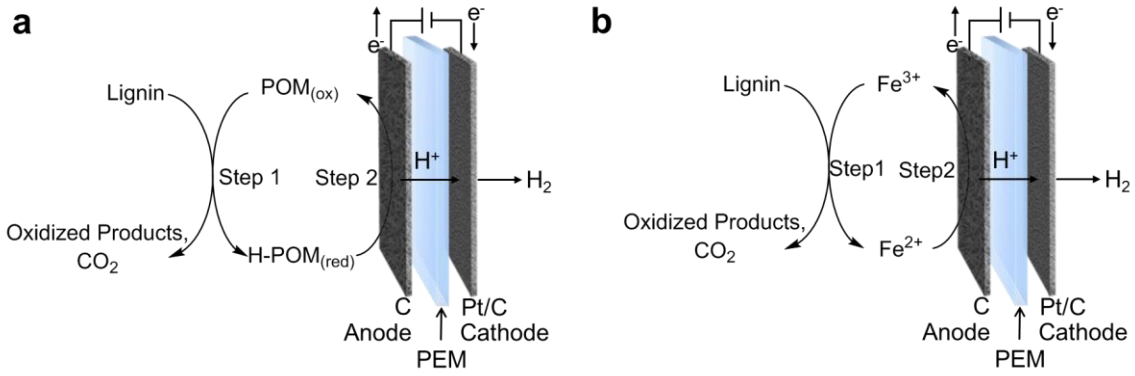

Figure 7.1 Schematic comparison of the mediated lignin electrolysis and water electrolysis. (a) PEM electrochemical reforming by POM-mediated and (b) PEM electrochemical reforming by Fe^{3+}-mediated

7.2 Experimental section

7.2.1 Materials

The lignin used in the experiments included: (1) pine Kraft lignin (KL), (2) alkline lignin (AL), and (3) sulfonated lignin (SL). Details and other chemicals used in this study was shown in 2.1 section of this dissertation.

7.2.2 Lignin oxidation with $FeCl_3$

See section 2.2.3 for details.

7.2.3 $FeCl_3$-mediated electrolysis process

See section 2.2.4 for details.

7.3 Results and discussion

7.3.1 The $FeCl_3$-mediated PEM electrolysis process

The chemical-electrolysis conversion process using lignin was conducted in a proton exchange membrane (PEM) electrolyzer as in chapter 6, which is schematically illustrated in Figure 7.1b. Instead of POM catalyst, Fe^{3+}/Fe^{2+} ion pair is a potential candidate to realize lignin oxidative degradation and anode discharge circles. Similarly, the lignin is oxidized by Fe^{3+} (from $FeCl_3$) under heating where the Fe^{3+} is reduced to Fe^{2+} at the anode side according to eqn (7.1). Electrons are transferred from lignin to Fe^{3+}, and release protons to electrolyte simultaneously.

$$Fe^{3+} + H_2O + \text{Lignin} \xrightarrow{\Delta} Fe^{2+} + 2H^+ + CO_2 + \text{Oxidized products} \quad (7.1)$$

At the second step, the Fe^{2+} is electro-oxidized by applying electric potential (eqn 7.2).

$$Fe^{2+} \xrightarrow{\text{Anode}} Fe^{3+} + e^- \quad (7.2)$$

The protons that are released from biomass (eqn 7.1) pass through the PEM into the cathode chamber to form hydrogen by taking the electrons at the cathode surface (eqn 7.3).

$$H^+ + e^- \xrightarrow{\text{Cathode}} 1/2\ H_2 \quad (7.3)$$

7.3.2 The $FeCl_3$ reduction by oxidation of lignin

$FeCl_3$ as a strong oxidant (E^{Θ} = +0.77 V)[219] can make the oxidative degradation of lignin taking place. During the reaction, the KL, AL and SL (10 g/L) were oxidized by $FeCl_3$ (1 mol/L with HCl) at 100 ^{o}C under N_2 protection. The concentration of Fe^{2+} (from Fe^{3+} reduction) was measured using ultraviolet-visible spectrophotometer (Agilent 8453) by spectrophotometric determination using 1,10-phenanthroline as chromogenic reagent (reference curve was shown in Figure 2.3b). As shown in Figure 7.2a, the concentration of Fe^{2+} rapidly increased in the first 3 hours, and finally reached to 0.38, 0.42 and 0.37 mol/L after 28 h reaction for KL, AL and SL, respectively.

7.3.3 The performance of $FeCl_3$-mediated electrolysis

For $FeCl_3$-electrolysis system, 50 ml aqueous electrolyte consisting of 1 mol/L $FeCl_3$ and 0.5 g different lignins after 6 h reaction was fed to the anode, and 80 ml 1 mol/L H_3PO_4 was fed to the cathode. Electrolysis polarization curves were obtained in the potential range from 0.1 to 1.2 V at 1 mV s^{-1} scan speed. The cell temperature was regulated at 80 ^{o}C. Figure 1b shows that the output current densities at a cell potential of 1.2 V were 0.341, 0.374 and 0.357 A cm^{-2} for KL, AL and SL, respectively. Moreover, the onsite potentials (bending point of I-V curve) were almost the same (~0.7 V), suggesting the source of lignin did not make a significant difference on the electrolysis performance. Actually, the concentration of Fe^{2+} is the key factor controlling the electrolysis performance because the actual electric oxidation on the anode during the electrolysis is Fe^{2+} ions (eq. 7.2). The higher concentration of Fe^{2+} means lower electrolysis potential so less electric energy is needed. In order to further confirm the relationship between the Fe^{2+} and applied potential at specific current density, the Fe^{3+}-KL solutions with different concentration of Fe^{2+} were prepared by controlling reaction time (Figure 7.2a). As shown

in Figure 7.2c, the higher concentration of Fe^{2+} (by longer reaction time) resulted in a higher current density at a fixed potential. However, there was no significant improvement in electrolysis performance after 6 h reaction due to the concentration of Fe^{2+} increased slowly. In order to evaluate the effect of lignin concentration in the pre-oxidation system, 2, 10, 20 and 30 g/L KL powders were fed to react with 1 mol/L $FeCl_3$. As shown in Figure 7.2d, no further improvement in the electrolysis performance was observed if the KL concentration was higher than 10 g/L. The onsite potential of $FeCl_3$-system (~0.7 V) is higher than PMo_{12} system (~0.6 V in Figure 6.3a in chapter 6), but the current density of $FeCl_3$-system increased faster than PMo_{12}-system (Figure 7.2e). When the applied potential was higher than ~0.8 V, the current density of $FeCl_3$-system is higher than PMo_{12}-system at same voltage. It is probably because of the higher concentration, fast diffusion of reduced ion (Fe^{2+}) in KL-$FeCl_3$ system (initial concentration: 1 mol/L $FeCl_3$) and faster discharge of Fe^{2+} comparing POM_{red} ions. When the initial concentration of $FeCl_3$ was 0.1 mol/L, the current density of $FeCl_3$-KL system was lower than KL-PMo_{12} system (initial concentration: 0.1 mol/L PMo_{12}).

As in chapter 6, the energy consumption and Faraday efficiency of the HER in the lignin-$FeCl_3$ based PEM electrolyzer were tested under a constant current density of 100 mA cm^{-2}. As shown in Figure 7.2f, the potential is almost stable during the process of 24 ml H_2 generation. The average Faraday efficiency is 92.71% for 1 mol/L $FeCl_3$-KL, which suggest a high electron transfer efficiency in our PEM electrolyzer. At current density 0.1 A cm^{-2}, the electric energy consumption was 2.30 kW h Nm^{-3} for $FeCl_3$-KL, which suggests 45.2% (for $FeCl_3$-KL) electric energy was saved compared to the reported PEM water electrolysis (4.2 kW h Nm^{-3})[207]. It also performed better than PMo_{12}-KL system.

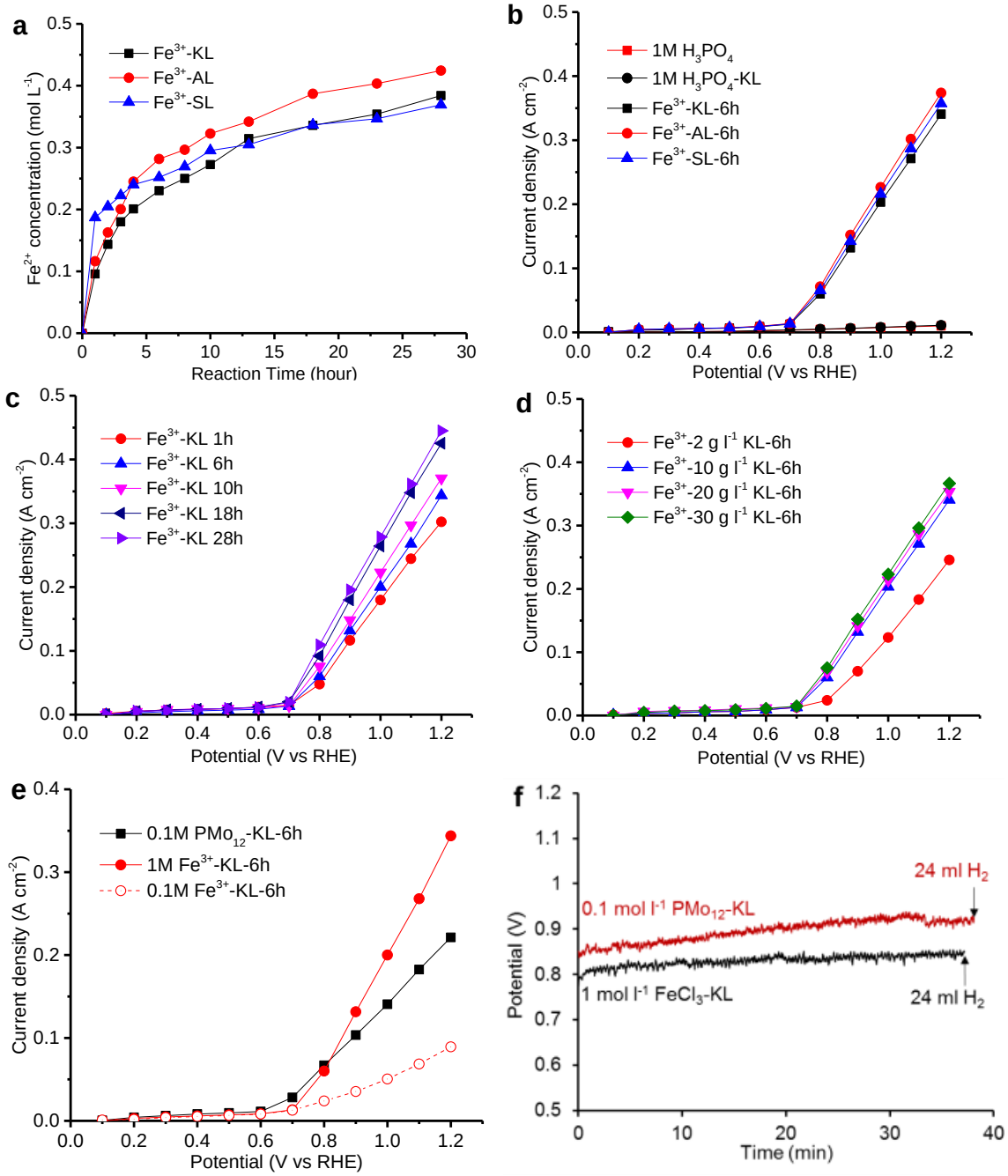

Figure 7.2 a) The concentration of Fe^{2+} along with the $FeCl_3$ (1 mol/L) reacted with KL, AL and SL under mild conditions; (Reaction conditions: 10 g/L KL/AL/SL, 1 mol/L $FeCl_3$, 100°C under N_2 protection.) The effects for polarization curves: b) $FeCl_3$ (1 mol/L) reacted with different kinds of lignin (KL, AL and SL), c) Different reaction time to obtain different Fe^{2+} concentration for KL, d) Different amount of KL with 1 mol/L $FeCl_3$, e) comparison of polarization curves of Fe^{3+} (1 and 0.1 mol/L) and PMo_{12} (0.1 mol/L) reacted with KL for 6 h, and f) hydrogen evolution during constant current density electrolysis. Applied potential *vs.* time during 0.1 A cm^{-2} constant current density electrolysis of PMo_{12}-KL (red) and $FeCl_3$-KL (black) (electrode area 1 cm^2).

7.3.4 The products of lignin depolymerization by POM oxidation

$FeCl_3$ is usually used as a catalyst in Fenton reagent with H_2O_2 for lignin depolymerization.[220-223] In the Fenton system, H_2O_2 is the oxidant rather than catalyst, which is consumed during reaction.[224] It should be noted that our $FeCl_3$ oxidation system is different from Fenton solution because no H_2O_2 was used in the process. Furthermore, in order to obtain fast hydrogen production rate, high concentration of Fe^{2+} was used in our PEM electrolysis. The oxidation of lignin is accompanied by reduction of the catalyst (Fe^{3+}). Then the reduced Fe^{2+} is reoxidized at anode under electric field, and the regenerated Fe^{3+} can be reused in the next oxidation cycle. After 3 oxidation-cycle heating (3 cycles × 6 hours/cycle = 18 hours) at 100°C, 77.6% of residual lignin still remain for $FeCl_3$ (1 mol/L). The GC results showed carbon dioxide (97%) and tiny amount of methane (3%) in the gas phase. It probably can be ascribed to the cleavage of C-C bond and C-O bond of methoxyl group (-O-CH_3) by oxidation. In aqueous phase, the total organic carbon analysis results showed 0.90 g/L organic materials were present in filtrated reaction solutions. The KL in the solid residual, liquid, gas and other part after reacted with $FeCl_3$ are shown in Figure 7.3a.

The oxidized products were extracted by diethyl ether and then analyzed by GC-MS. As shown in Figure 7.3b, vanillin, 4-methylbenzaldehyde, benzoic acid, phthalic anhydride and other chlorine substituted chemicals in the solution. The major depolymerized products of AL and SL also are similar as KL after $FeCl_3$ oxidation. It indicated $FeCl_3$ can depolymerize the lignin to small aromatics.

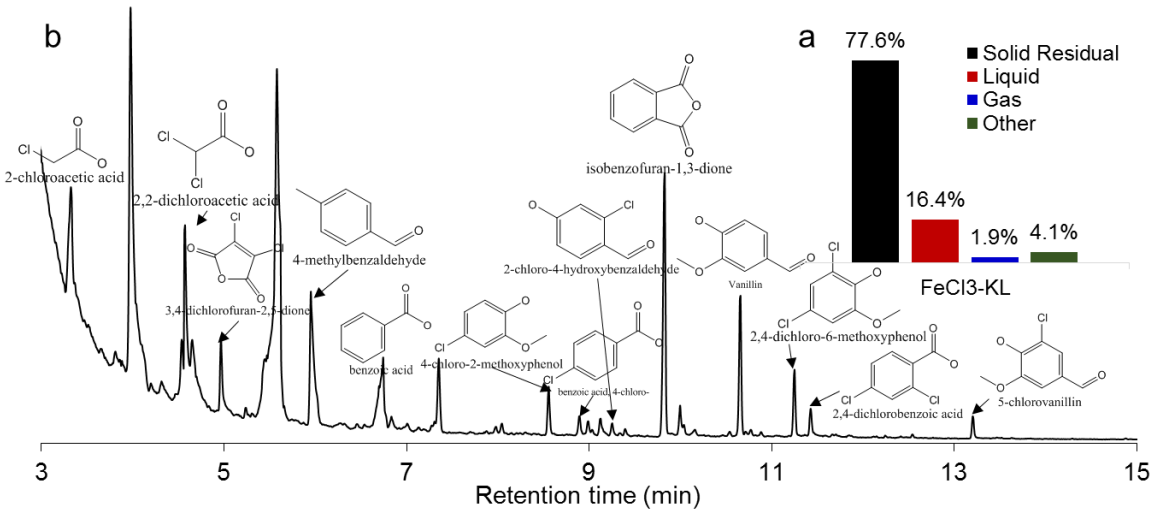

Figure 7.3 **a.** The solid, liquid and gas fractions after 3 oxidation-cycle reaction with $FeCl_3$. **b.** GC-MS analysis of Kraft lignin (KL) reaction with $FeCl_3$ ($FeCl_3$-KL) mixture. Reaction conditions: KL (10 g/L), $FeCl_3$ (1 mol/L), 100°C, 18 h under N_2 protection.

7.3.5 The functional groups and structure changes during $FeCl_3$ depolymerization

The KL solid residual was analyzed by solution-state 2D-NMR, phosphorus-31 (^{31}P) NMR, ATR-FTIR, and XPS to identify the functional groups and structure changes. Figure 7.4a shows the side chain regions of the HSQC NMR spectra of the original KL, and KL residuals after reacted with $FeCl_3$ (KL-$FeCl_3$). There are no ether linkages observed after reaction, which indicated $FeCl_3$ can effectively break the ether bonds in lignin structure. In the ^{31}P NMR spectra (Figure 7.4b), hydroxyl group contents in lignin reacted with $FeCl_3$ reduced compared with original lignin. Briefly, all the–OH were consumed after the reactions.

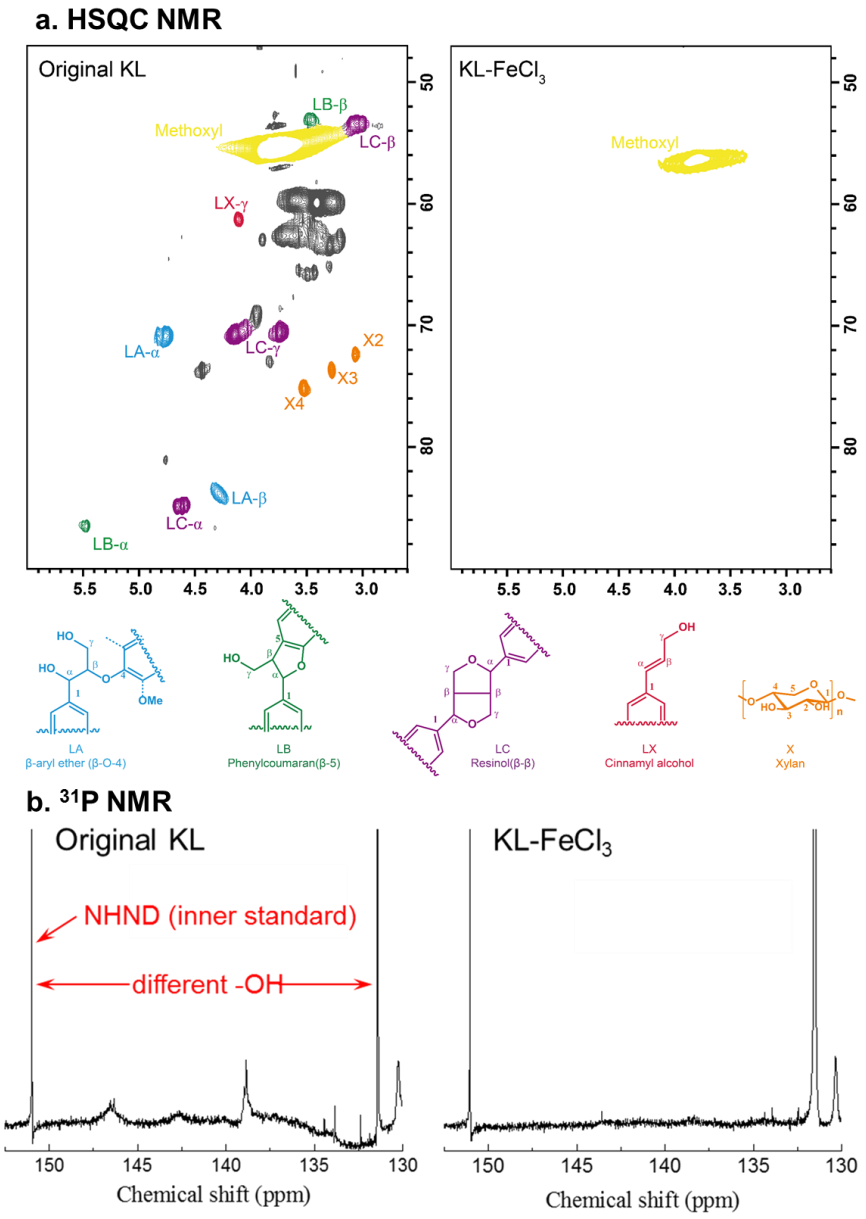

Figure 7.4 a) Side chain (*d*C/*d*H 48–91/2.0–6.0) regions in the 2D HSQC NMR spectra of original KL, and KL residuals after reaction with $FeCl_3$ (KL–$FeCl_3$). b) ^{31}P NMR spectra of original Kraft lignin (KL), lignin residual after reacted with $FeCl_3$ (KL-$FeCl_3$)

Figure 7.5a shows the ATR-FTIR spectra of original KL, and lignin residuals after reacted with $FeCl_3$. Same as in PMo_{12}-system, the –OH content in KL decreased after the oxidation which is confirmed by FTIR and ^{31}P NMR. The higher content of C=O in $FeCl_3$-KL was evidenced by a stronger band around 1,705 cm^{-1}. The reacted lignins were shifted

to a higher wavenumber values (1724 cm^{-1} for $FeCl_3$-KL), which is probably attributed to the new formed C=O (ketone, aldehyde, carboxylic acid, etc.) in different environments.

The surface chemistry of KL and $FeCl_3$ modified KL was also examined by XPS (Figure 7.5). As introduced in chapter 6, the peaks of carbon (C 1s) and oxygen (O 1s) were observed at 286 and 533 eV, respectively (Figure 7.5b). The oxygen/carbon (O/C) ratio of original KL (0.294) is much lower than the KL after $FeCl_3$ oxidation (0.355). It is probably because the oxidation reaction introduced more oxygen in lignin structure. The Gaussian peaks obtained through deconvolution of the C 1s peaks are shown in Figure 7.5c,d. Both C-O and C=O bonds increased and C=C bond (or C-C) decreased from original KL to $FeCl_3$-KL, indicating that more C-C (or C=C) bonds on the surface of KL were oxidized to C-O and C=O bonds by $FeCl_3$.

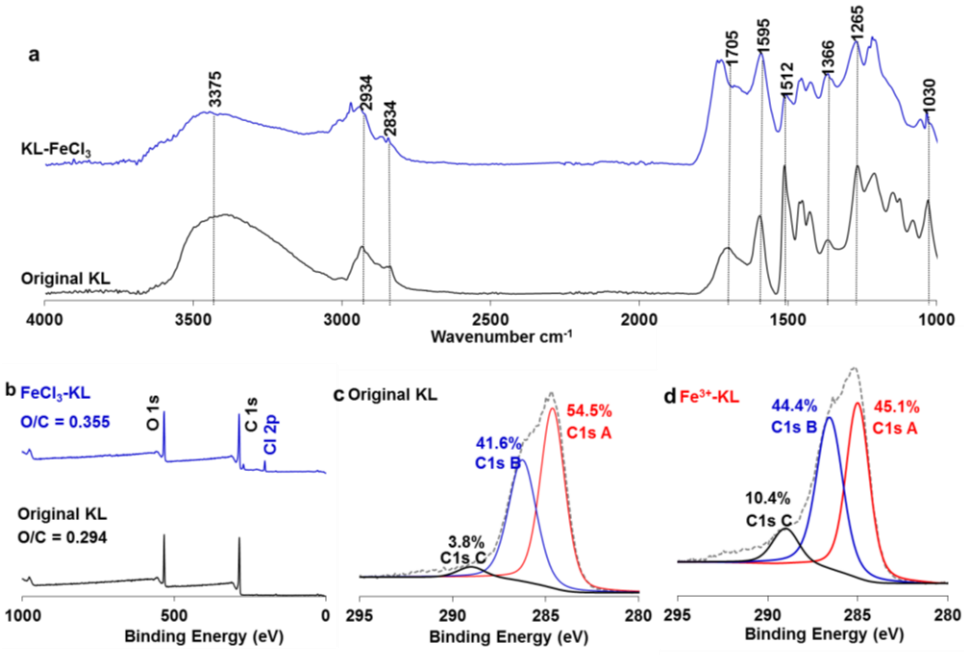

Figure 7.5 a) Analysis of KL before and after $FeCl_3$-mediated oxidation by FTIR (scan range 4000–600 cm^{-1} with a resolution of 4 cm^{-1}). b) XPS widescan spectra of KL c) before, d) after $FeCl_3$-mediated oxidation (scans taken with a 1.0 eV step and 80 eV pass energy; the highre solution regional spectra c), d) were recorded with a 0.1 eV step and 20 eV pass energy). Reaction conditions: KL (10 g/L), $FeCl_3$ (1 mol/L) 100 ^oC, 18 h, under N_2 protection.

Similarly, the HSQC NMR, ^{31}P NMR, ATR-FTIR and XPS results indicated that $FeCl_3$ not only have the potential to oxidize the –OH group on the surface of lignin structure, but also can cleave most ether bonds (e.g. β-O-4, β-5, β-β). The aromatic products in liquid further confirmed the ability of $FeCl_3$ as promising catalysts in lignin depolymerization. The companied reduction of high concentration $FeCl_3$ can be used in PEM electrolyzer to facilitate the electrolysis for hydrogen production. The lignin as only feedstock can be depolymerized to small molecules.

7.4 Conclusion

In conclusion, lignin as feedstock in the novel PEM electrolyzer was directly oxidized by high concentration $FeCl_3$ under mild conditions at the anode side, and Fe^{2+} could be completely regenerated to Fe^{3+} during the electrolysis. Around 16% of lignin was oxidized to small aromatic molecules, that is higher than 14.0% in PMo_{12} system, in 3 oxidation-discharge cycles at 100^{o}C. The functional groups and structure changes of lignin during depolymerization process were comprehensively characterized. The average Faraday efficiency (92.71%) for $FeCl_3$-KL system is higher than in PMo_{12} system (90.2%). The electrolysis at fixed current density of 0.1 A cm^{-2}, the electric energy saving could be 45.2% (for $FeCl_3$-KL) comparing to the reported best alkaline water electrolysis, which is higher than 39.5% for PMo_{12} system. This study provided another way to produce the aromatic monomers as well as hydrogen with a better performance in one process by simple metal ion compared with high-molecular-weight polyoxometaltate.

CHAPTER 8. OVERALL CONCLUSION AND FUTURE WORK

8.1 Overall conclusion

The present work reported in dissertation focused on lignin valorization considering 1) suppressing lignin condensation by selective oxidation of active benzyl alcohol to facilitate lignin depolymerization, 2) fractionating lignin from lignocellulose for *in situ* depolymerization towards complete biomass valorization; and 3) simultaneous processes of lignin depolymerization to chemicals and electrolysis to hydrogen to maximize lignin utilization.

In the first part, this study employed two-step oxidation strategies in two ways. In the preoxidation process under mild conditions, the secondary benzylic alcohol (C_α-OH) in the lignin structure is selectively oxidized to a ketone (C_α=O). In the second oxidation process at elevated temperature by POM oxidation, the lignin was depolymerized *via* an oxidative cleavage to aromatic chemicals. In the first strategy (chapter 3), TEMPO was used to selectively oxidize the C_α-OH moiety to ketone, [2, 3]. Then POM, which can be completely regenerated by oxygen under relatively mild conditions (150 ℃, 10 bar O_2), was used as an intermediate oxidizing agent for further oxidative degradation of the preoxidized lignin. The lignin depolymerization efficiency could be remarkably improved by converting the active C_α-OH to the stable C_α=O. Under optimized conditions, 74.5 wt% of the lignin was converted to low molecular weight compounds, and 32.8 wt% of the lignin (based total lignin mass) was converted to monomeric compounds. However, this process, similar as other two-step (stabilization-depolymerization) lignin treatment processes, need to be conducted in two different catalysis systems (*i.e.* solvents, catalysts),[2-5] which

becomes a significant hurdle for employing this strategy in industrial practice. Herein, we conducted another two-step oxidation protocol which can be achieved in one pot by the same polyoxometalate catalysis system (chapter 4). First, the benzyl alcohols in industrial lignin could be oxidized to ketones in methanol by POM under mild condition. Further, the preoxidized lignin was depolymerized to aromatics at an elevated temperature (e.g. 140℃). Total 58.0% of industrial lignin without purification can be converted to small molecules.

In the second part, a new lignin-first fractionation strategy was developed to improve the biomass valorization (chapter 5). Although the condensation of lignin in depolymerization was suppressed by applying preoxidation process, the recalcitrant condensed structure of lignin that is formed during biomass fractionation is a barrier for further lignin depolymerization. New biorefinery schemes are needed for complete utilization of biomass, where both the valorization of lignin and cellulose are regarded as a primary targets. In this study, the low concentration POM catalyst is employed to extract lignin from wood sawdust, under mild condition (100℃) in alcohol, while avoiding structural lignin condensation and degradation. Then extracted lignin is further oxidized to small aromatic molecules with 86.2% conversion, and the remaining cellulose can be further used to produce bio-ethanol towards biomass complete valorization.

The last part of my study focused on a novel proton exchange membrane (PEM) electrolysis process in which lignin was used as the hydrogen source at anode for hydrogen production. Either POM (chapter 6) or $FeCl_3$ (chapter 7) was used as the catalyst and charge transfer agent in anode. Over 90% Faraday efficiency was achieved. In a thermal insulation reactor, the input heat energy can be maintained at a very low stage for continuous operation. Compared to the alkaline water electrolysis reported in literature, the electrical

energy consumption could be 40% lower with novel lignin electrolysis method. At the anode, the Kraft lignin (KL) was oxidized to aromatic chemicals by POM or $FeCl_3$, and reduced POMs or iron ions were regenerated during the electrolysis. Structure analysis of the residual KL indicated the reduction of hydroxyl group number and the cleavage of ether bonds. Our results suggest that POM or $FeCl_3$ mediated electrolysis process can significantly reduce the electrolysis energy consumption in hydrogen production and, simultaneously, depolymerize lignin to low molecular weight value-added aromatic chemicals.[7]

In summary, this dissertation attempts to understand the catalytic valorization of lignin mainly using polyoxometalates as catalyst in terms of its special properties, including catalysis process design, catalyst preparation, depolymerization of lignin (or lignocellulose), and lignin (and its products) characterization. Most efforts has been put to develop the novel catalytic oxidation process in order to design an effective process for lignin conversion with high yield and low energy input. The developed processes in this dissertation show some advantages compared with current processes, such as easy to operate, potential to scale up and adapt in current refinery. I believe that the results achieved in this dissertation can provide feasible solutions to industry for using the industrial lignin, that is the most available and also a big waste in current biorefinery, as well as the lignocellulosic biomass to valuable outputs.

8.2 Future work

Several other studies might be conducted to further investigate the thermal conversion of biomass and its components to the fuel and chemicals. Some particularly attractive options are as follows: 1) complete separation and utilization of biomass by thermal catalysis; 2) electrochemical methods for biomass utilization.

8.2.1 Complete separation and utilization of biomass by thermal catalysis

All of three major components in biomass (cellulose, hemicellulose and lignin) should be considered as primary targets to maximize both economic and ecologic incentives. Due to the different properties of the three components, it is possible to separate and valorize them separately. Hemicellulose, has the potential to be an important renewable resource for furfural, which is mainly produced from corn cob now. The current production cannot meet the market demand (652.5 kilo tons in 2020), especially with the tougher environmental regulations in producing countries.[225] Therefore, developing an efficient method to isolate furfural from hemicellulose in agriculture waste and lignocellulose can become an important alternative. Due to its susceptible property, it can be easily isolated under mild condition in the first stage. [226] Lignin has great potential to be an important renewable feedstock for aromatic chemicals instead of the current primary resource, petroleum. My previous study suggests that it is possible to separate the lignin from cellulose by a catalytic method. Cellulose has a rigid semi-crystalline structure which is more stable towards degradation, and therefore meets the requirements to be valorized in a later stage.

To achieve the valorization of all lignocellulose constituents without pretreatment, a three stages strategy to fractionate hemicellulose, lignin and cellulose separately, and further valorize to value-added products. First, develop an efficient separation method for hemicellulose from biomass, and then move to separate the lignin and cellulose based on my previous work on lignin-first biomass fractionation. Moreover, the research will extend to study the properties of each isolated component, including purity, structure change, and explore its applications in various fields.

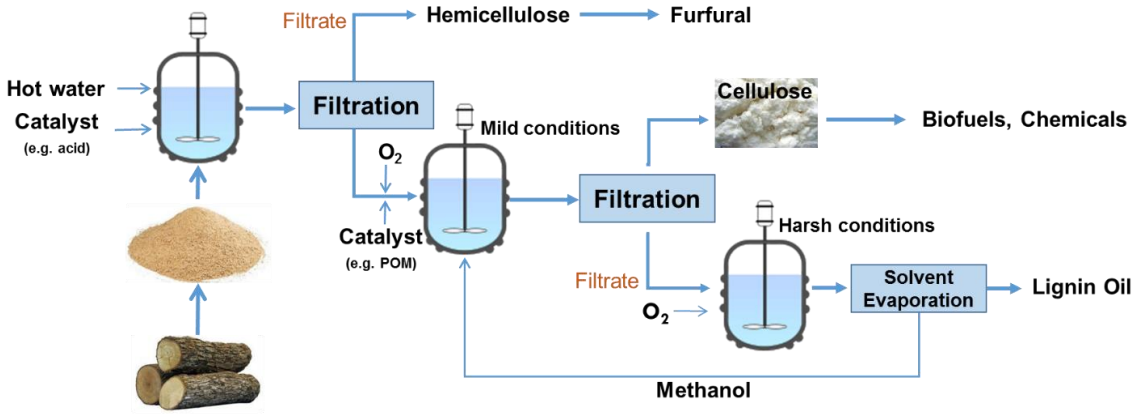

Figure 8.1 Lignocellulose separation and its complete utilization

8.2.2 Electrochemical method for biomass utilization

As mentioned in introduction part, there are two primary electro-oxidation strategies, namely indirect and direct. We have been extensively studied the indirect electro-oxidation of lignin using homogeneous catalysts (polyoxometalates[7, 128], ferric chloride [7, 227]). However, there are three key challenges for this process: 1) the necessary harsh conditions for the reaction between lignin and catalysts; 2) difficult separation of

products from catalysts; and 3) the catalyst regeneration process limited by electron diffusion in electrolyte. In direct electro-oxidation**,** the catalyst is usually immobilized on the surface of the electrode, and the catalytic depolymerization process and electrolysis happen simultaneously on the electrode. If we can immobilize the oxidative catalysts on electrode, it will greatly enhance the catalysts regeneration and facilitate the products separation.

In future study, it can combine the advantages of indirect and direct electro-oxidation processes together by fabricating a highly active oxidant-based catalyst on the anode with a 3D porous morphology to effectively convert lignin to aromatic chemicals. In this process, the lignin is either oxidized on the electrode with the assistance of applied potential or directly oxidized by immobilized catalyst which can be quickly regenerated by potential. The key challenges in this research include a) fabrication of electrode with a porous 3D morphology and high electrocatalytic activity, b) development of appropriate solvent systems with good lignin solubility, conductivity, and stability, and c) process optimization to maximize lignin monomer yield and selectivity.

APPENDIX A. THE EFFECTIVE CARBON NUMBER (ECN) OF LIGNIN MONOMERS

Chemical	MW	ECN
methyl 2,2-dimethoxyacetate	134.13	2.75
methyl 4-oxopentanoate	130.14	5.75
dimethyl succinate	146.14	5.5
dimethyl maleate	144.13	5.4
Dimethyl ethylidenemalonate	158.15	6.4
2-methoxyphenol	124.14	5
dimethyl 2-methylenesuccinate	158.15	4.9
dimethyl 2-methoxysuccinate	176.17	5.5
Tetramethoxyethene	148.16	1.9
Tricarbomethoxyethylene	202.16	7.15
syringol	154.17	5
Phthalic anhydride	148.12	7.75
Trimethyl 1,2,3-propanetricarboxylate	218.21	8.25
Trimethyl (1Z)-1-propene-1,2,3-tricarboxylate	216.19	8.15
Vanillin	152.15	6
4-Ethyl-1,3-benzenediol	138.07	6
methyl 2-propionylbenzoate	192.21	10.75
Dimethyl phthalate	194.19	9.5
Trimethyl 2-methoxypropane-1,2,3-tricarboxylate	248.23	8.25
methyl 3-hydroxybenzoate	152.15	6.75

dimethyl nonanedioate	216.28	10.5
Apocynin	166.18	7
Isovanillin	152.15	6
Methyl vanillate	182.06	6.75
methyl 3,4-dimethoxybenzoate	196.2	7.75
3,4,5-Trimethoxybenzaldehyde	196.2	7
Methyl syringate	212.2	6.75
Benzoic acid, 3,4,5-trimethoxy-, methyl ester	226.08	7.75
methyl palmitate	270.46	16.75
2-Hydroxy-1-(4-hydroxy-3-methoxyphenyl)ethanone	182.06	6.4
Acetosyringone	196.2	7
Benzoic acid, 2,4-dimethoxy-6-methyl, methyl ester	210.23	8.75
Acetosyringone	196.2	7
4-propylguaiacol	166.22	8
2-(3,4-dimethoxyphenyl)-2-hydroxypropanoate	225.22	9.07
methyl α-D-mannoside	194.18	2.6
2,6-dimethoxybenzoquinone	168.15	5.8
Benzaldehyde, 4-hydroxy-3,5-dimethoxy-	182.06	6
Propanedioic acid, dimethyl ester	132.12	4.5
dl-Malic acid, dimethyl ester	162.14	4.75
Methylparaben	152.15	6.75
Benzoic acid, 4-hydroxy-3-methoxy-, ethyl ester	196.2	7.75
dimethyl oxalate	118.09	3.5
methyl 2,2-dimethoxypropanoate	148.16	3.75
2-(2-methoxyethoxy)ethan-1-ol	120.15	2.4

dimethyl glutarate	160.17	6.5
Tricarbomethoxyethylene	202.16	7.15
methyl 4-hydroxy-3-methoxybenzoate	182.18	6.75
Ethanone, 1-(4-hydroxy-3-methoxyphenyl)-	166.18	7
Ethanone, 1-(4-hydroxy-3,5-dimethoxyphenyl)-	196.2	7

REFERENCES

1. Zakzeski, J., Bruijnincx, P.C.A., Jongerius, A.L., and Weckhuysen, B.M., The Catalytic Valorization of Lignin for the Production of Renewable Chemicals. *Chemical Reviews*, **2010**. 110(6): 3552-3599.

2. Rahimi, A., Azarpira, A., Kim, H., Ralph, J., and Stahl, S.S., Chemoselective Metal-Free Aerobic Alcohol Oxidation in Lignin. *Journal of the American Chemical Society*, **2013**. 135(17): 6415-6418.

3. Rahimi, A., Ulbrich, A., Coon, J.J., and Stahl, S.S., Formic-acid-induced depolymerization of oxidized lignin to aromatics. *Nature*, **2014**. 515(7526): 249-252.

4. Zhang, C.F., Li, H.J., Lu, J.M., Zhang, X.C., MacArthur, K.E., Heggen, M., and Wang, F., Promoting Lignin Depolymerization and Restraining the Condensation via an Oxidation-Hydrogenation Strategy. *Acs Catalysis*, **2017**. 7(5): 3419-3429.

5. Lancefield, C.S., Ojo, O.S., Tran, F., and Westwood, N.J., Isolation of Functionalized Phenolic Monomers through Selective Oxidation and C-O Bond Cleavage of the beta-O-4 Linkages in Lignin. *Angewandte Chemie-International Edition*, **2015**. 54(1): 258-262.

6. Renders, T., Van den Bosch, S., Koelewijn, S.F., Schutyser, W., and Sels, B.F., Lignin-first biomass fractionation: the advent of active stabilisation strategies. *Energy & Environmental Science*, **2017**. 10(7): 1551-1557.

7. Du, X., Liu, W., Zhang, Z., Mulyadi, A., Brittain, A., Gong, J., and Deng, Y.L., Low-Energy Catalytic Electrolysis for Simultaneous Hydrogen Evolution and Lignin Depolymerization. *Chemsuschem*, **2017**. 10(5): 847-854.

8. Corma, A., Iborra, S., and Velty, A., Chemical routes for the transformation of biomass into chemicals. *Chemical Reviews*, **2007**. 107(6): 2411-2502.

9. Gallezot, P., Conversion of biomass to selected chemical products. *Chemical Society Reviews*, **2012**. 41(4): 1538-1558.

10. Tuck, C.O., Perez, E., Horvath, I.T., Sheldon, R.A., and Poliakoff, M., Valorization of Biomass: Deriving More Value from Waste. *Science*, **2012**. 337(6095): 695-699.

11. Georgiadou, M., Biorefinery: From Biomass to Chemicals and Fuels. *Biorefinery: From Biomass to Chemicals and Fuels*, **2012**: 1-445.

12. Clark, J.H., Budarin, V., Deswarte, F.E.I., Hardy, J.J.E., Kerton, F.M., Hunt, A.J., Luque, R., Macquarrie, D.J., Milkowski, K., Rodriguez, A., Samuel, O., Tavener,

S.J., White, R.J., and Wilson, A.J., Green chemistry and the biorefinery: A partnership for a sustainable future. *Green Chemistry*, **2006**. 8(10): 853-860.

13. Gosselink, R.J.A., de Jong, E., Guran, B., and Abacherli, A., Co-ordination network for lignin - standardisation, production and applications adapted to market requirements (EUROLIGNIN). *Industrial Crops and Products*, **2004**. 20(2): 121-129.

14. Sun, Z.H., Fridrich, B., de Santi, A., Elangovan, S., and Barta, K., Bright Side of Lignin Depolymerization: Toward New Platform Chemicals. *Chemical Reviews*, **2018**. 118(2): 614-678.

15. Li, C.Z., Zhao, X.C., Wang, A.Q., Huber, G.W., and Zhang, T., Catalytic Transformation of Lignin for the Production of Chemicals and Fuels. *Chemical Reviews*, **2015**. 115(21): 11559-11624.

16. Ragauskas, A.J., Beckham, G.T., Biddy, M.J., Chandra, R., Chen, F., Davis, M.F., Davison, B.H., Dixon, R.A., Gilna, P., Keller, M., Langan, P., Naskar, A.K., Saddler, J.N., Tschaplinski, T.J., Tuskan, G.A., and Wyman, C.E., Lignin Valorization: Improving Lignin Processing in the Biorefinery. *Science*, **2014**. 344(6185): 709-719.

17. Chakar, F.S. and Ragauskas, A.J., Review of current and future softwood kraft lignin process chemistry. *Industrial Crops and Products*, **2004**. 20(2): 131-141.

18. Kacik, F., Durkovic, J., and Kacikova, D., Chemical Profiles of Wood Components of Poplar Clones for Their Energy Utilization. *Energies*, **2012**. 5(12): 5243-5256.

19. Isikgor, F.H. and Becer, C.R., Lignocellulosic biomass: a sustainable platform for the production of bio-based chemicals and polymers. *Polymer Chemistry*, **2015**. 6(25): 4497-4559.

20. Pettersen, R.C., The Chemical-Composition of Wood. *Advances in Chemistry Series*, **1984**(207): 57-126.

21. Jensen, A., Cabrera, Y., Hsieh, C.W., Nielsen, J., Ralph, J., and Felby, C., 2D NMR characterization of wheat straw residual lignin after dilute acid pretreatment with different severities. *Holzforschung*, **2017**. 71(6): 461-469.

22. Yue, F.X., Lu, F.C., Ralph, S., and Ralph, J., Identification of 4-O-5-Units in Softwood Lignins via Definitive Lignin Models and NMR. *Biomacromolecules*, **2016**. 17(6): 1909-1920.

23. del Rio, J.C., Rencoret, J., Prinsen, P., Martinez, A.T., Ralph, J., and Gutierrez, A., Structural Characterization of Wheat Straw Lignin as Revealed by Analytical Pyrolysis, 2D-NMR, and Reductive Cleavage Methods. *Journal of Agricultural and Food Chemistry*, **2012**. 60(23): 5922-5935.

24. Hedenstrom, M., Wiklund-Lindstrom, S., Oman, T., Lu, F.C., Gerber, L., Schatz, P., Sundberg, B., and Ralph, J., Identification of Lignin and Polysaccharide Modifications in Populus Wood by Chemometric Analysis of 2D NMR Spectra from Dissolved Cell Walls. *Molecular Plant*, **2009**. 2(5): 933-942.

25. Zhang, L.M., Gellerstedt, G., Ralph, J., and Lu, F.C., NMR studies on the occurrence of spirodienone structures in lignins. *Journal of Wood Chemistry and Technology*, **2006**. 26(1): 65-79.

26. Kim, H., Ralph, J., Lu, F.C., Ralph, S.A., Boudet, A.M., MacKay, J.J., Sederoff, R.R., Ito, T., Kawai, S., Ohashi, H., and Higuchi, T., NMR analysis of lignins in CAD-deficient plants. Part 1. Incorporation of hydroxycinnamaldehydes and hydroxybenzaldehydes into lignins. *Organic & Biomolecular Chemistry*, **2003**. 1(2): 268-281.

27. Marita, J.M., Ralph, J., Lapierre, C., Jouanin, L., and Boerjan, W., NMR characterization of lignins from transgenic poplars with suppressed caffeic acid O-methyltransferase activity. *Journal of the Chemical Society-Perkin Transactions 1*, **2001**(22): 2939-2945.

28. Marita, J.M., Ralph, J., Hatfield, R.D., and Chapple, C., NMR characterization of lignins in Arabidopsis altered in the activity of ferulate 5-hydroxylase. *Proceedings of the National Academy of Sciences of the United States of America*, **1999**. 96(22): 12328-12332.

29. Ralph, J., Hatfield, R.D., Piquemal, J., Yahiaoui, N., Pean, M., Lapierre, C., and Boudet, A.M., NMR characterization of altered lignins extracted from tobacco plants down-regulated for lignification enzymes cinnamyl-alcohol dehydrogenase and cinnamoyl-CoA reductase. *Proceedings of the National Academy of Sciences of the United States of America*, **1998**. 95(22): 12803-12808.

30. Adler, E., Lignin Chemistry - Past, Present and Future. *Wood Science and Technology*, **1977**. 11(3): 169-218.

31. Habibi, Y., Lucia, L.A., and Rojas, O.J., Cellulose Nanocrystals: Chemistry, Self-Assembly, and Applications. *Chemical Reviews*, **2010**. 110(6): 3479-3500.

32. Rubin, E.M., Genomics of cellulosic biofuels. *Nature*, **2008**. 454(7206): 841-845.

33. Ragauskas, A.J., Williams, C.K., Davison, B.H., Britovsek, G., Cairney, J., Eckert, C.A., Frederick, W.J., Hallett, J.P., Leak, D.J., Liotta, C.L., Mielenz, J.R., Murphy, R., Templer, R., and Tschaplinski, T., The path forward for biofuels and biomaterials. *Science*, **2006**. 311(5760): 484-489.

34. Sousa, L.D., Chundawat, S.P.S., Balan, V., and Dale, B.E., 'Cradle-to-grave' assessment of existing lignocellulose pretreatment technologies. *Current Opinion in Biotechnology*, **2009**. 20(3): 339-347.

35. Gaspar, A.R., Gamelas, J.A.F., Evtuguin, D.V., and Neto, C.P., Alternatives for lignocellulosic pulp delignification using polyoxometalates and oxygen: a review. *Green Chemistry*, **2007**. 9(7): 717-730.

36. Lawoko, M., Henriksson, G., and Gellerstedt, G., Characterization of lignin-carbohydrate complexes from spruce sulfite pulp. *Holzforschung*, **2006**. 60(2): 162-165.

37. Bunzel, M., Schussler, A., and Saha, G.T., Chemical Characterization of Klason Lignin Preparations from Plant-Based Foods. *Journal of Agricultural and Food Chemistry*, **2011**. 59(23): 12506-12513.

38. Kim, J.S., Lee, Y.Y., and Kim, T.H., A review on alkaline pretreatment technology for bioconversion of lignocellulosic biomass. *Bioresource Technology*, **2016**. 199: 42-48.

39. Kubes, G.J., Fleming, B.I., Macleod, J.M., and Bolker, H.I., Alkaline Pulping with Additives - a Review. *Wood Science and Technology*, **1980**. 14(3): 207-228.

40. Curran, C.E. and Bray, M.W., Reaction variables of the alkaline pulping process. *Industrial and Engineering Chemistry*, **1930**. 22: 830-836.

41. Zhu, J.Y., Pan, X.J., and Zalesny, R.S., Pretreatment of woody biomass for biofuel production: energy efficiency, technologies, and recalcitrance. *Applied Microbiology and Biotechnology*, **2010**. 87(3): 847-857.

42. Gierer, J., Chemistry of Delignification .1. General Concept and Reactions during Pulping. *Wood Science and Technology*, **1985**. 19(4): 289-312.

43. Gierer, J., Chemistry of Delignification .2. Reactions of Lignins during Bleaching. *Wood Science and Technology*, **1986**. 20(1): 1-33.

44. Bokinsky, G., Peralta-Yahya, P.P., George, A., Holmes, B.M., Steen, E.J., Dietrich, J., Lee, T.S., Tullman-Ercek, D., Voigt, C.A., Simmons, B.A., and Keasling, J.D., Synthesis of three advanced biofuels from ionic liquid-pretreated switchgrass using engineered Escherichia coli. *Proceedings of the National Academy of Sciences of the United States of America*, **2011**. 108(50): 19949-19954.

45. Pinkert, A., Marsh, K.N., Pang, S.S., and Staiger, M.P., Ionic Liquids and Their Interaction with Cellulose. *Chemical Reviews*, **2009**. 109(12): 6712-6728.

46. Brandt, A., Ray, M.J., To, T.Q., Leak, D.J., Murphy, R.J., and Welton, T., Ionic liquid pretreatment of lignocellulosic biomass with ionic liquid-water mixtures. *Green Chemistry*, **2011**. 13(9): 2489-2499.

47. Verdia, P., Brandt, A., Hallett, J.P., Ray, M.J., and Welton, T., Fractionation of lignocellulosic biomass with the ionic liquid 1-butylimidazolium hydrogen sulfate. *Green Chemistry*, **2014**. 16(3): 1617-1627.

48. Socha, A.M., Parthasarathi, R., Shi, J., Pattathil, S., Whyte, D., Bergeron, M., George, A., Tran, K., Stavila, V., Venkatachalam, S., Hahn, M.G., Simmons, B.A., and Singh, S., Efficient biomass pretreatment using ionic liquids derived from lignin and hemicellulose. *Proceedings of the National Academy of Sciences of the United States of America*, **2014**. 111(35): E3587-E3595.

49. George, A., Brandt, A., Tran, K., Zahari, S.M.S.N.S., Klein-Marcuschamer, D., Sun, N., Sathitsuksanoh, N., Shi, J., Stavila, V., Parthasarathi, R., Singh, S., Holmes, B.M., Welton, T., Simmons, B.A., and Hallett, J.P., Design of low-cost ionic liquids for lignocellulosic biomass pretreatment. *Green Chemistry*, **2015**. 17(3): 1728-1734.

50. Pu, Y.Q., Jiang, N., and Ragauskas, A.J., Ionic liquid as a green solvent for lignin. *Journal of Wood Chemistry and Technology*, **2007**. 27(1): 23-33.

51. Cheng, G., Kent, M.S., He, L.L., Varanasi, P., Dibble, D., Arora, R., Deng, K., Hong, K.L., Melnichenko, Y.B., Simmons, B.A., and Singh, S., Effect of Ionic Liquid Treatment on the Structures of Lignins in Solutions: Molecular Subunits Released from Lignin. *Langmuir*, **2012**. 28(32): 11859-11866.

52. Fort, D.A., Remsing, R.C., Swatloski, R.P., Moyna, P., Moyna, G., and Rogers, R.D., Can ionic liquids dissolve wood? Processing and analysis of lignocellulosic materials with 1-n-butyl-3-methylimidazolium chloride. *Green Chemistry*, **2007**. 9(1): 63-69.

53. Freudenberg, K., Belz, W., and Niemann, C., Die aromatische Natur des Lignins (10. Mitteilung über Lignin und Cellulose). *Berichte der deutschen chemischen Gesellschaft (A and B Series)*, **1929**. 62(6): 1554-1561.

54. Azadi, P., Inderwildi, O.R., Farnood, R., and King, D.A., Liquid fuels, hydrogen and chemicals from lignin: A critical review. *Renewable & Sustainable Energy Reviews*, **2013**. 21: 506-523.

55. Kang, S., Li, X., Fan, J., and Chang, J., Hydrothermal conversion of lignin: A review. *Renewable & Sustainable Energy Reviews*, **2013**. 27: 546-558.

56. Brebu, M. and Vasile, C., THERMAL DEGRADATION OF LIGNIN - A REVIEW. *Cellulose Chemistry and Technology*, **2010**. 44(9): 353-363.

57. Pandey, M.P. and Kim, C.S., Lignin depolymerization and conversion: a review of thermochemical methods. *Chemical Engineering & Technology*, **2011**. 34(1): 29-41.

58. Joffres, B., Laurenti, D., Charon, N., Daudin, A., Quignard, A., and Geantet, C., Thermochemical Conversion of Lignin for Fuels and Chemicals: A Review. *Oil & Gas Science and Technology-Revue D Ifp Energies Nouvelles*, **2013**. 68(4): 753-763.

59. Mu, W., Ben, H., Ragauskas, A., and Deng, Y., Lignin Pyrolysis Components and Upgrading-Technology Review. *Bioenergy Research*, **2013**. 6(4): 1183-1204.

60. Bugg, T.D.H., Ahmad, M., Hardiman, E.M., and Singh, R., The emerging role for bacteria in lignin degradation and bio-product formation. *Current Opinion in Biotechnology*, **2011**. 22(3): 394-400.

61. Zhang, X., Peng, X., and Masai, E., Recent advances in Sphingobium sp SYK-6 for lignin aromatic compounds degradation - A review. *Weishengwu Xuebao*, **2014**. 54(8): 854-867.

62. Lange, H., Decina, S., and Crestini, C., Oxidative upgrade of lignin - Recent routes reviewed. *European Polymer Journal*, **2013**. 49(6): 1151-1173.

63. Saidi, M., Samimi, F., Karimipourfard, D., Nimmanwudipong, T., Gates, B.C., and Rahimpour, M.R., Upgrading of lignin-derived bio-oils by catalytic hydrodeoxygenation. *Energy & Environmental Science*, **2014**. 7(1): 103-129.

64. Brandt, A., Grasvik, J., Hallett, J.P., and Welton, T., Deconstruction of lignocellulosic biomass with ionic liquids. *Green Chemistry*, **2013**. 15(3): 550-583.

65. Chatel, G. and Rogers, R.D., Review: Oxidation of Lignin Using Ionic Liquids-An Innovative Strategy To Produce Renewable Chemicals. *Acs Sustainable Chemistry & Engineering*, **2014**. 2(3): 322-339.

66. Deng, H.B., Lin, L., Sun, Y., Pang, C.S., Zhuang, J.P., Ouyang, P.K., Li, J.J., and Liu, S.J., Activity and Stability of Perovskite-Type Oxide LaCoO3 Catalyst in Lignin Catalytic Wet Oxidation to Aromatic Aldehydes Process. *Energy & Fuels*, **2009**. 23(1-2): 19-24.

67. Gu, X.L., Cheng, K.H., He, M., Shi, Y.J., and Li, Z.Z., La-Modified Sba-15/H2o2 Systems for the Microwave Assisted Oxidation of Organosolv Beech Wood Lignin. *Maderas-Ciencia Y Tecnologia*, **2012**. 14(1): 31-42.

68. Staerk, K., Taccardi, N., Boesmann, A., and Wasserscheid, P., Oxidative Depolymerization of Lignin in Ionic Liquids. *Chemsuschem*, **2010**. 3(6): 719-723.

69. Liu, S.W., Shi, Z.L., Li, L., Yu, S.T., Xie, C.X., and Song, Z.Q., Process of lignin oxidation in an ionic liquid coupled with separation. *Rsc Advances*, **2013**. 3(17): 5789-5793.

70. Yamamoto, K., Hosoya, T., Yoshioka, K., Miyafuji, H., Ohno, H., and Yamada, T., Tetrabutylammonium Hydroxide 30-Hydrate as Novel Reaction Medium for Lignin Conversion. *Acs Sustainable Chemistry & Engineering*, **2017**. 5(11): 10111-10115.

71. Xiang, Q. and Lee, Y.Y., Oxidative cracking of precipitated hardwood lignin by hydrogen peroxide. *Applied Biochemistry and Biotechnology*, **2000**. 84-6: 153-162.

72. Ma, R., Xu, Y., and Zhang, X., Catalytic Oxidation of Biorefinery Lignin to Value-added Chemicals to Support Sustainable Biofuel Production. *Chemsuschem*, **2015**. 8(1): 24-51.

73. Behling, R., Valange, S., and Chatel, G., Heterogeneous catalytic oxidation for lignin valorization into valuable chemicals: what results? What limitations? What trends? *Green Chemistry*, **2016**. 18(7): 1839-1854.

74. Barta, K., Matson, T.D., Fettig, M.L., Scott, S.L., Iretskii, A.V., and Ford, P.C., Catalytic disassembly of an organosolv lignin via hydrogen transfer from supercritical methanol. *Green Chemistry*, **2010**. 12(9): 1640-1647.

75. Chauvier, C. and Cantat, T., A Viewpoint on Chemical Reductions of Carbon-Oxygen Bonds in Renewable Feedstocks Including CO2 and Biomass. *Acs Catalysis*, **2017**. 7(3): 2107-2115.

76. Zaheer, M. and Kempe, R., Catalytic Hydrogenolysis of Aryl Ethers: A Key Step in Lignin Valorization to Valuable Chemicals. *Acs Catalysis*, **2015**. 5(3): 1675-1684.

77. Hensley, A.J.R., Zhang, R.Q., Wang, Y., and McEwen, J.S., Tailoring the Adsorption of Benzene on PdFe Surfaces: A Density Functional Theory Study. *Journal of Physical Chemistry C*, **2013**. 117(46): 24317-24328.

78. Sun, J.M., Karim, A.M., Zhang, H., Kovarik, L., Li, X.H.S., Hensley, A.J., McEwen, J.S., and Wang, Y., Carbon-supported bimetallic Pd-Fe catalysts for vapor-phase hydrodeoxygenation of guaiacol. *Journal of Catalysis*, **2013**. 306: 47-57.

79. Hong, Y.C., Hensley, A., McEwen, J.S., and Wang, Y., Perspective on Catalytic Hydrodeoxygenation of Biomass Pyrolysis Oils: Essential Roles of Fe-Based Catalysts. *Catalysis Letters*, **2016**. 146(9): 1621-1633.

80. Deuss, P.J. and Barta, K., From models to lignin: Transition metal catalysis for selective bond cleavage reactions. *Coordination Chemistry Reviews*, **2016**. 306: 510-532.

81. Shen, X.J., Huang, P.L., Wen, J.L., and Sun, R.C., Research Status of Lignin Oxidative and Reductive Depolymerization. *Progress in Chemistry*, **2017**. 29(1): 162-180.

82. Mohan, D., Pittman, C.U., and Steele, P.H., Pyrolysis of wood/biomass for bio-oil: A critical review. *Energy & Fuels*, **2006**. 20(3): 848-889.

83. Bu, Q., Lei, H.W., Zacher, A.H., Wang, L., Ren, S.J., Liang, J., Wei, Y., Liu, Y.P., Tang, J., Zhang, Q., and Ruan, R., A review of catalytic hydrodeoxygenation of lignin-derived phenols from biomass pyrolysis. *Bioresource Technology*, **2012**. 124: 470-477.

84. Zacher, A.H., Olarte, M.V., Santosa, D.M., Elliott, D.C., and Jones, S.B., A review and perspective of recent bio-oil hydrotreating research. *Green Chemistry*, **2014**. 16(2): 491-515.

85. Barta, K., Warner, G.R., Beach, E.S., and Anastas, P.T., Depolymerization of organosolv lignin to aromatic compounds over Cu-doped porous metal oxides. *Green Chemistry*, **2014**. 16(1): 191-196.

86. Gao, F., Webb, J.D., Sorek, H., Wemmer, D.E., and Hartwig, J.F., Fragmentation of Lignin Samples with Commercial Pd/C under Ambient Pressure of Hydrogen. *Acs Catalysis*, **2016**. 6(11): 7385-7392.

87. Jiang, Y.T., Li, Z., Tang, X., Sun, Y., Zeng, X.H., Liu, S.J., and Lin, L., Depolymerization of Cellulolytic Enzyme Lignin for the Production of Monomeric Phenols over Raney Ni and Acidic Zeolite Catalysts. *Energy & Fuels*, **2015**. 29(3): 1662-1668.

88. Konnerth, H., Zhang, J.G., Ma, D., Prechtl, M.H.G., and Yan, N., Base promoted hydrogenolysis of lignin model compounds and organosolv lignin over metal catalysts in water. *Chemical Engineering Science*, **2015**. 123: 155-163.

89. Si, X.Q., Lu, F., Chen, J.Z., Lu, R., Huang, Q.Q., Jiang, H.F., Taarning, E., and Xu, J., A strategy for generating high-quality cellulose and lignin simultaneously from woody biomass. *Green Chemistry*, **2017**. 19(20): 4849-4857.

90. Shao, Y., Xia, Q.N., Dong, L., Liu, X.H., Han, X., Parker, S.F., Cheng, Y.Q., Daemen, L.L., Ramirez-Cuesta, A.J., Yang, S.H., and Wang, Y.Q., Selective production of arenes via direct lignin upgrading over a niobium-based catalyst. *Nature Communications*, **2017**. 8.

91. Kim, S., Chmely, S.C., Nimos, M.R., Bomble, Y.J., Foust, T.D., Paton, R.S., and Beckham, G.T., Computational Study of Bond Dissociation Enthalpies for a Large Range of Native and Modified Lignins. *Journal of Physical Chemistry Letters*, **2011**. 2(22): 2846-2852.

92. Ragauskas, A.J., Beckham, G.T., Biddy, M.J., Chandra, R., Chen, F., Davis, M.F., Davison, B.H., Dixon, R.A., Gilna, P., Keller, M., Langan, P., Naskar, A.K., Saddler, J.N., Tschaplinski, T.J., Tuskan, G.A., and Wyman, C.E., Lignin Valorization: Improving Lignin Processing in the Biorefinery. *Science*, **2014**. 344(6185): 709-+.

93. Sousa, L.D., Jin, M.J., Chundawat, S.P.S., Bokade, V., Tang, X.Y., Azarpira, A., Lu, F.C., Avci, U., Humpula, J., Uppugundla, N., Gunawan, C., Pattathil, S., Cheh, A.M., Kothari, N., Kumar, R., Ralph, J., Hahn, M.G., Wyman, C.E., Singh, S., Simmons, B.A., Dale, B.E., and Balan, V., Next-generation ammonia pretreatment enhances cellulosic biofuel production. *Energy & Environmental Science*, **2016**. 9(4): 1215-1223.

94. Sousa, L.d.C., Foston, M., Bokade, V., Azarpira, A., Lu, F., Ragauskas, A.J., Ralph, J., Dale, B., and Balan, V., Isolation and characterization of new lignin streams derived from extractive-ammonia (EA) pretreatment. *Green Chemistry*, **2016**. 18(15): 4205-4215.

95. Bouxin, F.P., Jackson, S.D., and Jarvis, M.C., Isolation of high quality lignin as a by-product from ammonia percolation pretreatment of poplar wood. *Bioresource Technology*, **2014**. 162: 236-242.

96. Mittal, A., Katahira, R., Donohoe, B.S., Pattathil, S., Kandemkavil, S., Reed, M.L., Biddy, M.J., and Beckham, G.T., Ammonia Pretreatment of Corn Stover Enables Facile Lignin Extraction. *Acs Sustainable Chemistry & Engineering*, **2017**. 5(3): 2544-2561.

97. Sathitsuksanoh, N., Holtman, K.M., Yelle, D.J., Morgan, T., Stavila, V., Pelton, J., Blanch, H., Simmons, B.A., and George, A., Lignin fate and characterization during ionic liquid biomass pretreatment for renewable chemicals and fuels production. *Green Chemistry*, **2014**. 16(3): 1236-1247.

98. Kim, K.H., Simmons, B.A., and Singh, S., Catalytic transfer hydrogenolysis of ionic liquid processed biorefinery lignin to phenolic compounds. *Green Chemistry*, **2017**. 19(1): 215-224.

99. Luterbacher, J.S., Rand, J.M., Alonso, D.M., Han, J., Youngquist, J.T., Maravelias, C.T., Pfleger, B.F., and Dumesic, J.A., Nonenzymatic Sugar Production from Biomass Using Biomass-Derived gamma-Valerolactone. *Science*, **2014**. 343(6168): 277-280.

100. Luterbacher, J.S., Azarpira, A., Motagamwala, A.H., Lu, F., Ralph, J., and Dumesic, J.A., Lignin monomer production integrated into the gamma-valerolactone sugar platform. *Energy & Environmental Science*, **2015**. 8(9): 2657-2663.

101. Deuss, P.J., Lancefield, C.S., Narani, A., de Vries, J.G., Westwood, N.J., and Barta, K., Phenolic acetals from lignins of varying compositions via iron(III) triflate catalysed depolymerisation. *Green Chemistry*, **2017**. 19(12): 2774-2782.

102. Feghali, E., Carrot, G., Thuery, P., Genre, C., and Cantat, T., Convergent reductive depolymerization of wood lignin to isolated phenol derivatives by metal-free catalytic hydrosilylation. *Energy & Environmental Science*, **2015**. 8(9): 2734-2743.

103. Lancefield, C.S., Panovic, I., Deuss, P.J., Barta, K., and Westwood, N.J., Pre-treatment of lignocellulosic feedstocks using biorenewable alcohols: towards complete biomass valorisation. *Green Chemistry*, **2017**. 19(1): 202-214.

104. Constant, S., Wienk, H.L.J., Frissen, A.E., de Peinder, P., Boelens, R., van Es, D.S., Grisel, R.J.H., Weckhuysen, B.M., Huijgen, W.J.J., Gosselink, R.J.A., and Bruijnincx, P.C.A., New insights into the structure and composition of technical

lignins: a comparative characterisation study. *Green Chemistry*, **2016**. 18(9): 2651-2665.

105. Ferrini, P. and Rinaldi, R., Catalytic Biorefining of Plant Biomass to Non-Pyrolytic Lignin Bio-Oil and Carbohydrates through Hydrogen Transfer Reactions. *Angewandte Chemie-International Edition*, **2014**. 53(33): 8634-8639.

106. Galkin, M.V. and Samec, J.S.M., Selective Route to 2-Propenyl Aryls Directly from Wood by a Tandem Organosolv and Palladium-Catalysed Transfer Hydrogenolysis. *Chemsuschem*, **2014**. 7(8): 2154-2158.

107. Huang, X., Gonzalez, O.M.M., Zhu, J., Koranyi, T.I., Boot, M.D., and Hensen, E.J.M., Reductive fractionation of woody biomass into lignin monomers and cellulose by tandem metal triflate and Pd/C catalysis. *Green Chemistry*, **2017**. 19(1): 175-187.

108. Parsell, T., Yohe, S., Degenstein, J., Jarrell, T., Klein, I., Gencer, E., Hewetson, B., Hurt, M., Kim, J.I., Choudhari, H., Saha, B., Meilan, R., Mosier, N., Ribeiro, F., Delgass, W.N., Chapple, C., Kenttamaa, H.I., Agrawal, R., and Abu-Omar, M.M., A synergistic biorefinery based on catalytic conversion of lignin prior to cellulose starting from lignocellulosic biomass. *Green Chemistry*, **2015**. 17(3): 1492-1499.

109. Renders, T., Schutyser, W., Van den Bosch, S., Koelewijn, S.-F., Vangeel, T., Courtin, C.M., and Sels, B.F., Influence of Acidic (H3PO4) and Alkaline (NaOH) Additives on the Catalytic Reductive Fractionation of Lignocellulose. *Acs Catalysis*, **2016**. 6(3): 2055-2066.

110. Song, Q., Wang, F., Cai, J., Wang, Y., Zhang, J., Yu, W., and Xu, J., Lignin depolymerization (LDP) in alcohol over nickel-based catalysts via a fragmentation-hydrogenolysis process. *Energy & Environmental Science*, **2013**. 6(3): 994-1007.

111. Van den Bosch, S., Schutyser, W., Vanholme, R., Driessen, T., Koelewijn, S.F., Renders, T., De Meester, B., Huijgen, W.J.J., Dehaen, W., Courtin, C.M., Lagrain, B., Boerjan, W., and Sels, B.F., Reductive lignocellulose fractionation into soluble lignin-derived phenolic monomers and dimers and processable carbohydrate pulps. *Energy & Environmental Science*, **2015**. 8(6): 1748-1763.

112. Schutyser, W., Van den Bosch, S., Renders, T., De Boe, T., Koelewijn, S.F., Dewaele, A., Ennaert, T., Verkinderen, O., Goderis, B., Courtin, C.M., and Sels, B.F., Influence of bio-based solvents on the catalytic reductive fractionation of birch wood. *Green Chemistry*, **2015**. 17(11): 5035-5045.

113. Galkin, M.V., Smit, A.T., Subbotina, E., Artemenko, K.A., Bergquist, J., Huijgen, W.J.J., and Samec, J.S.M., Hydrogen-free catalytic fractionation of woody biomass. *Chemsuschem*, **2016**. 9(23): 3280-3287.

114. Van den Bosch, S., Renders, T., Kennis, S., Koelewijn, S.F., Van den Bossche, G., Vangeel, T., Deneyer, A., Depuydt, D., Courtin, C.M., Thevelein, J.M., Schutyser,

W., and Sels, B.F., Integrating lignin valorization and bio-ethanol production: on the role of Ni-Al2O3 catalyst pellets during lignin-first fractionation. *Green Chemistry*, **2017**. 19(14): 3313-3326.

115. Shuai, L., Amiri, M.T., Questell-Santiago, Y.M., Heroguel, F., Li, Y., Kim, H., Meilan, R., Chapple, C., Ralph, J., and Luterbacher, J.S., Formaldehyde stabilization facilitates lignin monomer production during biomass depolymerization. *Science*, **2016**. 354(6310): 329-333.

116. Rinaldi, R., A Tandem for Lignin-First Biorefinery. *Joule*, **2017**. 1(3): 427-428.

117. Di Marino, D., Stockmann, D., Kriescher, S., Stiefel, S., and Wessling, M., Electrochemical depolymerisation of lignin in a deep eutectic solvent. *Green Chemistry*, **2016**. 18(22): 6021-6028.

118. Di Marino, D., Aniko, V., Stocco, A., Kriescher, S., and Wessling, M., Emulsion electro-oxidation of kraft lignin. *Green Chemistry*, **2017**. 19(20): 4778-4784.

119. Stiefel, S., Marks, C., Schmidt, T., Hanisch, S., Spalding, G., and Wessling, M., Overcoming lignin heterogeneity: reliably characterizing the cleavage of technical lignin. *Green Chemistry*, **2016**. 18(2): 531-540.

120. Stiefel, S., Schmitz, A., Peters, J., Di Marino, D., and Wessling, M., An integrated electrochemical process to convert lignin to value-added products under mild conditions. *Green Chemistry*, **2016**. 18(18): 4999-5007.

121. Pardini, V.L., Smith, C.Z., Utley, J.H.P., Vargas, R.R., and Viertler, H., Electroorganic Reactions .38. Mechanism of Electrooxidative Cleavage of Lignin Model Dimers. *Journal of Organic Chemistry*, **1991**. 56(26): 7305-7313.

122. Chen, F.G., Lu, Z.M., and Tu, B., Electro-degradation of sodium lignosulfonate. *Journal of Wood Chemistry and Technology*, **2003**. 23(3-4): 261-277.

123. Cai, P., Fan, H.X., Cao, S., Qi, J., Zhang, S.M., and Li, G., Electrochemical conversion of corn stover lignin to biomass-based chemicals between Cu/Ni-Mo-Co cathode and Pb/PbO2 anode in alkali solution. *Electrochimica Acta*, **2018**. 264: 128-139.

124. Zhu, H., Chen, Y., Qin, T., Wang, L., Tang, Y., Sun, Y., and Wan, P., Lignin depolymerization via an integrated approach of anode oxidation and electro-generated H2O2 oxidation. *Rsc Advances*, **2014**. 4(12): 6232-6238.

125. Reichert, E., Wintringer, R., Volmer, D.A., and Hempelmann, R., Electro-catalytic oxidative cleavage of lignin in a protic ionic liquid. *Physical Chemistry Chemical Physics*, **2012**. 14(15): 5214-5221.

126. Kishioka, S. and Yamada, A., Kinetic study of the catalytic oxidation of benzyl alcohols by phthalimide-N-oxyl radical electrogenerated in acetonitrile using

rotating disk electrode voltammetry. *Journal of Electroanalytical Chemistry*, **2005**. 578(1): 71-77.

127. Shiraishi, T., Takano, T., Kamitakahara, H., and Nakatsubo, F., Studies on electro-oxidation of lignin and lignin model compounds. Part 2: N-Hydroxyphthalimide (NHPI)-mediated indirect electro-oxidation of non-phenolic lignin model compounds. *Holzforschung*, **2012**. 66(3): 311-315.

128. Liu, W., Cui, Y., Du, X., Zhang, Z., Chao, Z.S., and Deng, Y.L., High efficiency hydrogen evolution from native biomass electrolysis. *Energy & Environmental Science*, **2016**. 9(2): 467-472.

129. Weinstock, I.A., Homogeneous-phase electron-transfer reactions of polyoxometalates. *Chemical Reviews*, **1998**. 98(1): 113-170.

130. Evtuguin, D.V., Neto, C.P., Carapuca, H., and Soares, J., Lignin degradation in oxygen delignification catalysed by [PMo7V5O40](8-) polyanion. Part II. Study on lignin monomeric model compounds. *Holzforschung*, **2000**. 54(5): 511-518.

131. Weinstock, I.A., Hammel, K.E., Moen, M.A., Landucci, L.L., Ralph, S., Sullivan, C.E., and Reiner, R.S., Selective transition-metal catalysis of oxygen delignification using water-soluble salts of polyoxometalate (POM) anions. Part II. Reactions of alpha-[SiVW11O40](5-) with phenolic lignin-model compounds. *Holzforschung*, **1998**. 52(3): 311-318.

132. Weinstock, I.A., Atalla, R.H., Reiner, R.S., Houtman, C.J., and Hill, C.L., Selective transition-metal catalysis of oxygen delignification using water-soluble salts of polyoxomeralate (POM) anions. Part I. Chemical principles and process concepts. *Holzforschung*, **1998**. 52(3): 304-310.

133. Weinstock, I.A., Atalla, R.H., Reiner, R.S., Moen, M.A., Hammel, K.E., Houtman, C.J., Hill, C.L., and Harrup, M.K., A new environmentally benign technology for transforming wood pulp into paper - Engineering polyoxometalates as catalysts for multiple processes. *Journal of Molecular Catalysis a-Chemical*, **1997**. 116(1-2): 59-84.

134. Voitl, T. and von Rohr, P.R., Oxidation of Lignin Using Aqueous Polyoxometalates in the Presence of Alcohols. *Chemsuschem*, **2008**. 1(8-9): 763-769.

135. Zhao, Y., Xu, Q., Pan, T., Zuo, Y., Fu, Y., and Guo, Q.X., Depolymerization of lignin by catalytic oxidation with aqueous polyoxometalates. *Applied Catalysis a-General*, **2013**. 467: 504-508.

136. Gaspar, A., Evtuguin, D.V., and Neto, C.P., Lignin reactions in oxygen delignification catalysed by Mn(II)-substituted molybdovanadophosphate polyanion. *Holzforschung*, **2004**. 58(6): 640-649.

137. Weinstock, I.A., Barbuzzi, E.M.G., Wemple, M.W., Cowan, J.J., Reiner, R.S., Sonnen, D.M., Heintz, R.A., Bond, J.S., and Hill, C.L., Equilibrating metal-oxide cluster ensembles for oxidation reactions using oxygen in water. *Nature*, **2001**. 414(6860): 191-195.

138. Yokoyama, T., Chang, H.-m., Weinstock, I.A., Reiner, R.S., and Kadla, J.F., *Kinetic Analysis of Polyoxometalate (POM) Oxidation of Non-Phenolic Lignin Model Compound*, in *12th International Symposium on Wood and Pulping Chemistry*. 2003: Madison, Wisconsin USA. p. 43-46.

139. Yokoyama, T., Chang, H.M., Reiner, R.S., Atalla, R.H., Weinstock, I.A., and Kadla, J.F., Polyoxometalate oxidation of nonphenolic lignin subunits in water: Effect of substrate structure on reaction kinetics. *Holzforschung*, **2004**. 58(2): 116-121.

140. Liu, W., Mu, W., Liu, M.J., Zhang, X.D., Cai, H.L., and Deng, Y.L., Solar-induced direct biomass-to-electricity hybrid fuel cell using polyoxometalates as photocatalyst and charge carrier. *Nature Communications*, **2014**. 5.

141. Kupce, E. and Freeman, R., Fast multidimensional NMR by polarization sharing. *Magnetic Resonance in Chemistry*, **2007**. 45(1): 2-4.

142. Ben, H.X. and Ragauskas, A.J., NMR Characterization of Pyrolysis Oils from Kraft Lignin. *Energy & Fuels*, **2011**. 25(5): 2322-2332.

143. Santos, J.I., Martin-Sampedro, R., Fillat, U., Oliva, J.M., Negro, M.J., Ballesteros, M., Eugenio, M.E., and Ibarra, D., Evaluating Lignin-Rich Residues from Biochemical Ethanol Production of Wheat Straw and Olive Tree Pruning by FTIR and 2D-NMR. *International Journal of Polymer Science*, **2015**.

144. Liu, Y., Hu, T.J., Wu, Z.P., Zeng, G.M., Huang, D.L., Shen, Y., He, X.X., Lai, M.Y., and He, Y.B., Study on biodegradation process of lignin by FTIR and DSC. *Environmental Science and Pollution Research*, **2014**. 21(24): 14004-14013.

145. Wang, H.L., Ben, H.X., Ruan, H., Zhang, L.B., Pu, Y.Q., Feng, M.Q., Ragauskas, A.J., and Yang, B., Effects of Lignin Structure on Hydrodeoxygenation Reactivity of Pine Wood Lignin to Valuable Chemicals. *Acs Sustainable Chemistry & Engineering*, **2017**. 5(2): 1824-1830.

146. Scanion, J.T. and Willis, D.E., Calculation of Flame Ionization Detector Relative Response Factors Using the Effective Carbon Number Concept. *Journal of Chromatographic Science*, **1985**. 23(8): 333-340.

147. Zhang, J.G., Teo, J., Chen, X., Asakura, H., Tanaka, T., Teramura, K., and Yan, N., A Series of NiM (M = Ru, Rh, and Pd) Bimetallic Catalysts for Effective Lignin Hydrogenolysis in Water. *Acs Catalysis*, **2014**. 4(5): 1574-1583.

148. Hidajat, M.J., Riaz, A., Park, J., Insyani, R., Verma, D., and Kim, J., Depolymerization of concentrated sulfuric acid hydrolysis lignin to high-yield aromatic monomers in basic sub-and supercritical fluids. *Chemical Engineering Journal*, **2017**. 317: 9-19.

149. Deuss, P.J., Scott, M., Tran, F., Westwood, N.J., de Vries, J.G., and Barta, K., Aromatic monomers by in situ conversion of reactive intermediates in the acid-catalyzed depolymerization of lignin. *Journal of the American Chemical Society*, **2015**. 137(23): 7456-7467.

150. Song, Q., Wang, F., Cai, J., Wang, Y., Zhang, J., Yu, W., and Xu, J., Lignin depolymerization (LDP) in alcohol over nickel-based catalysts via a fragmentation–hydrogenolysis process. *Energy & Environmental Science*, **2013**. 6(3): 994-1007.

151. Zhao, Y., Xu, Q., Pan, T., Zuo, Y., Fu, Y., and Guo, Q.-X., Depolymerization of lignin by catalytic oxidation with aqueous polyoxometalates. *Applied Catalysis A: General*, **2013**. 467: 504-508.

152. Hatakka, A., Biodegradation of lignin. *Biopolymers Online*, **2005**.

153. Li, C., Zhao, X., Wang, A., Huber, G.W., and Zhang, T., Catalytic transformation of lignin for the production of chemicals and fuels. *Chem. Rev*, **2015**. 115(21): 11559-11624.

154. Shuai, L. and Saha, B., Towards high-yield lignin monomer production. *Green Chemistry*, **2017**. 19(16): 3752-3758.

155. Lahive, C.W., Deuss, P.J., Lancefield, C.S., Sun, Z., Cordes, D.B., Young, C.M., Tran, F., Slawin, A.M.Z., de Vries, J.G., Kamer, P.C.J., Westwood, N.J., and Barta, K., Advanced Model Compounds for Understanding Acid-Catalyzed Lignin Depolymerization: Identification of Renewable Aromatics and a Lignin-Derived Solvent. *Journal of the American Chemical Society*, **2016**. 138(28): 8900-8911.

156. Sturgeon, M.R., Kim, S., Lawrence, K., Paton, R.S., Chmely, S.C., Nimlos, M., Foust, T.D., and Beckham, G.T., A Mechanistic Investigation of Acid-Catalyzed Cleavage of Aryl-Ether Linkages: Implications for Lignin Depolymerization in Acidic Environments. *Acs Sustainable Chemistry & Engineering*, **2014**. 2(3): 472-485.

157. Bouxin, F.P., McVeigh, A., Tran, F., Westwood, N.J., Jarvis, M.C., and Jackson, S.D., Catalytic depolymerisation of isolated lignins to fine chemicals using a Pt/alumina catalyst: part 1-impact of the lignin structure. *Green Chemistry*, **2015**. 17(2): 1235-1242.

158. Zhang, C., Li, H., Lu, J., Zhang, X., MacArthur, K.E., Heggen, M., and Wang, F., Promoting Lignin Depolymerization and Restraining the Condensation via an Oxidation− Hydrogenation Strategy. *ACS Catalysis*, **2017**. 7(5): 3419-3429.

159. Gaspar, A.R., Gamelas, J.A., Evtuguin, D.V., and Neto, C.P., Alternatives for lignocellulosic pulp delignification using polyoxometalates and oxygen: a review. *Green Chemistry*, **2007**. 9(7): 717-730.

160. Voitl, T. and Rudolf von Rohr, P., Oxidation of lignin using aqueous polyoxometalates in the presence of alcohols. *ChemSusChem*, **2008**. 1(8‐9): 763-769.

161. Voitl, T. and Rohr, P.R.v., Demonstration of a process for the conversion of kraft lignin into vanillin and methyl vanillate by acidic oxidation in aqueous methanol. *Industrial & Engineering Chemistry Research*, **2009**. 49(2): 520-525.

162. Hiskia, A. and Papaconstantinou, E., Photocatalytic Oxidation of Organic-Compounds by Polyoxometalates of Molybdenum and Tungsten - Catalyst Regeneration by Dioxygen. *Inorganic Chemistry*, **1992**. 31(2): 163-167.

163. Florence, T.M., The Production of Hydroxyl Radical from Hydrogen-Peroxide. *Journal of Inorganic Biochemistry*, **1984**. 22(4): 221-230.

164. Birchmeier, M.J., Hill, C.G., Houtman, C.J., Atalla, R.H., and Weinstock, I.A., Enhanced wet air oxidation: Synergistic rate acceleration upon effluent recirculation. *Industrial & Engineering Chemistry Research*, **2000**. 39(1): 55-64.

165. Kim, Y.S., Chang, H.M., and Kadla, J.F., Polyoxometalate (POM) oxidation of milled wood lignin (MWL). *Journal of Wood Chemistry and Technology*, **2007**. 27(3-4): 225-241.

166. Studer, D.W. and Schaub, E.S., *Liquid phase methanol process with co-rich recycle*. 1994, Google Patents.

167. Liu, S., Shi, Z., Li, L., Yu, S., Xie, C., and Song, Z., Process of lignin oxidation in an ionic liquid coupled with separation. *RSC Advances*, **2013**. 3(17): 5789-5793.

168. Gao, P., Li, C., Wang, H., Wang, X., and Wang, A., Perovskite hollow nanospheres for the catalytic wet air oxidation of lignin. *Chinese Journal of Catalysis*, **2013**. 34(10): 1811-1815.

169. Lin, S.Y. and Dence, C.W., *Methods in lignin chemistry*. 2012: Springer Science & Business Media.

170. Sadakane, M. and Steckhan, E., Electrochemical properties of polyoxometalates as electrocatalysts. *Chemical Reviews*, **1998**. 98(1): 219-238.

171. Liu, W., Mu, W., and Deng, Y., High‐Performance Liquid‐Catalyst Fuel Cell for Direct Biomass‐into‐Electricity Conversion. *Angewandte Chemie*, **2014**. 126(49): 13776-13780.

172. Qi, S.-C., Hayashi, J.-i., Kudo, S., and Zhang, L., Catalytic hydrogenolysis of kraft lignin to monomers at high yield in alkaline water. *Green Chemistry*, **2017**. 19(11): 2636-2645.

173. Strassberger, Z., Alberts, A.H., Louwerse, M.J., Tanase, S., and Rothenberg, G., Catalytic cleavage of lignin β-O-4 link mimics using copper on alumina and magnesia–alumina. *Green Chemistry*, **2013**. 15(3): 768-774.

174. Brebu, M. and Vasile, C., Thermal degradation of lignin—a review. *Cellulose Chemistry & Technology*, **2010**. 44(9): 353.

175. Weinstock, I.A., Hammel, K.E., Moen, M.A., Landucci, L.L., Ralph, S., Sullivan, C.E., and Reiner, R.S., Selective Transition-Metal Catalysis of Oxygen Delignification. Using Water-Soluble Salts of Polyoxometalate (POM) Anions. Part II. Reactions of α-[SiVW 11 O 40] 5-with Phenolic Lignin-Model Compounds. *Holzforschung-International Journal of the Biology, Chemistry, Physics and Technology of Wood*, **1998**. 52(3): 311-318.

176. Patil, S.V. and Argyropoulos, D.S., Stable Organic Radicals in Lignin: A Review. *Chemsuschem*, **2017**. 10.

177. Cronin, D.J., Zhang, X., Bartley, J., and Doherty, W.O.S., Lignin Depolymerization to Dicarboxylic Acids with Sodium Percarbonate. *Acs Sustainable Chemistry & Engineering*, **2017**.

178. Ma, R., Guo, M., Prof., #x, and Zhang, D.X., Selective Conversion of Biorefinery Lignin into Dicarboxylic Acids. *Chemsuschem*, **2014**. 7(2): 412-415.

179. Waggoner, D.C., Chen, H., Willoughby, A.S., and Hatcher, P.G., Formation of black carbon-like and alicyclic aliphatic compounds by hydroxyl radical initiated degradation of lignin. *Organic Geochemistry*, **2015**. 82: 69-76.

180. ‡, A.C.S., †,, And, A.G.M., †, §, and †, W.T.C., Exact Masses and Chemical Formulas of Individual Suwannee River Fulvic Acids from Ultrahigh Resolution Electrospray Ionization Fourier Transform Ion Cyclotron Resonance Mass Spectra. *Analytical Chemistry*, **2003**. 75(6): 1275-1284.

181. Weinstock, I.A., Hammel, K.E., Moen, M.A., Landucci, L.L., Ralph, S., Sullivan, C.E., and Reiner, R.S., Selective transition-metal catalysis of oxygen delignification using water-soluble salts of polyoxometalate (POM) anions. Part II. Reactions of alpha- SiVW11O40 (5-) with phenolic lignin-model compounds. *Holzforschung*, **1998**. 52(3): 311-318.

182. Kim, H., Ralph, J., and Akiyama, T., Solution-state 2D NMR of Ball-milled Plant Cell Wall Gels in DMSO-d(6). *Bioenergy Research*, **2008**. 1(1): 56-66.

183. Kim, H. and Ralph, J., Solution-state 2D NMR of ball-milled plant cell wall gels in DMSO-d(6)/pyridine-d(5). *Organic & Biomolecular Chemistry*, **2010**. 8(3): 576-591.

184. Mansfield, S.D., Kim, H., Lu, F.C., and Ralph, J., Whole plant cell wall characterization using solution-state 2D NMR. *Nature Protocols*, **2012**. 7(9): 1579-1589.

185. Vassilev, P., Louwerse, M.J., and Baerends, E.J., Hydroxyl radical and hydroxide ion in liquid water: A comparative electron density functional theory study. *Journal of Physical Chemistry B*, **2005**. 109(49): 23605-23610.

186. Weinstock, I.A., Atalla, R.H., Reiner, R.S., Moen, M.A., Hammel, K.E., Houtman, C.J., and Hill, C.L., A new environmentally benign technology and approach to bleaching kraft pulp. Polyoxometalates for selective delignification and waste mineralization. *New Journal of Chemistry*, **1996**. 20(2): 269-275.

187. Evtuguin, D.V. and Neto, C.P., New polyoxometalate promoted method of oxygen delignification. *Holzforschung*, **1997**. 51(4): 338-342.

188. Sonnen, D.M., Reiner, R.S., Atalla, R.H., and Weinstock, I.A., Degradation of pulp-mill effluent by oxygen and Na-5 PV2Mo10O40 , a multipurpose delignification and wet air oxidation catalyst. *Industrial & Engineering Chemistry Research*, **1997**. 36(10): 4134-4142.

189. Evtuguin, D.V., Neto, C.P., Carapuca, H., and Soares, J., Lignin degradation in oxygen delignification catalysed by PMo7V5O40 (8-) polyanion. Part II. Study on lignin monomeric model compounds. *Holzforschung*, **2000**. 54(5): 511-518.

190. Evtuguin, D.V., Neto, C.P., and Rocha, J., Lignin degradation in oxygen delignification catalysed by PMo7V5O40 (8-) polyanion. Part I. Study on wood lignin. *Holzforschung*, **2000**. 54(4): 381-389.

191. Ruuttunen, K. and Vuorinen, T., Developing catalytic oxygen delignification for kraft pulp: Kinetic study of lignin oxidation with polyoxometalate anions. *Industrial & Engineering Chemistry Research*, **2005**. 44(12): 4284-4291.

192. Sun, N., Jiang, X., Maxim, M.L., Metlen, A., and Rogers, R.D., Use of Polyoxometalate Catalysts in Ionic Liquids to Enhance the Dissolution and Delignification of Woody Biomass. *Chemsuschem*, **2011**. 4(1): 65-73.

193. Pan, X.J., Kadla, J.F., Ehara, K., Gilkes, N., and Saddler, J.N., Organosolv ethanol lignin from hybrid poplar as a radical scavenger: Relationship between lignin structure, extraction conditions, and antioxidant activity. *Journal of Agricultural and Food Chemistry*, **2006**. 54(16): 5806-5813.

194. Sluiter, A., Hames, B., Ruiz, R., Scarlata, C., Sluiter, J., Templeton, D., and Crocker, D., Determination of structural carbohydrates and lignin in biomass. *Laboratory analytical procedure*, **2008**. 1617: 1-16.

195. Lawoko, M., Henriksson, G., and Gellerstedt, G., Structural differences between the lignin-carbohydrate complexes present in wood and in chemical pulps. *Biomacromolecules*, **2005**. 6(6): 3467-3473.

196. Yuan, T.Q., Sun, S.N., Xu, F., and Sun, R.C., Structural Characterization of Lignin from Triploid of Populus tomentosa Carr. *Journal of Agricultural and Food Chemistry*, **2011**. 59(12): 6605-6615.

197. Akgul, M. and Kirci, H., An environmentally friendly organosolv (ethanol-water) pulping of poplar wood. *Journal of Environmental Biology*, **2009**. 30(5): 735-740.

198. Goyal, G.C., Lora, J.H., and Pye, E.K., Autocatalyzed Organosolv Pulping of Hardwoods - Effect of Pulping Conditions on Pulp Properties and Characteristics of Soluble and Residual Lignin. *Tappi Journal*, **1992**. 75(2): 110-116.

199. Chen, J.Z., Lu, F., Si, X.Q., Nie, X., Chen, J.S., Lu, R., and Xu, J., High Yield Production of Natural Phenolic Alcohols from Woody Biomass Using a Nickel-Based Catalyst. *Chemsuschem*, **2016**. 9(23): 3353-3360.

200. Rausch, B., Symes, M.D., Chisholm, G., and Cronin, L., Decoupled catalytic hydrogen evolution from a molecular metal oxide redox mediator in water splitting. *Science*, **2014**. 345(6202): 1326-1330.

201. Dincer, I., Green methods for hydrogen production. *International Journal of Hydrogen Energy*, **2012**. 37(2): 1954-1971.

202. Turner, J., Sverdrup, G., Mann, M.K., Maness, P.-C., Kroposki, B., Ghirardi, M., Evans, R.J., and Blake, D., Renewable hydrogen production. *International Journal of Energy Research*, **2008**. 32(5): 379-407.

203. Parthasarathy, P. and Narayanan, K.S., Hydrogen production from steam gasification of biomass: Influence of process parameters on hydrogen yield - A review. *Renewable Energy*, **2014**. 66: 570-579.

204. Levin, D.B. and Chahine, R., Challenges for renewable hydrogen production from biomass. *International Journal of Hydrogen Energy*, **2010**. 35(10): 4962-4969.

205. Lu, X., Xie, S., Yang, H., Tong, Y., and Ji, H., Photoelectrochemical hydrogen production from biomass derivatives and water. *Chemical Society Reviews*, **2014**. 43(22): 7581-7593.

206. Wong, Y.M., Wu, T.Y., and Juan, J.C., A review of sustainable hydrogen production using seed sludge via dark fermentation. *Renewable & Sustainable Energy Reviews*, **2014**. 34: 471-482.

207. Carmo, M., Fritz, D.L., Merge, J., and Stolten, D., A comprehensive review on PEM water electrolysis. *International Journal of Hydrogen Energy*, **2013**. 38(12): 4901-4934.

208. Anh Tuan, P., Baba, T., and Shudo, T., Efficient hydrogen production from aqueous methanol in a PEM electrolyzer with porous metal flow field: Influence of change in grain diameter and material of porous metal flow field. *International Journal of Hydrogen Energy*, **2013**. 38(24): 9945-9953.

209. Take, T., Tsurutani, K., and Umeda, M., Hydrogen production by methanol-water solution electrolysis. *Journal of Power Sources*, **2007**. 164(1): 9-16.

210. Sahlin, S.L., Andreasen, S.J., and Kaer, S.K., System model development for a methanol reformed 5 kW high temperature PEM fuel cell system. *International Journal of Hydrogen Energy*, **2015**. 40(38): 13080-13089.

211. Lamy, C., Jaubert, T., Baranton, S., and Coutanceau, C., Clean hydrogen generation through the electrocatalytic oxidation of ethanol in a Proton Exchange Membrane Electrolysis Cell (PEMEC): Effect of the nature and structure of the catalytic anode. *Journal of Power Sources*, **2014**. 245: 927-936.

212. Caravaca, A., Sapountzi, F.M., de Lucas-Consuegra, A., Molina-Mora, C., Dorado, F., and Valverde, J.L., Electrochemical reforming of ethanol-water solutions for pure H-2 production in a PEM electrolysis cell. *International Journal of Hydrogen Energy*, **2012**. 37(12): 9504-9513.

213. Ehteshami, S.M.M., Vignesh, S., Rasheed, R.K.A., and Chan, S.H., Numerical investigations on ethanol electrolysis for production of pure hydrogen from renewable sources. *Applied Energy*, **2016**. 170: 388-393.

214. Marshall, A.T. and Haverkamp, R.G., Production of hydrogen by the electrochemical reforming of glycerol-water solutions in a PEM electrolysis cell. *International Journal of Hydrogen Energy*, **2008**. 33(17): 4649-4654.

215. Chen, Y.X., Lavacchi, A., Miller, H.A., Bevilacqua, M., Filippi, J., Innocenti, M., Marchionni, A., Oberhauser, W., Wang, L., and Vizza, F., Nanotechnology makes biomass electrolysis more energy efficient than water electrolysis. *Nature Communications*, **2014**. 5.

216. Lv, H., Geletii, Y.V., Zhao, C., Vickers, J.W., Zhu, G., Luo, Z., Song, J., Lian, T., Musaev, D.G., and Hill, C.L., Polyoxometalate water oxidation catalysts and the production of green fuel. *Chemical Society Reviews*, **2012**. 41(22): 7572-7589.

217. Symes, M.D. and Cronin, L., Decoupling hydrogen and oxygen evolution during electrolytic water splitting using an electron-coupled-proton buffer. *Nature Chemistry*, **2013**. 5(5): 403-409.

218. Ragland, K.W., Aerts, D.J., and Baker, A.J., Properties of Wood for Combustion Analysis. *Bioresource Technology*, **1991**. 37(2): 161-168.

219. Mao, L., Zhang, L., Gao, N., and Li, A., FeCl3 and acetic acid co-catalyzed hydrolysis of corncob for improving furfural production and lignin removal from residue. *Bioresource Technology*, **2012**. 123: 324-331.

220. Zeng, J., Yoo, C.G., Wang, F., Pan, X., Vermerris, W., and Tong, Z., Biomimetic Fenton-Catalyzed Lignin Depolymerization to High-Value Aromatics and Dicarboxylic Acids. *Chemsuschem*, **2015**. 8(5): 861-871.

221. Seesuriyachan, P., Kuntiya, A., Kawee-ai, A., Techapun, C., Chaiyaso, T., and Leksawasdi, N., Improvement in efficiency of lignin degradation by Fenton reaction using synergistic catalytic action. *Ecological Engineering*, **2015**. 85: 283-287.

222. Kent, M.S., Avina, I.C., Rader, N., Busse, M.L., George, A., Sathitsuksanoh, N., Baidoo, E., Timlin, J., Giron, N.H., Celina, M.C., Martin, L.E., Polsky, R., Chavez, V.H., Huber, D.L., Keasling, J.D., Singh, S., Simmons, B.A., and Sale, K.L., Assay for lignin breakdown based on lignin films: insights into the Fenton reaction with insoluble lignin. *Green Chemistry*, **2015**. 17(10): 4830-4845.

223. Bentivenga, G., Bonini, C., D'Auria, M., and De Bona, A., Degradation of steam-exploded lignin from beech by using Fenton's reagent. *Biomass & Bioenergy*, **2003**. 24(3): 233-238.

224. Neyens, E. and Baeyens, J., A review of classic Fenton's peroxidation as an advanced oxidation technique. *Journal of Hazardous Materials*, **2003**. 98(1-3): 33-50.

225. *Furfural Market Analysis By Application (Furfuryl Alcohol, Solvent) And Segment Forecasts To 2020*. 2015 [cited 2018 May 7]; Available from: https://www.grandviewresearch.com/industry-analysis/furfural-market.

226. Mamman, A.S., Lee, J.M., Kim, Y.C., Hwang, I.T., Park, N.J., Hwang, Y.K., Chang, J.S., and Hwang, J.S., Furfural: Hemicellulose/xylosederived biochemical. *Biofuels Bioproducts & Biorefining-Biofpr*, **2008**. 2(5): 438-454.

227. Yang, L., Liu, W., Zhang, Z., Du, X., Gong, J., Dong, L.C., and Deng, Y.L., Hydrogen Evolution from Native Biomass with Fe3+/Fe2+ Redox Couple Catalyzed Electrolysis. *Electrochimica Acta*, **2017**. 246: 1163-1173.